

**SPATIO-TEMPORAL GROUNDWATER DROUGHT
ASSESSMENT BASED ON ANN MODEL AND GIS FOR A
SUB-BASIN OF BHARATHAPUZHA**

By

RABEEA ASSAINAR K K

(2020-18-005)



**DEPARTMENT OF IRRIGATION AND DRAINAGE ENGINEERING
KELAPPAJI COLLEGE OF AGRICULTURAL ENGINEERING AND
TECHNOLOGY**

TAVANUR - 679573, MALAPPURAM

2022

**SPATIO-TEMPORAL GROUNDWATER DROUGHT
ASSESSMENT BASED ON ANN MODEL AND GIS FOR A
SUB-BASIN OF BHARATHAPUZHA**

By

RABEEA ASSAINAR K K

(2020-18-005)

THESIS

Submitted in partial fulfilment of the requirement for the degree of

MASTER OF TECHNOLOGY

IN

AGRICULTURAL ENGINEERING

(Soil and Water Engineering)

Faculty of Agricultural Engineering & Technology

Kerala Agricultural University



DEPARTMENT OF IRRIGATION AND DRAINAGE ENGINEERING

KELAPPAJI COLLEGE OF AGRICULTURAL ENGINEERING AND

TECHNOLOGY

TAVANUR - 679573, MALAPPURAM

KERALA, INDIA

2022

DECLARATION

I, hereby declare that this thesis entitled “**Spatio-Temporal Groundwater Drought Assessment Based on ANN Model and GIS for a Sub-Basin of Bharathapuzha**” is a bonafide record of research work done by me during the course of research and that the thesis has not previously formed the basis for the award of any degree, diploma, associateship, fellowship or other similar title of any other University or Society.

Place: Tavanur

Rabeea Assainar K K

Date:

(2020-18-005)

CERTIFICATE

Certified that this thesis entitled “**Spatio-Temporal Groundwater Drought Assessment Based on ANN Model and GIS for a Sub-Basin of Bharathapuzha**” is a record of research work done independently by **Mrs. Rabeea Assainar K K (2020- 18- 005)** under my guidance and supervision and that it has not previously formed the basis for the award of any degree, diploma, fellowship or associateship to her.

Place: Tavanur

Date:

Dr. Asha Joseph.

Professor,

Dept. of Irrigation and

Drainage Engineering,

KCAET, Tavanur.

Malappuram, Kerala

CERTIFICATE

We, the undersigned members of the Advisory Committee of **Mrs. Rabeea Assainar K K (2020- 18- 005)**, a candidate for the degree of Master of Technology in Agricultural Engineering, agree that the thesis entitled **“Spatio-Temporal Groundwater Drought Assessment Based on ANN Model and GIS for a Sub-Basin of Bharathapuzha”** may be submitted by **Mrs. Rabeea Assainar K K**, in partial fulfilment of the requirement for the degree.

Committee:

Dr. Asha Joseph

(Chairman, Advisory Committee)

Professor

Dept. of IDE,

KCAET, Tavanur.

Dr. Rema K.P.

(Member, Advisory Committee)

Professor & Head,

Dept. of IDE,

KCAET, Tavanur.

Dr. Josephina Paul

(Member, Advisory Committee)

Assistant Professor

Dept. of BEAS,

KCAET, Tavanur.

Dr. Sajeena S.

(Member, Advisory Committee)

Associate Professor,

Dept. of IDE,

KCAET, Tavanur.

EXTERNAL EXAMINER

ACKNOWLEDGEMENT

ACKNOWLEDGEMENT

*First of all, I offer million gratitude to **God**, the almighty who made me do this task and made every job a success for me. He was the greatest source of all resources and provision, moral or without whose grace nothing is possible.*

*Words cannot express by deepest sense of gratitude and heartfelt thanks to Chairman of my Advisory committee, **Dr. Asha Joseph.**, professor, Department of Irrigation and Drainage Engineering, Kelappaji college of Agricultural Engineering and technology, Tavanur. Her level of guidance, constructive criticism and generous assistance at every stage of my research work is beyond measure. It is my proud privilege to express my heartfelt indebtedness and deepest sense of gratitude for laying out the guidelines of research work. I have real admiration and regards for her whole-hearted support and untiring help.*

*It is my pleasure to pay tribute to **Dr. Jayan P.R**, Dean, Professor & Head, Department of Farm Machinery and Power Engineering, KCAET, Tavanur, for his interest and support given to me at all stages of my research work.*

*I avail this opportunity to express my sincere thanks to my advisory committee members **Dr. Rema. K.P**, Professor & Head, Department of Irrigation and Drainage Engineering, KCAET, Tavanur, **Dr. Sajeena S**, Associate Professor, Department of Irrigation and Drainage Engineering, KCAET, Tavanur, **Dr. Josephina Paul**, Assistant Professor, Department of Basic Engineering and Applied Sciences, KCAET, Tavanur for their valuable counsel, note-worthy guidance and cordial co-operation during my research programme.*

*I would like to extend my sincere thanks to **Dr. Pramada S.K**, Assistant Professor, NIT Calicut for her profound suggestion and encouragement by providing kind advises during my research work.*

*It is my pleasure to thank **Er. Renu S**, **Er. Angitha K A**, **Er. Akhina P**, **Dr. T. Roshni**, and **Er. Yesubabu Vinnakota** for their invaluable help and support during my research work.*

I use this opportunity to sincerely thank my loving teachers of KCAET, Tavanur, Dept. of IDE and SWCE for their support during my research work.

With extreme pleasure, I express my wholehearted gratitude to my dearest friends, juniors and seniors for their great support and constant encouragement provided throughout my work.

*I express my thanks to all the **faculty members of Library, KCAET, Tavanur**, for their ever willing help and cooperation. I express my sincere thanks and gratitude to **KCAET** for giving me an opportunity to undergo my PG studies and **Kerala Agricultural University** for having proffered me a chance to study in this institution.*

*Words are inadequate to express my heartfelt gratitude and love towards my husband **Noushad K.P** for his everlasting love and affection, help, support, incessant motivation and constant encouragement throughout my journey.*

*I am in dearth of words to express my soulful gratitude to my loving parents **Assainar K K** and **Ayissummu C** and my siblings **Sirajudheen K, Muneer Assainar K K, Sirajunnisa K K** for their blessings, selfless support, boundless patience, prayers, inspiration, sacrifices, unflagging interest and eternal love which sustains peace in my life.*

One last word since it is practically impossible to list all contributions to my work, it seems proper to issue a blanket of thanks to those who helped me directly or indirectly for the successful completion of my work.

RABEEA ASSAINAR K K

(202-18-005)

*DEDICATED TO MY LOVING
FAMILY*

CONTENTS

Chapter No.	Title	Page No.
	LIST OF TABLES	i
	LIST OF FIGURES	iii
	LIST OF PLATES	vi
	SYMBOLS AND ABBREVIATIONS	vii
I	INTRODUCTION	1
II	REVIEW OF LITERATURE	5
III	MATERIALS AND METHODS	28
IV	RESULTS AND DISCUSSION	65
V	SUMMARY AND CONCLUSIONS	116
	REFERENCES	121
	APPENDICES	129
	ABSTRACT	

LIST OF TABLES

Table No.	Title	Page No.
3.1	Details of data used, its source and utility	38
3.2	Details of wells selected for the study	39
3.3	Overall modelling strategies used for prediction of groundwater level	59
3.4	Drought intensity categories by Bloomfield and Marchant (2013)	63
3.5	Projected bias corrected data of 2023 from CMIP6 climate model for SSP 245 scenario	65
4.1	Mean monthly groundwater level w.r.t MSL (m) during 2007-2021	71
4.2	Annual mean groundwater level w.r.t MSL (m)	72
4.3	Monthly standard deviation of groundwater level (m)	73
4.4	Monthly CV (%) of groundwater level	74
4.5	Skewness values of groundwater level	75
4.6	Kurtosis values of groundwater level	76
4.7	Mann-Kendall trend analysis of pre-monsoon groundwater level	77
4.8	Mann-Kendall trend analysis of post-monsoon groundwater level	78
4.9	Mann-Kendall trend analysis of annual groundwater level	79
4.10	The developed ANN configuration and its structure for groundwater level prediction	84

4.11	Performance indicators of ANN models developed for different wells	86
4.12	Estimated SGI values of well 160 PKD-12	96
4.13	Estimated SGI values of well PKD S-3	97
4.14	Estimated SGI values of well PKD S-4	98
4.15	Estimated SGI values of well 128	98
4.16	Estimated SGI values of well 129	99
4.17	Estimated SGI values of well 160 PKD-8	100
4.18	Estimated SGI values of well 133	101
4.19	Estimated SGI values of well 140	101
4.20	Estimated SGI values of well 142	102
4.21	Estimated SGI values of well PKD S-15	103
4.22	Estimated SGI values of well 139	103
4.23	Estimated SGI values of well PKD S-7	104

LIST OF FIGURES

Figure No.	Title	Page No.
3.1	Location map of the study area	31
3.2	Map showing groundwater exploitation status of the study area	32
3.3	Location Map of wells selected in the study area	33
3.4	Google earth imagery of study area with well location	34
3.5	Classified Digital Elevation Model of the study area	34
3.6	Log-sigmoid activation function (log-sig)	50
3.7	Hyperbolic tangent activation function (Tansig)	50
3.8	Purelin transfer function (purelin)	51
3.9	Single layer perceptron	54
3.10	Multi-layer perceptron (MLP)	54
3.11	General Procedure for Development of ANN models	56
3.12	Working environment of MATLAB software	60
3.13	Neural network toolbox in MATLAB (nntool)	61
3.14	New network creation window in MATLAB	61

3.15	Model of a neural network in MATLAB	62
3.16	Workflow of groundwater level modelling and drought assessment	64
3.17	nftool window showing MATLAB Matrix-Only function	65
3.18	MATLAB Code generated for GWL prediction	66
4.1	Skewness of groundwater level	69
4.2	Kurtosis of groundwater level	70
4.3	Spatial distribution of groundwater level trend in the study area	80
4.4	Water table contour map of the study area	81
4.5	Average annual seasonal fluctuation of groundwater level	83
4.6	Regression plot of different ANN models for training and testing dataset	87
4.7	Observed vs ANN predicted groundwater level of different wells	92
4.8	Variation of SGI in the pre-monsoon months	105
4.9	SGI values estimated by ANN model and observed groundwater level data of well 160 PKD-12 of Kuzhalmannam block	109
4.10	SGI values estimated by ANN model and observed groundwater level data of well 160 PKD-8 of Palakkad block	110
4.11	SGI values estimated by ANN model and observed groundwater level data of well 140 of Malampuzha block	110
4.12	SGI values estimated by ANN model and observed groundwater level data of well 139 of Chittur block	110

4.13	Spatial distribution of SGI during April 2013	111
4.14	Spatial distribution of SGI during May 2013	111
4.15	Spatial distribution of SGI during April 2016	112
4.16	Spatial distribution of SGI during May 2016	112
4.17	Spatial distribution of SGI during April 2017	113
4.18	Spatial distribution of SGI during May 2017	113
4.19	Monthly predicted groundwater level (bgl) of well 142	113
4.20	Monthly forecasted SGI values of well 142 for the year 2023	114
4.21	Monthly predicted groundwater level (bgl) of well 160 PKD-12	115
4.22	Monthly forecasted SGI values of well 160 PKD-12 for the year 2023	115

LIST OF PLATES

Plate No.	Title	Page No.
3.1	Drought scene- Malampuzha reservoir area, Palakkad	35
3.2	Drought scene- Kalpathypuzha during summer months	35
3.3	Drought scene- Dried up Chitturpuzha	36
3.4	Drinking water scenario in Vadakarapathi GP, Palakkad during 2017	36

SYMBOLS AND ABBREVIATIONS

%	: Percentage
=	: Equal to
°	: Degree
°C	: Degree Celsius
ANFIS	: Adaptive Neuro-Fuzzy Interference System
ANN	: Artificial Neural Networks
ARIMA	: Autoregressive Integrated Moving Average
bgl	: below ground level
CFN	: Cascade Forward Network
CGWB	: Central Groundwater Board
CLSM	: Catchment Land Surface Model
CMIP6	: Coupled Model Intercomparison Project Phase 6
COE	: Coefficient of Efficiency
CRD	: Cumulative rainfall departure
CV	: Coefficient of Variation
DGWL	: depth to groundwater level
DITI	: Directed Information Transfer Index
DTW	: depth to water table
ELM	: Extreme Learning Machine
EP	: evaporation
ESRI	: Environmental Systems Research Institute
<i>et al.</i>	: and others
EVP	: potential evapotranspiration

FFANN	: Feed Forward Artificial Neural Network
FFBPNN	: feed-forward back-propagation neural network
FFN-LM Network	: Levenberg-Marquardt Feed Forward Neural
FFNN	: Forward Neural Network
GA	: Genetic Algorithms
GDI	: Groundwater Drought Index
GDM	: Departure with momentum
GEC	: Ground Water resource Estimation Committee
GGDI	: GRACE Groundwater Drought Index
GIS	: Geographic Information System
GLDAS	: Global Land Data Assimilation System
GP	: Gaussian Process
GPR	: Gaussian Process Regression
GRACE	: Gravity Recovery and Climate Experiment
GSM	: grey self-memory model
GT	: Gamma and M-tests
GWI	: Groundwater Drought Index
GWL	: Groundwater Level
GWS	: Groundwater Storage
GWSA-DSI	: Drought Severity Index of Groundwater Storage Anomalies.
H	: humidity
i.e.	: that is
IBIS	: Indus Basin Irrigation System

IDW	: Inverse Distance Weighted
IMD	: Indian Meteorological Department
ISA	: Interior Search Algorithms
ITA	: Innovative Trend Analysis
km/hr	: kilometer per hour
KNN-RF	: K-Nearest Neighbours Random Forest
KZN	: KwaZulu-Natal
LM	: Levenberg-Marquardt
LM	: The Levenberg-Marquardt
Log-sig	: Log-Sigmoid activation function
LSSVM	: Least-Squares Support Vector Machine
LSTM	: Long Short-Term Memory
m	: Meter
m/year	: Meter per year
M5Tree	: M5 Model Tree
MAE	: Mean Absolute Error
MATLAB	: Matrix Laboratory
M-K	: Mann-Kendall test
MLP	: Multi-Layer Perceptron
mm	: millimeter
mm/year	: Millimeter per year
MODFLOW groundwater flow model	: Modular three-dimensional finite difference
MSE	: Mean Square Error
MSL	: Mean Sea Level

NARX inputs	: Non-linear autoregressive model with exogenous inputs
NCP	: North China Plain
nftool	: Neural Fitting Tool
NIDIS	: National Integrated Drought Information System
nntool	: Neural Network Tool
NSE	: Nash-Sutcliffe efficiency
P	: precipitation
PDSI	: Palmer Drought Severity Index
PHSs	: Permanent Hydrograph Stations
PR	: Pearson coefficient
PSO-SVM Optimization	: Support Vector Machine with Particle Swarm Optimization
Purelin	: Purelin Transfer function
R	: Correlation coefficient
R	: Pearson correlation
R^2	: Coefficient of Determination
RBF	: Radial Basis Function
RBF-NN	: Radial Basis Function-Neural Network
RBF-SVM	: Radial Basis Function-Support Vector Machine
RF	: Random Forest
RMSE	: Root Mean Squared Error
RP	: Resilient back Propagation
SCG	: Scaled Conjugate Gradient
SGI	: Standardized Groundwater Level Index
SGI	: Standardized Groundwater Level Index

SOM	: Self-Organising Maps
SPEI Index	: Standardized Precipitation-Evapotranspiration
SPI	: Standardised Precipitation Index
SSP	: Shared Socio-economic Pathways
SVM	: Support Vector Machine
SVR	: Support Vector Regression
T	: temperature
Tansig	: Hyperbolic tangent activation function
Tmean	: mean temperature
TRMM	: Tropical Rainfall Measuring Mission
TWS	: Terrestrial Water Storage
UK	: United Kingdom
USA	: United States of America
viz	: namely
VLSI	: very large-scale integrated circuit
w.r.t	: with respect to
W3	: World-Wide Water
WA-ANN	: Wavelet ANN
WT-FFNN	: wavelet hybrid neural network
XG-Boost	: Extreme Gradient Boosting
XRB	: Xijiang River Basin
YRC	: Yellow River catchments
YZRC	: Yangtze River catchments
Z	: test statistics

INTRODUCTION

CHAPTER-I

INTRODUCTION

Water is the most essential natural resource which supports life on the globe and it is one of the principal elements which influences the economical, industrial and agricultural growth of human beings. Ever increasing demands of water for irrigation, domestic, industrial and livestock sectors have created water scarcity worldwide. Groundwater is the only reliable source of water, which is becoming scarce in almost all parts of hard rock terrain of the country. There are many reasons for this condition such as over exploitation of groundwater, decrease in infiltration rate, deforestation etc. The significance of water can be seen in all sectors as the demand and needs are growing exponentially. Groundwater represents the terrestrial subsurface component of the hydrologic cycle. Since groundwater is generally in motion, it moves from higher-elevation recharge locations to lower-elevation discharge areas. Groundwater is estimated to make up around 30% of the world's fresh water, followed by surface water (0.3%), atmospheric water (0.04%), and ice (70%) (GEC, 2015).

Groundwater is very important for India's agriculture and drinking water security in urban and rural areas. The 90% of domestic use in rural areas is relied on groundwater whereas 70% of the water used in agriculture is drawn from aquifers. Groundwater accounts for 50% of urban water usage. In the case of the industrial sector, unregulated groundwater may result in serious inter-sectoral disputes. Therefore, India's ability to manage groundwater resources, particularly the aquifer in various parts of the country, is crucial to the growth of both agriculture and industry. There is currently a serious groundwater crisis in India as a result of excessive groundwater extraction and contamination, which affects nearly 60% of the country's districts and poses a threat to the population's access to safe drinking water (GEC, 2015).

Drought is an extreme natural hazard caused by a temporary shortage of water availability that lasts for a long time. Drought has been divided into meteorological, hydrological, agricultural, and socioeconomic droughts based on

the availability of water in various water resource sectors (American Meteorological Society, 2004). The groundwater drought is a hydrological drought category that deals specifically with the characteristics of groundwater resources and can be assessed using groundwater recharge, discharge, levels, and volume. Lack of groundwater recharge or a lack of groundwater expressed in terms of storages or groundwater heads in a specific area and over a specific period of time are two definitions of groundwater drought (Lanen and Peters, 2000). A groundwater drought begins with a decline in recharge brought on by a lack of rainfall, which causes the water table to sink and exhausts all available groundwater reserves. The groundwater drought is, however, made worse by excessive pumping (Mishra and Singh, 2010 and Gleeson *et al.* 2012)

Groundwater level is an indication of groundwater flow, availability of groundwater and aquifer's or groundwater system's physical properties. Any event that causes an aquifer's pressure to change will cause the groundwater level to alter. The quantity of storage, the amount of discharge and recharge, the variance of stream stages, and evaporation all can affect the groundwater level. Hence, understanding the groundwater level variability and trend is crucial for water resource planning in a region.

The method for trend evaluation of groundwater level is an efficient tool for groundwater conservation measures. Time-series analysis is used in groundwater trend assessment and to provide a greater knowledge of long-term changes in groundwater levels. It can assist in figuring out whether an aquifer's groundwater storage is steady, increasing, or decreasing. Several researchers have evaluated how groundwater levels have changed over time using trend analysis approaches (Patle *et al.*, 2015).

Natural and human activities both have an impact on groundwater systems; therefore, targeted and ongoing management is required to keep these conditions within acceptable bounds while achieving the desired economic and social advantages. Groundwater management and policy decisions must be based on knowledge of the past and present behaviour of the groundwater system, the

probable response to changes in the future, and the degree of uncertainty in those responses. Groundwater modelling is an effective technique for managing water resources, protecting groundwater, and remediation. Before starting a project or carrying out a remediation, decision-makers utilise models to forecast how a groundwater system would behave. Any computational technique that represents an approximation of an underground water system is referred to as a groundwater model. Although groundwater models are by definition a simplification of a more complicated reality, they have shown to be effective tools for addressing a variety of groundwater issues and assisting the decision-making process throughout the course of several decades. Population growth and industrialisation have raised the demand for water supplies. Furthermore, groundwater recharge is being impacted by the shift in land use pattern caused by urban development. Hence, accurate groundwater forecasting has become essential for effective groundwater resource development.

For forecasting groundwater table depth, numerous models have been created and used till date. These models can be divided into two categories: physical descriptive models and empirical time series models. The empirical time series models have been frequently employed for water table depth modelling. The main drawback of empirical approaches is that they are inadequate for forecasting when the hydrological system's dynamical behaviour changes over time (Bierkens, 1998). The relationships between precipitation, canal releases, and groundwater level in an aquifer's water table are probably not linear but rather nonlinear, and the models that try to approximate these relationships in linear form fail to accurately capture these relationships. Very few truly non-linear empirical models, such as stochastic differential equation and threshold autoregressive self-extracting open-loop models, have been reported for shallow water table modelling due to the challenges associated with identifying non-linear model structure and parameter estimation (Bierkens, 1998). Artificial neural networks (ANNs) have been employed in many branches of science and engineering recently for forecasting. ANNs have been proven to be effective in modelling virtually any nonlinear function to an arbitrary degree of accuracy. The key benefit of this approach over conventional methods is

that it does not require the explicit mathematical formulation of the complicated nature of the underlying process under investigation. This makes ANN an appealing technique for simulating changes in the water table.

ANN is a mathematical model that simulates functioning of a nerve cell. Without knowing how the input and output are physically connected, ANN may recognise the relationship between them. The best architecture of an ANN model is one that retains a simple and compact structure while producing the least amount of error possible based on performance indicators (Tawfik *et al.*, 1997). The critical component of a good ANN architecture is the number of hidden layers and the number of neurons in each hidden layer. ANN models produce approximate and near solution to such non-linear phenomenon.

Once the groundwater level is modelled, it is easy to assess the groundwater drought condition of a region. Drought indices are true communication tools to quantify the drought severity, magnitude, duration, frequency and spatial extent. Standardized Groundwater Level Index (SGI), is a new drought index developed by (Bloomfield *et al.*, 2013). The SGI proves that the occurrence of drought events is reflected in changes in the groundwater level (NIDIS, 2021).

Kalpathypuzha, sub-basin of Bharathapuzha coming under Palakkad district of Kerala is a severe drought prone area. The area contains over-exploited, critical and semi critical classes of groundwater exploited areas of the district. Ground water development in some parts of the area has reached to a critical stage resulting in decline of ground water levels, thus there is need to adopt an integrated approach of development of ground water resources. In view of the above facts a study was taken up in Kalpathypuzha with the following specific objectives:

1. To analyze the groundwater level variability and trend during 2007-2021 period.
2. To develop an ANN model for groundwater level prediction.
3. To generate spatio-temporal groundwater drought map of the basin.

REVIEW OF LITERATURE

CHAPTER-II

REVIEW OF LITERATURE

Groundwater is among the most precious and significant sources of water worldwide and is essential to various facets of human existence, including agriculture, the growth of industry, and the provision of drinking water (Qadir *et al.*, 2007). Understanding the effects of both natural and human-made factors on groundwater reserves (and exploitation) is crucial for developing appropriate management strategies to deal with unsustainable use (Tillman and Leake, 2010). The availability and accessibility of groundwater can be measured directly and easily using the groundwater level (Tao *et al.*, 2020). The understanding of groundwater level variability and trend is crucial for water resource planning in a region. Groundwater level fluctuation is a non-linear phenomenon. Artificial Neural Networks (ANN) proves to be one of the best tools for modelling non-linear relationship between input and output datasets in hydrology (Dawson and Wilby, 1999). Once the groundwater level is modelled, it is easy to assess the groundwater drought condition of a region. Drought indices are trusted tools for communicating the extent, magnitude, frequency, and severity of droughts. The Standardized Groundwater Level Index (SGI) demonstrates how alterations in groundwater levels correlate with the instances of drought events (NIDIS, 2021). This chapter briefly summarises the previous research works conducted with respect to variability and trend of groundwater level, prediction of groundwater level using physical, empirical and machine learning techniques and groundwater drought assessment using various indices. The details are reviewed under the following sub heads:

1. Variability and trend analysis of groundwater level
2. Groundwater level prediction using physical and empirical models
3. Groundwater level prediction using machine learning models
 - i. Application of ANN models
 - ii. Fuzzy logic and neuro-fuzzy model's applications

- iii. Kernel model's applications
 - iv. Hybrid model's applications
4. Groundwater drought assessment using various indices

2.1 VARIABILITY AND TREND ANALYSIS OF GROUNDWATER LEVEL

Shamsudheen et al. (2009) used a nonparametric seasonal-trend decomposition approach (STL) to observations obtained from 1985 to 2005 in Bangladesh to resolve trend and seasonal components in weekly groundwater levels in the Ganges-Brahmaputra-Meghna (GBM) Delta. Although seasonal variation in groundwater levels predominates, declining groundwater levels (>1 m/yr) have been observed in urban and peri-urban areas near Dhaka as well as in the north-central, north-western, and south-western regions of the nation (0.1-0.5 m/yr), where intensive groundwater abstraction is being done for dry-season rice cultivation. In the estuarine and southern coastal zones, groundwater levels are rising (0.5–2.5 cm/yr).

By using the non-parametric Mann-Kendall trend test and Sen's slope estimator, Bui et al. (2012) identified trends in groundwater level (1995–2009) in 57 wells in the Holocene unconfined aquifer and 63 wells in the Pleistocene confined aquifer. 17 time series (such as yearly, seasonal, and monthly) generated from the original data were examined at each well. According to an analysis of the yearly groundwater-level averages, 35% of the wells in the unconfined aquifer had tendencies towards decline, while 21% had trends towards increase. Contrarily, groundwater levels in constrained aquifers showed decreasing trends practically everywhere. Strongly falling trends (>0.3 m/year) were mostly identified in metropolitan areas around Hanoi, where groundwater is actively being extracted, according to spatial distributions of trends.

In order to estimate the pre- and post-monsoon water levels in the Haryana district of Karnal, Patle *et al.* (2015) used the Mann-Kendall test and Sen's slope estimator to identify patterns in pre- and post-monsoon groundwater levels. The findings revealed that the groundwater levels had decreased drastically between

1974 and 2010. The average rates of water level fall during the pre- and post-monsoon seasons were 0.228 and 0.267 m/year, respectively.

Gibrilla *et al.* (2017) employed non-parametric tools such the Mann-Kendall test, Sen's slope estimator, and ARIMA models to analyse trends in rainfall, temperature, and groundwater levels in the Upper East Region of Ghana during the period from 2005 to 2014. The average depth of groundwater (below the surface of the ground) in Gowrie, Bawku, and Kabingo varied between 1.24 and 5.46 m, which was a smaller variation than Datoku and Bongo. Every well in the research area except Kabingo, showed rising seasonal trends according to both the Mann-Kendall and Sen's slope estimators. The Kabingo well displayed a seasonal decline of 0.312-0.097 m/year. Yet, none of the monitoring wells observed any appreciable upward or downward trends in groundwater levels on an annual basis.

Kumar *et al.* (2018) applied non-parametric techniques to assess the trends in groundwater level. Modified Mann-Kendall and Sen's slope estimator at significance level of 5% were used for the groundwater level during the period from 1998 to 2012 at 13 sites in the Uttar Pradesh, India, districts of Hardoi, Laxmipur, Lucknow, and Sitapur. The trend in groundwater levels revealed negative values for 7 places spanning 54% of the area, and positive values at six sites covering 46% of the area in the pre-monsoon season. However, in the post-monsoon period, 9 sites spanning 69 percent of the area demonstrated positive patterns, whereas 4 locations covering 31% of the area displayed negative trends. Recharge by rainfall in the post-monsoon season might be responsible for the variation in water level trends between the two distinct seasons.

Ndlovu and Demlie (2018) reported the findings of analysis of groundwater level variations and their association with rainfall in South Africa's KwaZulu-Natal (KZN) Province. 15 rainfall stations and 32 groundwater level monitoring locations dispersed throughout the region were employed for the study. The Mann-Kendall test was employed at a 10% significance level to investigate whether there were any trends in the groundwater level and rainfall data. Sen's slope estimator was used to assess the trend's slope. To better understand the cause-and-effect relationship

between rainfall and changes in groundwater level, cumulative rainfall departure (CRD) was determined at each individual rainfall station influencing the groundwater monitoring site. The findings indicated a varying, but generally decreasing trend.

Pathak and Dodamani (2019) examined groundwater level trends and evaluated regional groundwater drought characteristics in India's drought-prone Ghataprabha river basin. Groundwater level fluctuations during the monsoon (June to September), post-monsoon (October to December), winter (January to February), pre-monsoon (March to May), and annually (January to December) have been evaluated using the nonparametric Mann-Kendall test at a significance threshold of $\alpha = 0.05$. A significant decreasing trends were seen in more than 61% of wells with an average loss of 0.21 m during the course of all seasons. This could be attributable to either declining precipitation or intensive exploitation of groundwater, or even both.

Kumar and Rathnam (2019) investigated the monthly, yearly, and seasonal groundwater fluctuation patterns of the forty observation wells were used in the Warangal district (2000–2015) for four non-parametric Mann-Kendall approach variations. With the help of the Sen's slope estimator, trend magnitudes were calculated. According to the findings, three observation wells on a monthly time series showed substantial positive trends (positive Z-statistics), while other wells among forty showed significant negative trends. The monthly, seasonal, and annual median trend slopes for groundwater levels were all negative. A decreasing trend in the seasonal trend slope was seen in pre-monsoon season. The annual variation in trend slope ranged between -0.4 and +0.4 millimetres per year.

Halder *et al.* (2020) investigated groundwater degradation to examine the seasonal trend in their groundwater levels using Mann-Kendall test statistics between 1996 and 2018. For that twenty wells from a river basin in West Bengal was chosen. It was found that 60 percent of wells showed a drop in water level, especially in the post-monsoon season. According to a socio-economic survey, these wells were mostly situated close to agricultural land where there was

substantial groundwater extraction using submersible pumping wells. The amount of recharge following monsoonal precipitation is indicated by the groundwater level increase in post-monsoon period.

Nygren *et al.* (2021) studied the association between groundwater storage and hydro climate in Sweden and Finland, an area with a temperate and cold climate. Two regional and one global reanalysis datasets were used in the study to examine annual, frost-free season and frost season temperature and precipitation changes in the climate regions. groundwater level trends for the same time period between 1980 and 2010 were compared to the trends in effective precipitation and rainy-day frequency. Sen's slope and the Mann-Kendall test were used to calculate trends. groundwater levels in southern Finland and south-eastern Sweden were dropping significantly, while groundwater levels in south-western Sweden were substantially rising. According to the findings, trends in the frost season have no relation on annual groundwater level trends in southern Finland and are only related to rainy day frequency and effective precipitation patterns during that season. Groundwater level trends in southern Sweden seem to be correlated with yearly and frost-free season trends in effective precipitation.

Noori and Singh (2021) applied the nonparametric Mann-Kendall test at a significance level of 0.05 to evaluate seasonal spring (Mar to May), summer (June to Aug), fall (Sept to Nov), winter (Dec to Feb), and annual trends of groundwater-table for all observation points, which is a part of the Kabul basin of Afghanistan. Before integrating the seasonal and annual groundwater level data in the Mann-Kendall trend-test, an autocorrelation test was performed. The annual and seasonal groundwater level revealed significant trend. Only six of the sixty-six observational wells with annual groundwater levels exhibit increasing trends, the remaining sixty wells show falling trends, frequently with considerable trends.

Gautam *et al.* (2021) conducted statistical analysis and geospatial technology to investigate the trend in groundwater level in the Jakham River basin of southern Rajasthan. The Mann-Kendall statistical test was used for the water level trend analysis in 75 wells. According to trend analysis statistics, a relatively

small percentage of wells show a fall in water level during the post-monsoon season, while 15% of wells experienced it during the pre-monsoon. Pre-monsoon water level reduction averaged 0.245 m/a, and post-monsoon water level decline averaged 0.05 m/a. The potential to recharge the aquifer was also declining annually.

Fu *et al.* (2022) used three trend analysis methods to figure out the annual mean, minimum, and maximum depth to water table (DTW) trends in 910 bores over the long term (1971–2021). This study was conducted in eight major alluvial systems of Australia's Murray-Darling Basin (MDB), which concentrated nearly 75 percent of groundwater use. The findings demonstrated (a) an overall increasing trend in DTW across alluvial aquifers, which could be attributed to changes in groundwater extraction and recharging from rainfall; (b) similar statistical significances and magnitudes were shown by the analysis methods employed; (c) Annual maximum DTW had a bigger trend magnitude than mean DTW, while annual lowest DTW had a smaller trend magnitude; (d) Groundwater patterns were consistent with trends in the quantity of production bores, potential evaporation, and yearly rainfall; (e) Irrigation was partially responsible for the downward trend in groundwater level.

Swain *et al.* (2022) presented the trend in groundwater levels in three districts of India's Jharkhand State viz, Purbi Singhbhum, Ranchi, and Saraikela. The depth to groundwater level (DGWL) data from twenty four wells in the three districts from 1996 to 2018 for the pre and post-monsoon seasons were gathered. In this investigation, Innovative Trend Analysis (ITA) was used to examine groundwater level trends. The findings showed a considerably rising trend in DGWL for 14 sites during the post-monsoon season and 17 sites during the pre-monsoon season. The growing DGWL patterns in majority of the locations indicated a significant fall in groundwater levels over time.

2.2 GROUNDWATER LEVEL PREDICTION USING PHYSICAL AND EMPIRICAL MODELS

Chen *et al.* (2002) based on a water budget model and a groundwater flow model, developed an empirical model that links climatic variables to groundwater level. An incomplete data set comprising historical records of water levels from more than 80 wells in a monitoring network for the carbonate rock aquifer in southern Manitoba, Canada, was utilised to evaluate the empirical model. The results of the tests revealed that for the most part, the predicted and observed groundwater levels were very similar. In general, there was a 0.92 average correlation coefficient between the projected and observed water levels. A climate change impact assessment could employ the proposed empirical statistical model to predict changes in groundwater level in response to various climate scenarios.

39 piezometric wells monitored over a 12-year period by Ahmadi et al. (2007) underwent geographical and temporal investigation of monthly groundwater level changes. Many scholars have employed geostatistics, which has been presented as a management and decision-making tool, to expose the geographical and temporal structure of groundwater level variation. The findings demonstrated that extremely weak nugget impacts caused groundwater level variations to have a substantial geographical and temporal pattern. Groundwater level fluctuations have a temporal pattern, according to a temporal analysis that also revealed a significant structure of groundwater level decline across the research region. Groundwater level decline and groundwater level fluctuations were understated by 3% and 6% for geographical and temporal analysis, respectively, according to results of ordinary and universal krigings.

In the dry and semi-arid regions of western Jilin province of China, Yang et al. (2009) employed Integrated Time Series (ITS) and Back-Propagation Artificial Neural Network (BPANN) models to empirically estimate groundwater level. On the basis of Root Mean Squared Error (RMSE), Mean Absolute Error (MAE), and coefficient of efficiency (CE), the modelling procedure and accuracy of these two

methodologies were investigated. The simulation results showed that the CE is 0.98 and 0.97, respectively, and that both ITS and BPANN are accurate in replicating (fitting) the groundwater levels. The BPANN model outperformed the ITS in forecasting the time series for groundwater levels, according to a comparison of the prediction accuracy of the two models during the validation phase..

Mohanty *et al.* (2012) assessed the effectiveness of the finite difference-based numerical model MODFLOW and ANN model in simulating groundwater levels in the Kathajodi-Surua Inter-basin of Odisha. The MODFLOW was calibrated using weekly groundwater level data for two years and four months (February 2004 to May 2006), and the model was validated using data for one year (June 2006 to May 2007). The model was calibrated using a combination of the automated calibration technique and the trial-and-error method, with a mean RMSE (root mean squared error) value of 0.62 m and a mean NSE (Nash-Sutcliffe efficiency) value of 0.915. For the validation period, groundwater levels at 18 monitoring wells were simulated. In addition, ANN models for 18 observation wells in the basin were created to forecast groundwater levels one-time step (or week) ahead. The input variables to the ANN model were weekly rainfall, evaporation, river stage, water level in the drain, tube well pumping rate, and groundwater levels in these wells at the previous time step. The observed groundwater levels and the predicted groundwater levels produced by the MODFLOW and ANN models were compared. The ANN model outperformed the numerical model in predicting groundwater levels in the research area for forecasts with short time horizons.

Devarajan and Sindhu (2015) compared the effectiveness of the MODFLOW-based numerical model and the Radial basis Function Neural Network (RBFNN) machine learning model for predicting groundwater levels in the Trivandrum district's Athiyannoor Block Panchayath, which is designated as a semi-critical zone due to the rapid drop in groundwater level. Weekly groundwater level data from January 2014 to December 2014 were used to create the groundwater flow model. The groundwater levels at ten observation wells were simulated to calibrate the model using the trial-and-error method. The groundwater

levels were forecasted and validated using the simulated model between January 2015 and March 2015. The inputs to the RBFNN model were weekly groundwater recharge, evapotranspiration, the rate at which the pumping wells are being pumped, and the groundwater levels in these wells at the previous time step. The trained RBFNN model was then validated. During the validation period, the predicted groundwater levels by the numerical model and RBFNN models were compared with the actual groundwater levels. The performance characteristics of both models showed that the RBFNN model performed better for forecasting weekly groundwater levels than a numerical model utilising MODFLOW.

A comparison study between a physical model and a phenomenological model was undertaken by Wei *et al.* (2020) in order to determine which approach would be more effective for predicting groundwater levels in relation to deep-seated landslides. The physical model was a finite-element seepage code named Slide by Rocscience. A Support Vector Machine with Particle Swarm Optimization (PSO-SVM) served as the phenomenological model. The physical seepage model's input parameters were calibrated using trial and error method to compare the computed results with real monitoring data in order to acquire more accurate calculated results from the physical seepage model. To get more precise calculated results, the phenomenological model's input data were additionally processed. The outcomes demonstrated that the physical seepage model performed poorly because it was hard to calibrate correctly under the conditions of limited data. The phenomenological model outperformed the other models, according to the validation results. The RMSE and MAE of physical seepage model were 0.92 m and 0.81 m, and that of the phenomenological models were 0.052 m and 0.043 m, respectively.

Yin *et al.* (2021) used the Australian state of Victoria as a case study to compare and contrast how well machine learning and physical models predicted groundwater dynamics. Groundwater levels were predicted using two traditional machine learning models (Random Forest (RF) and A NN) plus a deep learning model (Long Short-Term Memory, LSTM). The groundwater level estimations were compared with the in-situ groundwater level observations from ground

networks and the simulated groundwater storage from two different physical models, World-Wide Water (W3) and Catchment Land Surface Model with GRACE data assimilation (CLSM-DA). The evaluation demonstrated that LSTM greatly outperformed machine learning models in terms of accuracy, with increases in Pearson coefficient (PR) values of 23.89% (compared to ANN) and 41.32% (compared to RF) respectively during the prediction period. Since the CLSM-DA groundwater levels products outperformed the W3 model in terms of accuracy, this proved the value of incorporating GRACE data into land surface models. Also, the results indicated that in plain terrain, the LSTM model had higher accuracy.

The main drawback of empirical and physical models is that they are insufficient for forecasting when the hydrological system's dynamical behaviour changes over time (Bierkens, 1998). The relationships between precipitation, canal releases, and groundwater level in an aquifer's water table are probably not linear but rather nonlinear, and models that try to approximate these relationships in linear form fall short of accurately capturing these relationships. Few really non-linear empirical models, such as threshold autoregressive self-extracting open-loop models and stochastic differential equations, have been described for shallow water table modelling due to the difficulties in detecting non-linear model structure and parameter estimation (Bierkens, 1998). In recent years, machine learning techniques have been used for forecasting in many areas of science and engineering. ANNs have been proven to be effective in modelling successfully any nonlinear function to an arbitrary level of accuracy.

2.3 GROUNDWATER LEVEL PREDICTION USING MACHINE LEARNING MODELS

2.3.1 Application of ANN models

Daliakopoulos *et al.* (2004) examined the performance of different neural networks in groundwater level forecasting in Messara Valley in Crete (Greece), where groundwater resources had been overexploited during the previous fifteen years and the groundwater level had been steadily declining, in order to identify an

optimal ANN architecture that could simulate the decreasing trend of the groundwater level and provide acceptable predictions up to 18 months ahead. A typical feedforward neural network trained with the Levenberg-Marquardt algorithm yields the best results for up to 18 months of forecasts when seven different types of network designs and training techniques are examined and compared.

Nayak *et al.* (2006) investigated the use of ANN for groundwater level forecasting in shallow aquifers in India. The water levels of two observation wells had been predicted, up to six months ahead using various ANN models. The outcomes demonstrated that ANNs were an effective technique for predicting monthly groundwater levels. For one month ahead prediction of groundwater levels, the performance assessment parameters (RMSE, coefficient of correlation) were found to be reliable and consistent. The forecast error was also within a reasonable range. Even though good results were obtained for Munganda observation well for forecasts up to 4 months in advance, the model performance for Cheyyeru observation well was observed to degrade after a 2-month lead forecast.

Jothiprakash and Suhasini (2008) developed an artificial neural network model (ANN) to predict the groundwater level fluctuation in an observation well in Sri Ram Reservoir Project, Andhra Pradesh, India. The ANN model, configured with back propagated algorithm, single hidden layer, and tanh activation function. The ANN models were assessed on the basis of statistical performance criteria namely, mean square error, root mean square error and correlation coefficient. The result showed that the best correlation coefficient obtained was 0.76, while on the basis of other two performance indicators, the model results were promising. The study revealed that ANN model could be used to predict the groundwater level fluctuations within reasonable accuracy.

Sreekanth *et al.* (2009) conducted research on the use of ANNs for groundwater level forecasting. The effectiveness and accuracy of the model were evaluated based on root means square error and regression coefficient. The root

means square error and the regression coefficient were 0.93 and 4.50 respectively. It was found that a typical feed forward neural network that had been trained using the Levenberg-Marquardt algorithm was able to make the precise predictions.

Mayilvaganan and Naidu (2011) developed Feed-Forward Network based Artificial Neural Network (ANN) model to predict the groundwater levels in hard rock region. Model was trained using back propagation algorithm with two hidden layer, and log-sig activation function. The models were evaluated using three statistical performance criteria namely, mean average error (MAE), root mean squared error (RMSE) and regression coefficient (R). The most suitable configuration of the ANN structure was found to be 12-20-1 feed forward network trained with the Levenberg–Marquardt function. This configuration showed the most accurate predictions of the decreasing groundwater levels in the study area. It was also concluded that A NN could be used to predict groundwater level in a hard rock region with good accuracy even with limited data.

In dry and semi-arid environments, Mirzavand *et al.* (2014) suggested ANNs to predict groundwater levels (Kashan plain aquifer, Iran). Rainfalls, rivers, spring discharges (as aquifer recharge components) and transitional water resources from other basin, evaporation, and aquifer discharges were taken as input variables, and the output was groundwater levels of Kashan plain aquifer in five clusters of 36 Piezometric wells. Simulated groundwater levels were compared with actual groundwater of all clusters in the study area. The results demonstrated an excellent fit between the calculated and observed data.

Chitsazan *et al.* (2015) investigated the forecasting of groundwater level using ANNs as an alternative for groundwater modelling. Departure with momentum (GDM), Levenberg-Marquardt (LM), resilient back propagation (RP), and scaled conjugate gradient (SCG) were the four different techniques employed for modelling. The input layer was made up of rainfall, evaporation, relative humidity, temperature, irrigation canal discharge, and groundwater recharge from the plain boundary, while the output layer was made up of the future groundwater level. The effectiveness of ANN's prediction was examined using statistical

analysis in terms of Mean-Square-Error (MSE) and correlation coefficient (R). In the current investigation, the FFN-LM algorithm produced the best results across all three hydrogeological groups.

Djurovic *et al.* (2015) compared the performance of Artificial Neural Network (ANN) and Adaptive Neuro-Fuzzy Interference System (ANFIS) for forecasting one month ahead water table at various wells situated at different distance from the Danube River. The performance criteria such as root mean squared error (RMSE), coefficient of determination (R^2), and coefficient of efficiency (COE) were used to compare the performance of two techniques. The result of the study revealed that each of the studied techniques could be considered as useful tool for hydrological process modelling in water resource engineering.

Lohani and Krishan (2015) conducted research on the application of ANNs for groundwater level simulation in Amritsar and Gurdaspur Districts of Punjab, India. Different network designs and training procedures were researched and compared for forecasting the model's efficiency and accuracy. The results demonstrated that accurate forecasting was possible, with the standard feed forward neural network trained with Levenberg-Marquardt algorithm and showed best performance. From the analysis, it was concluded that the accuracy of the ANN model in forecasting groundwater level was inside acceptable limits.

Nair and Sindhu (2016) conducted a study for estimating the groundwater level in the Mamom river basin in the Trivandrum region, India. They developed an ANN model based on hydrological factors for the purpose of estimating the groundwater level in three wells during monsoon and non-monsoon seasons. Only four meteorological variables—rainfall (Raf), potential evapotranspiration (EVP), temperature (T), and humidity (H%)—were used to build the predictive models. The Levenberg-Marquardt (LM) algorithm was used to train a number of ANN model structures in order to select the weight and bias values in the best way possible. The outcomes demonstrated that, in comparison to other methods, an ANN using the LM back-propagation algorithm offered more accurate predictions.

Hong (2017) conducted a study using a feed-forward back-propagation neural network (FFBPNN), that estimated hourly groundwater level with the

intention of achieving two main goals: (1) predicting next hour groundwater level and (2) forecasting the fluctuations and changes in groundwater level between the current and one-lag-ahead groundwater level. The results showed that the suggested model was able to mimic groundwater level changes between lags more accurately than one lag-ahead groundwater level prediction.

Shamsuddin *et al.* (2017) used ANNs to anticipate groundwater levels by combining river recharge and river bank infiltration. Daily rainfall, river stage, water level, stream flow rate, temperature, and groundwater level were taken as input variables to ANN models. To predict the fluctuation of groundwater tables, two different types of ANNs structures were applied, and the best forecasting results were compared. The coefficient correlation (R), mean square error (MSE), root mean square error (RMSE), and coefficient determination (R^2) were the selection criteria for the best model. Two pumping experiments were carried out, and it was discovered that the first test had a better performance criterion and provided an accurate projection of the groundwater level.

Yadav *et al.* (2017) employed the Extreme Learning Machine (ELM) and Support Vector Regression (SVR) models to conduct a study for the prediction of groundwater level in Canada. Both forecasting models were created using inputs from the hydrological and meteorological data. The outcomes demonstrated that ELM outperformed SVR in monthly groundwater level forecasting.

Lee *et al.* (2019) used an (Feed Forward Artificial Neural Network) FFANN model to predict hourly groundwater level at eight wells in South Korea. The study used groundwater abstraction and surface water level as input variables. The suggested model was thought to be effective in capturing the non-linear connection between the targets and predictors because the predicted groundwater level values were quite precise and in line with the actual magnitudes of groundwater level.

In order to determine the monthly groundwater level in four aquifers of the Nebhana watershed, in Tunisia, Africa, Nouri and Derbela (2020) developed an ANN model. To create the forecasting models, only three input parameters viz, rainfall, antecedent groundwater level, and evaporation were used. The ANN model was able to capture the dynamic fluctuations in piezometric values and provided

predictions with a greater degree of accuracy. According to the study, the monthly groundwater level was mostly dependent on the monthly precipitation, evaporation, and antecedent values of groundwater level.

Hasda *et al.* (2020) implemented a non-linear autoregressive model with exogenous inputs (NARX) of ANN in order to simulate groundwater level and predict its weekly level up to 52 weeks in advance at 14 Permanent Hydrograph Stations (PHSs) in the drought-prone Barind Tract in the northwest of Bangladesh. To forecast groundwater level, the weekly historical time series climatological data from 1980 to 2017 were utilised as input variables (rainfall, temperature, humidity, and evaporation). There was a relatively good fit between predicted and observed groundwater level in a selected PHS. Hence, they concluded that this methodology could be simply used for groundwater planning and management aspects in water scarce areas.

2.3.2 Fuzzy logic and neuro-fuzzy model's applications

Emamgholizadeh *et al.* (2014) conducted in-depth research and compared the effectiveness of Adaptive Neuro Fuzzy Inference System (ANFIS) and Feed Forward Neural Network (FFNN) models in simulating groundwater level in various parts of the world. They claimed that when using either only antecedent groundwater level or meteorological data along with antecedent groundwater level as inputs, ANFIS was preferable to the FFNN model for groundwater level prediction.

Khaki *et al.* (2015) modelled the monthly groundwater level measured at the Langat Basin located in the southeast of Malaysia's Selangor state. There were many regressors employed, including prior groundwater level, precipitation, evaporation, relative humidity, maximum temperature, and min temperature. Adaptive Neuro Fuzzy Inference System (ANFIS), Feed Forward Neural Network (FFNN), and the Cascade Forward Network (CFN) were the three models employed. R and MSE were used to analyse their performances. The findings

revealed that among the different models used the ANFIS model had much superior accuracy with $R^2 = 0.94$ and $MSE = 0.005$.

Raghavendra and Deka (2016) suggested the multi-step-ahead forecasting of monthly groundwater level utilising Adaptive Neuro Fuzzy Inference System (ANFIS) and Gaussian Process Regression (GPR) techniques in the river basin near Sullia Taluk, India. The groundwater level measured in the preceding four months was one of four input factors that were used to predict groundwater level, up to six months in advance. The findings demonstrated that the GPR model outperformed the ANFIS model in terms of prediction accuracy. It was also demonstrated that the performances of the two models (i.e., ANFIS and GPR) decreased from one to three months ahead prediction.

Zhang *et al.* (2017) analysed the differences in groundwater level prediction by three AI models: ANFIS, RBFNN, and the grey self-memory model (GSM). All models were used to simulate the groundwater level. It was found that the ANFIS model showed the highest performance metrics (i.e., R^2 , NSE, and RMSE) with good accuracy.

Bak and Bae (2019) used the ANFIS model to predict groundwater level using precipitation (P) and mean temperature (T_{mean}) and reported acceptable results, with RMSE and MAPE of 0.1381 and 37.869%, respectively.

Moravej *et al.* (2020) applied Adaptive Neuro Fuzzy Inference System (ANFIS) and Gaussian Process (GP) models to predict monthly groundwater level from evaporation (EP) and precipitation (P). They also used genetic algorithms (GA), interior search algorithms (ISA), and metaheuristic optimization techniques to enhance the performance of the least-squares support vector machine (LSSVM). According to a comparative performance analysis of the ANFIS, GP, GA-LSSVM, and ISA-LSSVM models the maximum accuracy was attained utilising the ISA-LSSVM algorithm. The investigation also revealed that the addition of P and EP had no impact on the model's performance.

2.3.3 Kernel model's applications

The Radial Basis Function-Neural Network (RBF-NN) and Radial Basis Function-Support Vector Machine (RBF-SVM) models were used by Nie *et al.* (2017) to forecast the monthly groundwater level fluctuation in Jilin, China. The SVM model structure was set up by using the RBF kernel function. The uncertainties resulting from measured input and output variable errors were estimated based on 95% confidence intervals. The study revealed that the RBF-SVM model outperformed the RBF-NN model in terms of accuracy and reliability for predicting the monthly groundwater level fluctuation.

Sattari *et al.* (2017) applied the SVR and M5 Model Tree (M5Tree) models in order to forecast the variance of monthly groundwater level in the Ardebil plain, Iran. The SVR model networks were created with a polynomial kernel function. The prior groundwater level, precipitation volume, and well discharge were the variables of the input combination, with groundwater level being the output variable. The variance of the monthly groundwater level could be accurately predicted by both models. However, the research demonstrated that using the M5Tree model for prediction was simpler and easier than using the SVR model.

Guzman *et al.* (2019) developed the non-linear autoregressive with exogenous inputs-based ANN (NARX-ANN) and RBF-based support vector regression (RBF-SVR) models, in order to evaluate groundwater level in irrigation wells in Mississippi, USA. To find the best SVR model with the smallest training error, three kernel functions—polynomial, radial basis function, and sigmoid—were applied. The RBF kernel function provided the most accurate results out of the three. The entire historical time series was divided into seasons of withdrawal (summer) and recharging (winter). For each season (summer or winter), the RBF-SVR model outperformed the NARX-ANN model in terms of prediction.

2.3.4 Hybrid Machine Learning model's applications

Adamowski and Chan (2011) coupled a hybrid WA-ANN (Wavelet ANN) for groundwater level prediction by employing several hydro-climatology factors. Monthly groundwater level data were collected from the Chateauguay watershed in Quebec, Canada for a period from 2002 to 2009. Based on assessment and comparison, the groundwater level simulation results showed that the hybrid WA-ANN model outperformed ANN and Autoregressive Integrated Moving Average (ARIMA) models.

Nourani and Mousavi (2016) integrated a wavelet hybrid neural network (WT-FFNN) for groundwater level simulation utilising Self-Organising Maps (SOM) clustering approaches at various piezometer places in the Ardabil plain. The output showed that the hybrid WT-FFNN improved the average performance by up to 15.3% above the classic Feed Forward Neural Network (FFNN) and Autoregressive Integrated Moving Average (ARIMA) models.

Chang *et al.* (2016) created a novel hybrid soft-computing approach using Self organising Maps- non-linear autoregressive with exogenous inputs (SOM-NARX) approaches. Monthly regional groundwater level data were collected from 203 sites in Taiwan's Zhuoshui River basin between 2000 and 2013. The outcomes, based on statistical indicators, showed that the hybrid SOM-NARX technique was suitable and reliable for modelling groundwater level. The results also showed that the suggested strategies could offer a healthy approach to manage water resources.

In order to predict the groundwater level using ANN and hybrid PSO-ANN, Balavalikar *et al.* (2018) analysed monthly groundwater level fluctuation data from 2000 to 2013 in Brahmavar, Kundapur, and Hebri in the Udupi district, India. The models were calibrated for this purpose using a variety of input configurations. The performance results showed that PSO-ANN could model groundwater level better than ANN.

Kombo *et al.* (2020) proposed a long-term multistep groundwater level estimation in eastern Rwanda employing climate variable (Temperature,

Precipitation, solar radiation, and groundwater level) using a hybrid K-Nearest Neighbours Random Forest (KNN-RF) technique. The modelling outcomes using NSE, RMSE, MAE, and R^2 demonstrated that the hybrid model provided a solid strategy.

Roshni *et al.* (2020) developed a standard FFNN with a hybrid WANN (Wavelet ANN) model for the purpose of predicting complex groundwater level in an alluvial aquifer in Konan groundwater basin of Japan. Gamma and M-tests (GT) technique was combined with the results and a different evaluation matrix was employed to gauge the model's effectiveness. The calibrated results demonstrated the reliability of GT combined WANN for the estimation of groundwater level.

2.4 GROUNDWATER DROUGHT ASSESSMENT USING VARIOUS INDICES

According to Lanen and Peters (2000), natural groundwater shortages result from reduced recharge over a prolonged period of time, and these shortages are frequently made worse by human activity (e.g. abstractions). Droughts are brought on by low groundwater heads and small groundwater gradients. Low well yields, which have an impact on the public water supply and irrigation methods are the main cause of groundwater droughts (e.g. agricultural droughts).

Shahid and Hazarika (2010) have researched groundwater scarcity and drought in three north western areas of Bangladesh. The Cumulative Deficit technique from a threshold groundwater level was used for the calculation of the severity of groundwater droughts. Monthly groundwater fluctuation data gathered from 85 sites were used. According to the report, groundwater scarcity affects 42% of the region's land every year. According to analysis of groundwater hydrographs and rainfall time-series, groundwater level decline in the area was caused by increasing groundwater withdrawal for irrigation during the dry season and frequent droughts.

To identify groundwater shortages and standardise groundwater level time series, Bloomfield and Marchant (2013) described the Standardized Groundwater Level Index (SGI). The SGI is a modification of the Standardised Precipitation

Index (SPI) that takes into account the differences in the form and characteristics of precipitation and groundwater level time series. The study employed hydrographs of groundwater levels from 14 different locations throughout the UK. It was determined that if the SPI approach was appropriately modified to take into account the form and nature of groundwater level time series, it could be used to groundwater level data to produce a Standardised Groundwater Level Index (SGI). The study also noted that SGI offers a reliable quantification of groundwater drought if strong correlations between SPI and SGI are established and SGI time series are in good agreement with previously independently proven droughts.

Li and Rodell (2015) estimated a Groundwater Drought Index (GWI) derived from monthly groundwater storage output from the Catchment Land Surface Model (CLSM) using a GWI derived similarly from in situ groundwater observations. From eight different parts of the central and north-eastern United States, unconfined or semi-confined aquifers were used to collect groundwater observations. With correlation values ranging from 0.43 to 0.92, the regional average GWI generated from CLSM showed a significant correlation with that derived from observation wells. GWI from both in situ data and CLSM was generally better correlated with the Standard Precipitation Index (SPI) at 12 and 24 month timescales than at shorter timescales, however it varied depending on climate conditions. The correlation between GWI and SPI determined from the CLSM generally declines with increasing depth to the water table, which is dependent on both bedrock depth (a CLSM parameter) and mean annual precipitation.

Thomas *et al.* (2017) used the GRACE Groundwater Drought Index (GGDI) over the Central Valley of California, a regional aquifer that has experienced major drought times throughout the GRACE record and is exposed to extensive human activity. The capacity to identify drought delays specific to groundwater drought is highlighted by relationships between GGDI and other hydrological drought indices. The findings showed that, in contrast to the groundwater storage deviation technique, GRACE-derived groundwater storage anomalies may allow for an assessment of groundwater variations but do not adequately capture groundwater

drought as measured by an in situ-based groundwater drought index (GWI). The increased connection between GGDI and GWI suggested that additional processing of GRACE-derived groundwater storage anomalies is required to identify groundwater drought.

To estimate monthly groundwater drought status from 1960 to 2013, Marchant and Bloomfield (2018) developed an empirical (geo)statistical modelling technique and evaluated it using groundwater level measurements from 948 observation boreholes spread over the Chalk aquifer (UK). To create spatially distributed monthly maps of the Chalk's SGI drought status for 54 years, the modelled groundwater levels were standardised using the Standardized Groundwater Index (SGI), and the monthly SGI values were interpolated across the aquifer. With no prerequisite understanding of catchment or aquifer parameters, the empirical modelling approach allows for the estimation of confidence bounds on the predicted groundwater levels and SGI values. The results of the modelling scheme were illustrated for three major episodes of multi-annual drought (1975–1976; 1988–1992; 2011–2012). The findings supported the earlier published analysis of the groundwater shortages while also offering a systematic, characterization of the events for the first time.

Lee *et al.* (2018) analysed the groundwater drought in the Mangyeong River Basin by analysing precipitation, surface water (river stage and streamflow at four gauging stations), and groundwater (groundwater level at five monitoring stations) data for 11 years (2005 to 2015). Correlations were analysed between surface water, rainfall and groundwater. The threshold and 95% probability occurrence line methods were employed to evaluate groundwater drought using the SPI index, an extensively used meteorological drought index. Results from the SPI index showed that there were severe droughts in 2008–2009 and 2015. The groundwater drought assessment also indicated that weak droughts happened annually and a severe drought was in 2009; however only two monitoring wells (G-4 and G-5) in the upstream region registered a groundwater drought in 2015. This might be because majority of the annual rainfall was concentrated in the rainy season. The usage of

agricultural water for farming in June was responsible for the groundwater level drop below the threshold level.

Seo and lee (2019) evaluated groundwater drought based on comparatively high spatial resolution groundwater storage change data. Global Land Data Assimilation System (GLDAS) models and satellite data from the Gravity Recovery and Climate Experiment (GRACE) and Tropical Rainfall Measuring Mission (TRMM) were used to develop an ANN model. The Standardized Groundwater Level Index (SGI) was developed by normalising groundwater storage variations in South Korea between 2003 and 2015 and that were predicted by ANN. The Standardized Precipitation-Evapotranspiration Index (SPEI) and the Palmer Drought Severity Index (PDSI) were utilised to validate the SGI. According to the findings, the SGI followed a pattern that was comparable to the PDSI, SPEI-1 and SPEI-2.

Rose *et al.* (2020) conducted analysis of the occurrence and persistence of the drought in Kerala's Bharathapuzha river basin. The results revealed that the river basin had seen several drought conditions in both the past and the future. Water availability was measured using the SPEI tool, which took temperature and precipitation into account to look for anomalies in the climatic water balance.

The evolution of groundwater drought has been studied by Wang *et al.* (2022) using a high-resolution GRACE mass concentration (mascon) model perspective. The spatiotemporal changes and gridded trend characteristics of groundwater drought were thoroughly identified throughout China between 2003 and 2018. The GRACE's verification results for evaluating groundwater droughts were credible and reliable. The most severe groundwater drought, with an average groundwater drought index (GDI) value of -0.86, occurred in April 2011, and the gridded drought trend characteristic revealed that the severity of the drought increased from 2003 to 2018.

Noori and Singh (2021) determined groundwater drought index (SGI) values for the 66 observational points of the research area to determine the severity

and spatial distribution of groundwater drought conditions in Kabul city in Afghanistan. According to the SGI report, the majority of wells have been suffering from a severe and continuous drought since 2014. The continuous management of groundwater resources is concerned by the observation of persistent and frequent drought conditions in representative wells from each group. The calculated SGI values in wells 1 and 60, which make up a significant portion of the wells in the city, indicated the severity and extent of groundwater depletion in the area and show that management actions are urgently required to solve the issue.

Han *et al.* (2021) employed the Standardized Precipitation Index (SPI) to describe meteorological drought and the Drought Severity Index of Groundwater Storage Anomalies (GWSA-DSI) to describe groundwater droughts in the Xijiang River Basin (XRB) of China. A probabilistic methodology was presented to find the high-resolution propagation thresholds from meteorological to groundwater drought on 0.25 grid. The propagation time from meteorological to groundwater drought ranged from 8 to 42 months, according to the results, and GWSA-DSI could consistently identify groundwater drought episodes. Despite being in a humid area with plenty of precipitation, the probability of a groundwater drought occurred at the XRB was 43.8%, 54.8%, 61.2%, and 64.2%, during light, moderate, severe, and extreme meteorological drought events respectively.

Thompson *et al.* (2021) carried out a study on the principles for the groundwater drought index in the Chaliyar river basin in Kerala. The applicability of the standard groundwater drought index (GWDI) on the occurrence of groundwater shortage conditions was examined. In the Chaliyar river basin, the development of the drought and its related impact on the groundwater regime were studied. A modified GWDI was proposed based on the typical responses to drought situations in various physiographic zones.

Guo *et al.* (2021) measured groundwater drought using the standardised precipitation index (SPI) using the long-term groundwater level data (1981–2010) gathered from the Climate Response Network wells across the conterminous United States to. As the primary research objects, four monitoring wells in Georgia,

Massachusetts, Oklahoma, and Washington were chosen. The pattern of the lag time between the SGI and SPI in various time scales was then examined in order to calculate the SGI and assess the groundwater drought status when combined with the SPI. Due to the complexity of geographic position, agricultural irrigation, population, and other aspects of the natural environment and human activities, groundwater drought differed greatly in different places. The results showed that beginning and ending times for drought conditions as well as the intensity of both flooding and drought at various time frames in the same location were found to vary. The cross-correlation coefficients increased as the time scales lengthened. Wells in Georgia, Massachusetts, Oklahoma, and Washington had average correlation values between SPI and SGI of -0.568, -0.634, -0.667, and -0.496, respectively.

Zhu and Zhang (2022) identified the spatiotemporal characteristics and evolution trend of the groundwater drought in the Yangtze River catchments (YZRC) and Yellow River catchments (YRC) between 2002 and 2020 by using a GRACE-based groundwater drought index. The study assessed the influence of the influencing factors, and quantitatively identified the main influencing factors. According to the findings, the majority of groundwater droughts in the YZRC occurred between 2002 and 2009 in the middle and lower reaches of the catchments, and most catchments showed a decreasing trend. But most of the catchments in YRC had experienced an increasing trend between 2015 and 2019, and had impact on all the nearby catchments.

Zhao *et al.* (2022) explored propagation dynamics from meteorological droughts to groundwater droughts and their spatial-temporal evolution in order to monitor and evaluate the danger of groundwater droughts. In this work, groundwater droughts in the North China Plain (NCP) were evaluated using the Standardized Precipitation and Evapotranspiration Index (SPEI) and the Gravity Recovery and Climate Experiment (GRACE) Groundwater Drought Index (GDI). The Directed Information Transfer Index (DITI) was used to track the spread of groundwater droughts from meteorological droughts. The results showed that

GRACE data for estimating drought occurrences in the NCP had good dependability. When there was a temporal change, the SPEI1 first dropped and then rose; its lowest point occurred in 2011. The peak year for the GDI was 2008, after which it was first elevated, then declined. But prior to 2011, the SPEI-1's spatial distribution in the NCP's core region dramatically declined. SPEI-1 showed a rising trend for the 2011–2020 period in numerous NCP regions. The centre and western regions of the NCP showed an increasing trend in GDI before 2008, while several areas revealed a falling trend in GDI over the 2008–2020 period.

Ali *et al.* (2022) examined the trend characteristics, temporal evolution, and spatial distribution of GRACE Groundwater Drought Index (GGDI) from 2003 to 2016 in the Indus Basin Irrigation System (IBIS). Four machine learning models (XG-Boost, RF, SVM, ANN) were used to train the datasets of the Gravity Recovery and Climate Experiment (GRACE), Terrestrial Water Storage (TWS), and Groundwater Storage (GWS) data to increase the resolution from 1° to 0.25°. Extreme Gradient Boosting (XG-Boost) model outperformed the other models with performance indications of Pearson correlation (R) as 0.99, Nash Sutcliff Efficiency (NSE) as 0.99, Root Mean Square Error (RMSE) as 5.22 mm, and Mean Absolute Error (MAE) as 2.75 mm. The GRACE Groundwater Drought Index (GGDI) was calculated by normalizing XGBoost-downscaled GWS.

MATERIALS AND METHODS

CHAPTER-III

MATERIALS AND METHODS

This chapter gives a brief description of the study area, its geographic location, climatic condition, geomorphology and hydrogeology. It also explains the various methodologies employed for variability and trend analysis of groundwater level, modelling of groundwater level by Artificial Neural Network and estimation of Standardized Groundwater level Index (SGI) for drought analysis.

3.1 GENERAL DESCRIPTION OF THE STUDY AREA

3.1.1 Study area location

The Kalpathypuzha watershed one of the principal tributaries and the most water stressed regions of the Bharathapuzha River basin was selected for the study. The Kalpathypuzha originates at the higher slopes of the Western Ghats deep inside Palakkad district from the place called Chenthamarakulam in the hills, north of Walayar. Four tributaries, including the Malampuzha River, Walayar River, Korayar River, and Varattar River, come together to make it. Kalpathypuzha is crossed by the Malampuzha Dam. The area of the Kalpathypuzha watershed is shared between Tamil Nadu and Kerala and only the part coming in the Kerala region is taken in this study. The study area covers parts of Kuzhalmannam, Palakkad, Malampuzha and Chittur blocks of Palakkad district. It is located in between 10.939443 °N and 10.684076 °N latitude and 76.428872 °E and 76.900910 °E longitude. The geographic area of the study portion is 759 km². The elevation of the study area ranges from 24 to 2028 m (Drisya *et al*, 2020). The location map of the study area is shown in the Fig 3.1.

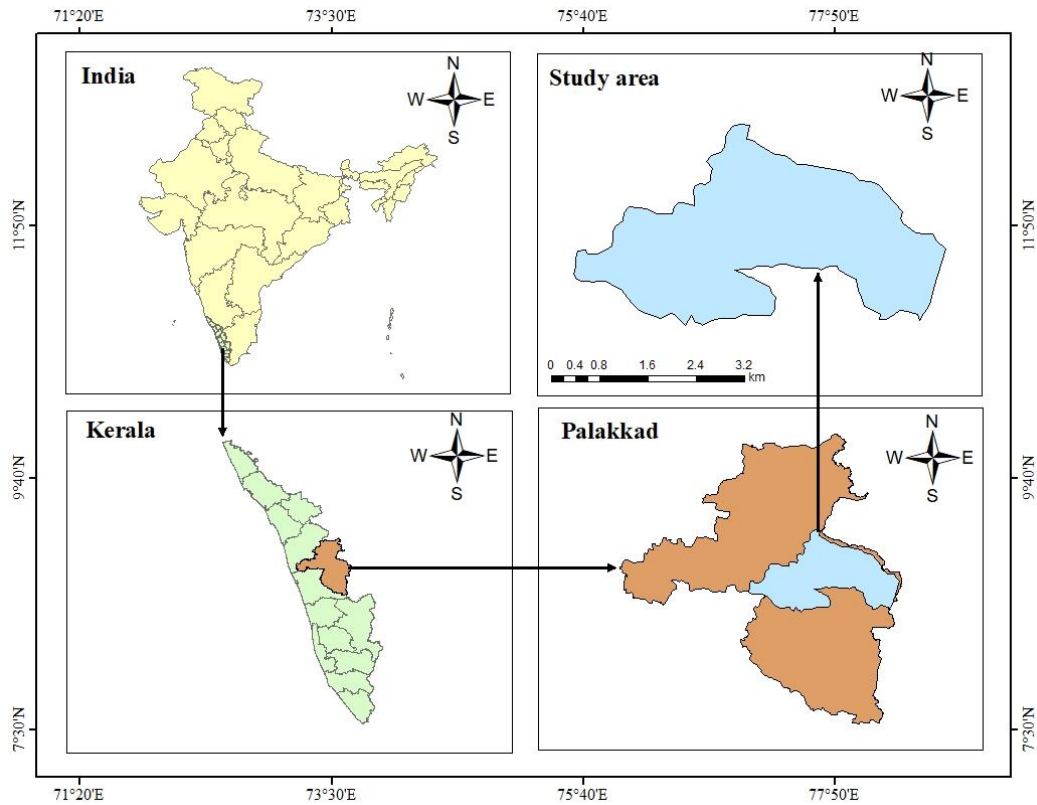


Fig 3.1 Location map of the study area

3.1.2 Climate

The study area falls under tropical dry and wet climate. The average annual rainfall is about 2400 mm. The average maximum and minimum temperatures are 32.45 °C and 23.50 °C respectively. The average annual relative humidity is about 72% and the average annual wind speed is about 5.75km/hr.

3.1.3 Geomorphology and soil

Physiographically the study area contains high land and the mid land and the main soil type of the area is laterite and alluvial soil.

3.1.4 Groundwater scenario

Archaean metamorphic complex rocks provide the foundation of the Palakkad district. These consist of the granulite group and the gneisses, which are found beneath laterite and alluvium. All geological formations, from Archaean

crystallines (hard rock) to Recent alluvium (soft rock), contain groundwater. Phreatic groundwater is found in laterite, alluvium, and worn crystalline materials.

3.1.5 Hydrogeology

The hard rock province covers major portion of the study area. The hornblende biotite gneiss is the main hard rock aquifer.

3.1.6 Groundwater exploitation status of Palakkad

The Fig 3.2 shown is collected from the Ground Water Information Booklet of Palakkad District, CGWB- 2013 which reveals the groundwater exploitation status of Palakkad district. The map clearly indicated that the Chittur block is overexploited and the Malampuzha block is critical zone and both these areas comes under the study area.

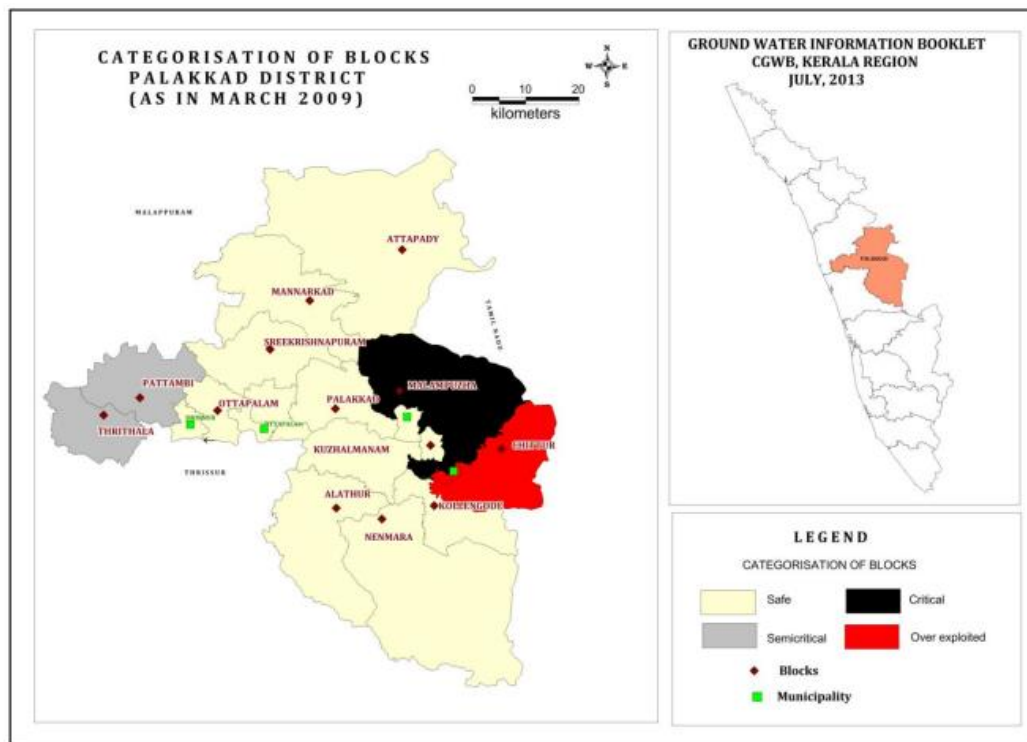


Fig 3.2 Map showing groundwater exploitation status of the study area
(source: Ground Water Information Booklet of Palakkad District, CGWB- 2013)

The Fig 3.3 shows the location map of various wells selected in the study area. Twelve observation wells evenly distributed in four blocks Kuzhalmannam, Palakkad, Malampuzha and Chittur of Palakkad district were selected for study. Three wells 160 PKD-12, PKD S-3 and PKD S-4 in Kuzhalmannam block, three wells 128, 129 and 160 PKD-8 in Palakkad block, four wells 133, 140, 142 and PKD S-15 in Malampuzha block and two wells 139 and PKD S-7 in Chittur block. The wells are denoted as per ID number given by Groundwater Dept. Palakkad. The google earth imagery of various well locations is also shown in Fig 3.4.

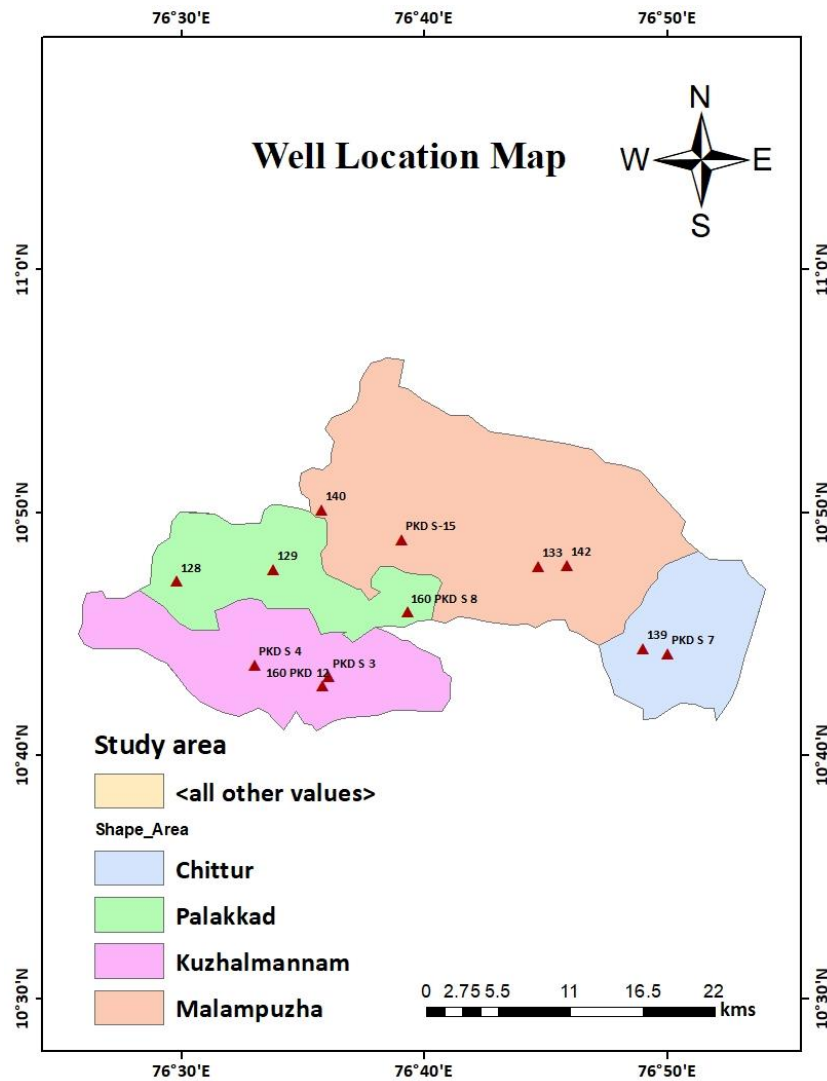


Fig 3.3 Location Map of wells selected in the study area

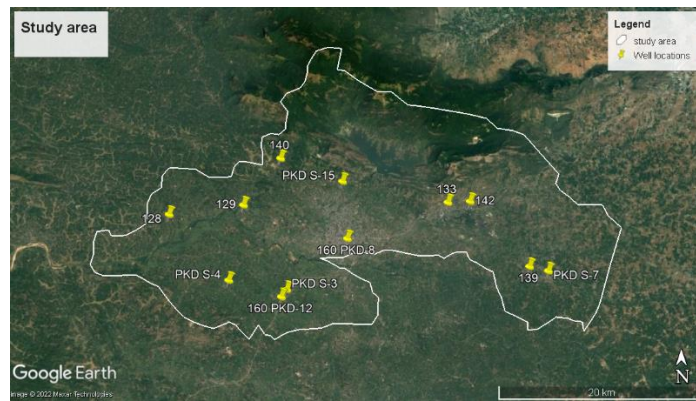


Fig 3.4 Google earth imagery of study area with well location

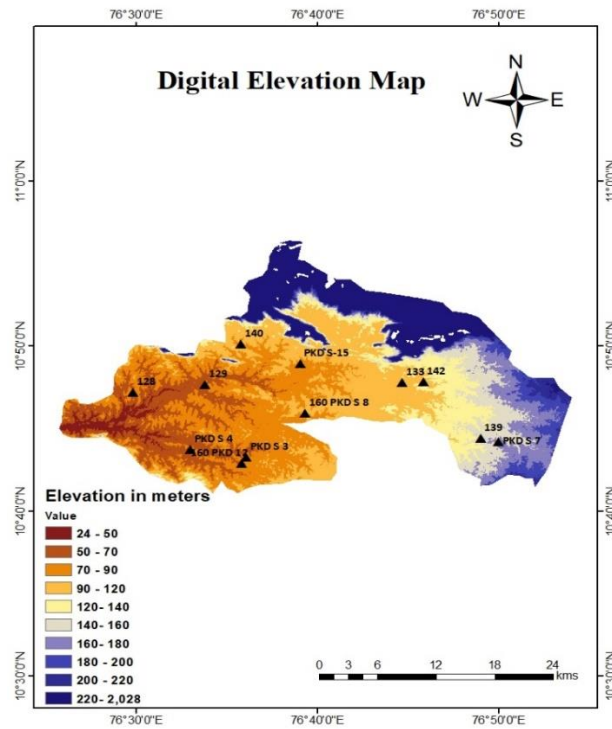


Fig 3.5 Classified Digital Elevation Model of the study area

The classified digital elevation model of the study area prepared for the study is shown in the Fig 3.5. The elevation of the entire study area ranges from 24 to 2028 m. The average elevation is 1026. No observation wells are located in the highly elevated areas as it is forest. The elevation difference between wells ranges from 67 to 152 m. Some of the drought scenes (Drought - Situation Assessment

Report, 2017, Kerala State Drought Monitoring Cell) of the study area are shown in the Plate 3.1, Plate 3.2, Plate 3.3 and Plate 3.4.



Plate 3.1 Drought scene- Malampuzha reservoir area, Palakkad



Plate 3.2 Drought scene- Kalpathypuzha during summer months



Plate 3.3 Drought scene- Dried up Chitturpuzha



Plate 3.4 Drinking water scenario in Vadakarapathi GP, Palakkad during 2017

3.1.7 Software and Tools used

Software and tools employed in the study are briefly described as follows

3.1.7.1 ArcGIS – ArcGIS 10.4

ArcGIS is geospatial software used to view, alter, store, and analyze geographic data. ArcGIS software released by the Environmental Systems Research

Institute (ESRI) is used. ArcGIS is a collection of programmes that includes ArcMap, ArcCatalog, ArcGIS Pro, ArcScene, and ArcGlobe. ArcGIS 10.4 version is used in this study. ArcGIS is mainly used in this study for generating contours, location map and spatial distribution maps. The spatial distribution maps were generated using IDW interpolation technique in ArcGIS.

3.1.7.2 Google earth

A free geospatial desktop programme called Google Earth Pro gives users the ability to view the entire planet and make incredibly precise maps. The 3D mapping system in Earth Pro, designed for customers with complex feature requirements, enables the import and export of GIS data as well as the analysis and collection of geographic data. It is employed in this study to define the study region and pinpoint the latitude and longitude of the well locations.

3.1.7.3 MATLAB-R2016a

MATLAB is a programming and numeric computing platform which allows matrix manipulations, plotting of functions and data, implementation of algorithms, creation of user interfaces. In this study it is used for ANN modelling of groundwater level.

3.1.7.4 XLSTAT

XLSTAT is a complete analysis and statistics add-in for Excel, used to analyze, customize, and share results within Microsoft Excel. In this study it is used for variability and trend analysis of groundwater level.

3.1.8 Data Availability

Precipitation data, temperature data, well location data and its groundwater level data were the dataset used in this study. The data were collected for a period of 15 years from 2007 to 2021. The details of data used, its source and utility are shown in Table 3.1.

Table 3.1 Details of Data used, its source and utility

Data	Source	Utility
Precipitation	http://dsp.imdpune.gov .in/ (IMD Pune)	Input for groundwater level modelling
Temperature (Max temperature and Min temperature)	http://dsp.imdpune.gov .in/ (IMD Pune)	Input for groundwater level modelling
Well Data (The well location data and groundwater level data of 12 observation wells located evenly in the study area.)	District Groundwater Department, Palakkad.	GWL trend analysis GWL modelling Groundwater drought assessment

3.1.8.1 Precipitation data

The daily precipitation data in mm for a period of 15 years from 2007 to 2021 was collected from IMD station Palakkad, India Meteorological Department (IMD) portal, it is given in Appendix-III. IMD is the principal agency responsible for meteorological observations and weather forecasting in the country. The daily rainfall data is converted into monthly rainfall and monthly rainfall data is used in the study.

3.1.8.2 Temperature data

The Maximum temperature and minimum temperature data required in this study were collected as IMD gridded data from the IMD portal, it is given in Appendix-IV and V. The gridded data is then extracted using gridded data extractor to daily minimum temperature and daily maximum temperature data for the location. The daily temperature data is then converted into monthly data for the study. The temperature data was collected for the study period of 15 years (2007-2021).

3.1.8.3 Well data

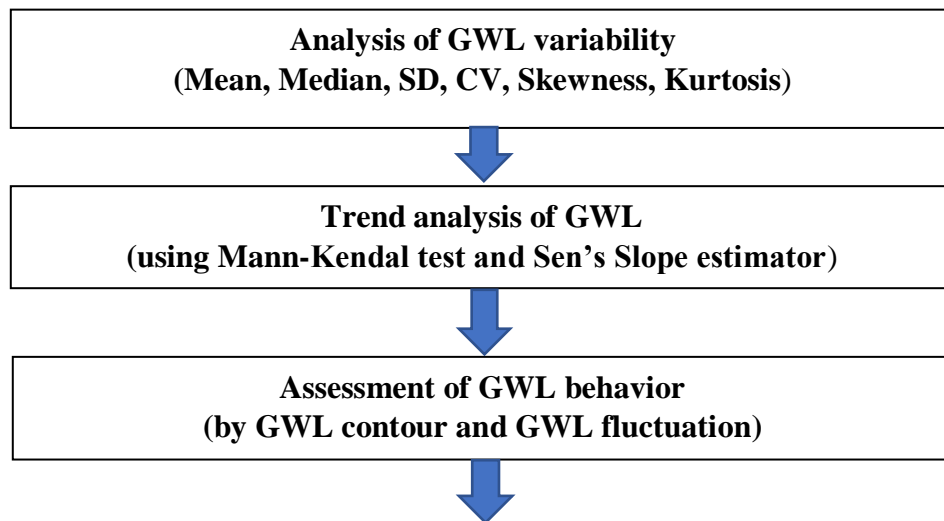
A total of 12 observation wells evenly distributed in the study area were selected for the study. These wells are distributed in four blocks of Palakkad district namely, Malampuzha, Palakkad, Kuzhalmannam and Chittur. The well location data and monthly groundwater level data of all the wells was collected from the District Groundwater Department, Palakkad for a period of 15 years (2007-2021). The monthly groundwater level data is given in Appendix-I. Out of twelve wells selected seven wells were dug wells and six wells were borewells. Details of wells selected for the study are shown in the Table 3.2.

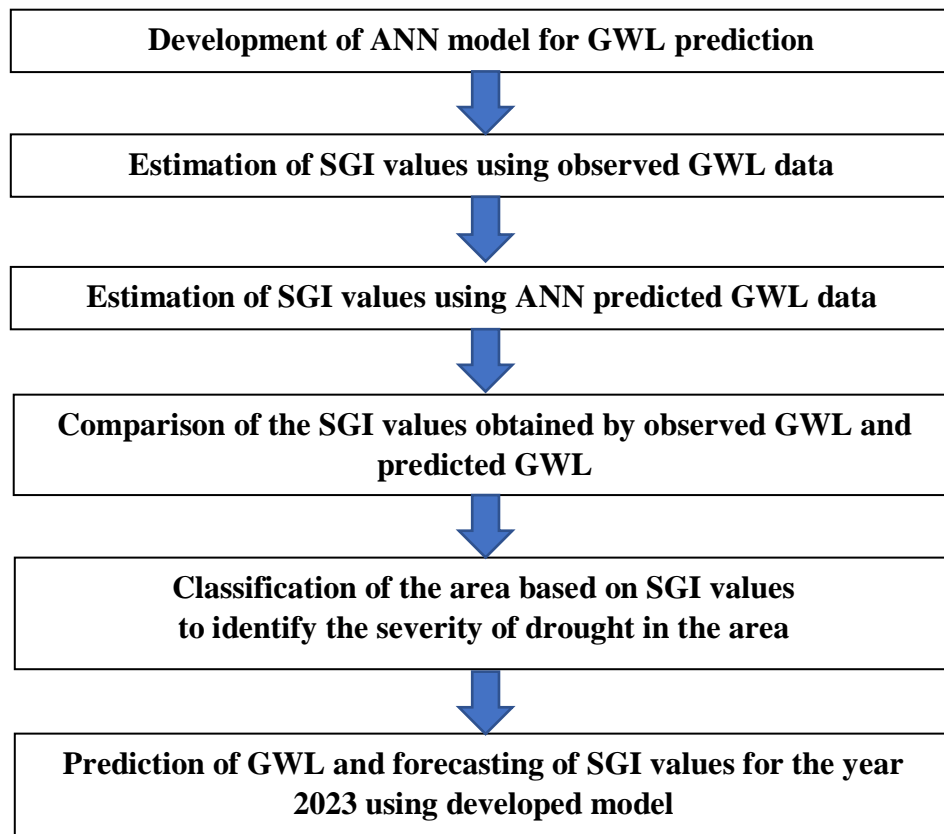
Table 3.2 Details of wells selected for the study

Sl. No	Well (ID as per state GW Dept. norms)	Block	Latitude (Decimal degrees)	Longitude (Decimal degrees)	Well type	Elevation (m)
1	160 PKD-12	Kuzhalmannam	10.715	76.597	Bore well	70
2	PKD S-3	Kuzhalmannam	10.721	76.601	Dug well	74
3	PKD S-4	Kuzhalmannam	10.729	76.550	Dug well	67

4	128	Palakkad	10.787	76.497	Dug well	68
5	129	Palakkad	10.795	76.563	Dug well	71
6	160 PKD-8	Palakkad	10.765	76.655	Bore well	92
7	133	Malampuzha	10.797	76.745	Dug well	113
8	140	Malampuzha	10.835	76.596	Bore well	90
9	142	Malampuzha	10.797	76.764	Bore well	113
10	PKD S-15	Malampuzha	10.815	76.651	Dug well	93
11	139	Chittur	10.741	76.817	Bore well	152
12	PKD S-7	Chittur	10.737	76.837	Dug well	152

3.1.9 Over-all Conceptual Framework of the study





3.2 ANALYSIS OF GROUNDWATER LEVEL VARIABILITY

In order to study the variability of groundwater level, the statistical parameters mean, standard deviation, coefficient of variation, skewness and kurtosis were computed for the groundwater level data.

3.2.1 Mean

The mean is one of the measurements of central tendency in statistics. It is a mathematical representation of the average value of a set of numbers, calculated as the sum of the numbers divided by the total number of numbers in the set. The arithmetic mean is calculated by using the formula (Helsel and Hirsch, 1992).

$$\mu = \frac{\sum X}{N}$$

Where, μ - sample mean

X - variable of a sample

N - number of variables in a sample

3.2.2 Standard Deviation

The statistics, data dispersion is measured by standard deviation. It is the positive square root of the arithmetic mean of the squares of deviation of the given values from arithmetic mean. The standard deviation is calculated by using the formula (Helsel and Hirsch, 1992).

$$\sigma = \sqrt{\frac{\sum(X - \mu)^2}{N}}$$

Where,

σ – Standard deviation

X – the variable of the sample

N – Number of variables in a sample

μ - sample mean

3.2.3 Coefficient of Variation (CV)

The statistical indicator of how widely apart individual data points are from the mean value is called the coefficient of variation (CV). The coefficient of variation is calculated by using the formula (Helsel and Hirsch, 1992)

$$CV = \frac{\sigma}{\mu} \times 100$$

Where, CV – coefficient of variation

σ – Standard deviation

μ - sample mean

3.2.4 Skewness

Skewness is a metric for the asymmetry of a real-valued random variable's probability distribution with respect to its mean. A positive, zero, negative, or undefined value for the skewness can occur. Positive skew typically implies that the distribution's tail is on the right, whereas negative skew typically indicates that it is on the left (Helsel and Hirsch, 1992).

3.2.5 Kurtosis

Kurtosis is a measure for a distribution's degree of tailedness. Tailedness is how often outliers occur. The tailedness of a distribution in comparison to a normal distribution is known as excess kurtosis. Mesokurtic distributions are those with medium kurtosis (medium tails), platykurtic distributions are those with low kurtosis (thin tails), and leptokurtic distributions are those with high kurtosis (fat tails). The tapering endpoints on either side of a distribution are known as the tails. They show the likelihood or frequency of values that are drastically high or low in comparison to the mean (Helsel and Hirsch, 1992).

3.3 TREND ANALYSIS OF GROUNDWATER LEVEL

The process of gathering data and looking for patterns or trends in it is known as trend analysis. It is a technique for time series data analysis that compares a specific item over a considerable amount of time in order to find a general pattern in the relationships between related components or variables and predict the future course of this pattern.

Trend analysis of groundwater level data was statistically examined in two phases. The non-parametric Mann-Kendall test was applied first. The normalised test statistic (Z) value was used to determine if there was an upward or downward trend. Using the non-parametric Sen's slope estimator, the rate of trend rise or fall was calculated in the second phase. The annual groundwater level data were subjected to trend analysis using the following techniques to determine whether there was an upward or downward trend.

3.3.1 Mann-Kendall Test (M-K)

A non-parametric test called the M-K test is used to identify trends and the non-linear trend that results from Kendall test statistics. The Mann-Kendall test was employed for trend analysis of time series data. Based on the normalised Z statistics value, the monotonic trend (increasing or decreasing) in the annual groundwater level time series was examined. The groundwater level's decreasing trend is

represented by the Z statistic's negative value, and its rising trend is shown by its positive value. It has been discovered to be a good tool for trend recognition.

Mann-Kendall test evaluates the relative magnitudes of data rather than the values itself. Each data value in the time series is compared to all succeeding values in this test. When a data value is increased by one, the Mann-Kendall statistics is initially believed to be zero, and vice versa. The final value of S is the sum of all such increments and decrements. In contrast to the alternative hypothesis (H1), which predicts an increasing or declining monotonic trend, the null hypothesis (H0) for the Mann-Kendall test is that there is no trend or serial correlation among the population under study Halder et al., (2020).

The Mann-Kendall statistics (S) is given by the equation

$$S = \sum_{i=1}^{n-1} \sum_{j=i+1}^n \text{sign}(x_j - x_i) \quad \text{Halder et al., (2020)}$$

Where,

$$\text{sign}(x_j - x_i) = 1, \text{ if } (x_j - x_i) > 0$$

$$\text{sign}(x_j - x_i) = 0, \text{ if } (x_j - x_i) = 0$$

$$\text{sign}(x_j - x_i) = -1, \text{ if } (x_j - x_i) < 0$$

S values that are positive or negative represent an upward or downward trend, respectively. To determine the significance of the trend, statistical analysis is required. Kendall describes the normal approximation test technique (1975). This test assumes that the dataset only contains a small number of tied values. The variance (S) is calculated by the following equation

$$\text{Var}(S) = \frac{1}{18} [n(n-1)(2n+5) - \sum_{p=1}^g t_p(t_p-1)(2t_p+5)]$$

Halder et al., (2020)

Where,

n – number of data points

g – number of tied groups

t_p - number of data points in the pth group

The normal Z- statistics is computed as follows:

$$Z = \frac{S-1}{\sqrt{\text{Var}(S)}}, \text{ if } S > 0$$

$$Z = 0, \text{ if } S = 0$$

$$Z = \frac{S+1}{\sqrt{\text{Var}(S)}}, \text{ if } S < 0$$

If Z is negative and the computed Z-statistics is higher than the Z-value corresponding to the 5% level of significance, the trend is considered to be falling. If Z is positive and the computed Z-statistics is higher than the Z value corresponding to the 5% level of significance, the trend is considered to be rising. There is no trend if the calculated Z-statistics is smaller than the Z-value equivalent to the 5% level of significance.

Z value is 1.645 at 10% level of significance

Z value is 1.96 at 5% level of significance

Z value is 2.33 at 1% level of significance

3.3.2 Sen's slope Estimator

One of the most popular models to find linear trends is simple linear regression. However, this approach necessitates the residuals' normality being assumed. Sen's slope is superior to the regression slope in that it is less impacted by significant data errors and outliers. The median of the pair-wise slopes between each pair of points in the dataset is used to determine the Sen's slope. Each individual slope (m_{ij}) is estimated using the equation:

$$m_{ij} = \frac{(Y_j - Y_i)}{(j - i)}$$

Halder *et al.*, (2020)

Where,

$i = 1$ to $n-1$ and $j = 2$ to n ,

Y_j and Y_i are data values at time j and i ($j > i$), respectively.

If there are n values of Y_j in the time series, there will be $N = n(n-1)/2$ slope estimates. The median slope of these N values of slopes is known as the Sen's slope.

The Sen's slope is:

$$m = m_{(\frac{N+1}{2})}, \text{ if } n \text{ is odd}$$
$$m = \frac{1}{2}(m_{(\frac{N}{2})} + m_{(\frac{N+1}{2})}), \text{ if } n \text{ is even}$$

Halder *et al.*, (2020)

Sen's slope suggests a rising trend when it is positive, while Sen's slope reveals the declining tendency when it is negative.

3.4 STUDY OF GROUNDWATER LEVEL BEHAVIOUR

The groundwater level behavior of the study area was studied based on the groundwater level data available from 12 observation wells evenly distributed in the study area. The water table contour and groundwater level fluctuations were analyzed.

3.4.1 Water table Contour maps

The elevations of the water table at the piezometric stations are plotted on a base map of the field by the standard mapping procedures used for the ground surface contour plotting. Lines of equal water table elevations was drawn. The locus of points on the water table where the hydraulic head is constant is known as a water table contour line. Water table contour maps of pre-monsoon, post-monsoon and annual were prepared with the help ArcGIS software.

3.4.2 Groundwater level fluctuations

Groundwater level is known to fluctuate depending on recharge and discharge of groundwater. Recharge due to rainfall, return flow of irrigation, canal seepage and seepage from tanks and ponds are the major components of groundwater recharge whereas draft from minor irrigation structure for irrigation use, industrial use, domestic use and livestock use are the main components of groundwater discharge in the area. Groundwater level fluctuation is calculated as the difference between post-monsoon (Sept-Nov) and pre-monsoon (Mar-May) groundwater levels.

3.5 MODELLING GROUNDWATER LEVEL

Artificial Neural Network (ANN) was used for modelling the groundwater level. The details of ANN modelling are explained in the following subheads

3.5.1 Artificial Neural Network

The human brain or nervous system, which consists of a massively large parallel interconnection of a large number of neurons, is where neural networks get their beginning because it completes tasks like perceptron tasks, recognition tasks, etc. in a fraction of the time required by high-performance computers of today.

The artificial neural network is inspired by the biological neural network that is the brain. The human brain has a highly complex and non-linear parallel computer. And this can organize its structural constituent elements, which are 'neurons'. They are interconnected in a highly complex way. Typically, there are 10 billion neurons and approximately 60 trillion interconnections. Rather than considering the structure of the human brain in totality, it is possible to mimic only an extremely small part of it in order to perform some very small task.

3.5.2 Usefulness and Capabilities of ANN models (Haykin, 2001)

- a) Nonlinearity: If the relationship between inputs and output cannot be described in terms of a simple linear equation. Real-life problems are highly non-linear in nature. ANN is interconnections of non-linear neurons, and nonlinearity is distributed throughout.
- b) Input-output mapping: Specifying what is going to be the output or desired response for a given input. The computational unit has a set of free parameters. If the obtained output is not close to the desired output, free parameters can be adjusted such that the difference between the actual and the desired is minimized, that have to be done several times. This learning ability makes neural networks remarkably different from the conventional computational unit.
- c) Adaptivity: Neural network can modify its free parameters to the changes in the surrounding environment.

- d) Evidential response: Neural network not only reports what the response is, but it can also tell the response is with what confidence level. It gives a decision with a measure of confidence.
- e) Fault tolerance: If some connections malfunction, it leads to some performance degradation, called graceful degradation.
- f) VLSI implement ability: very large-scale integrated circuit. A very large number of neurons can be integrated together.
- g) Neurobiological analogy: motivated by the biological neural network system.

Because of the above-mentioned advantages and due to the non-linear nature of groundwater level changes, ANN was selected for modelling groundwater level in this study.

3.5.3 Components of ANN (Haykin, 2001)

- a) Input Nodes (input layer): The information is typically passed to the next layer (hidden layer) without any computation taking place in this layer. A layer is another name for a group of nodes.
- b) Hidden nodes (hidden layer): Hidden layers are the locations of intermediary processing or computation; they carry out calculations and then pass weights (signals or information) from the input layer to the next layer (another hidden layer or to the output layer). It is possible to have a neural network without a hidden layer.
- c) Output Nodes (output layer): Use an activation function here that maps to the specified output format (e.g. softmax for classification).
- d) Connections and weights: The network consist of connections; each connection transfer the output of a neuron 'i' to the input of a neuron 'j'. In this meaning 'i' is the predecessor of 'j' and 'j' is the successor of 'i', each connection is assigned a weight W_{ij} .
- e) Activation function: A node's output in response to an input or combination of inputs is determined by the activation function of that node. It is a non-linear activation function commonly used. In artificial neural networks this function is also called the transfer function.

- f) Learning rule: The learning rule is a rule or algorithm that adjusts the neural network's parameters so that a particular input will result in a preferred output. The weights and thresholds are typically changed as a result of this learning process.

3.5.4 Mathematical representation of neuron

The mathematical representation of neuron described by (Haykin, 2001) is as follows

$$u_k = \sum_{j=1}^m (w_{kj} x_j)$$

$$y_k = \varphi(u_k + b_k)$$

Where, Bias denoted by b_k , has the effect of raising or reducing the net input of the activation function. x_1, x_2, \dots, x_m are the inputs; $w_{k1}, w_{k2}, \dots, w_{km}$ are the weights of the neuron k ; u_k is the linear combiner output due to input signals; $\varphi(.)$ is the activation function; y_k is the output signal of the neuron.

3.5.5 Various Activation Functions in ANN (Haykin, 2001)

Additionally, known as a transfer function. It is a mathematical description of the relationship between the input and output, expressed in terms of spatial or temporal frequency. There are several activation functions for neural network. Three of them which are available in the GUI of Neural Network toolbox of MATLAB software are explained as follows:

3.5.5.1 Log-Sigmoid activation function (Log-sig)

$$a = \text{Logsig}(n) = \frac{1}{1 + e^{-n}}$$

Log-sigmoid transfer function is one of the most commonly used transfer functions. This transfer function compresses the output into the range of 0 to 1 from the input, which may be any value between plus and minus infinity. A graphical representation of Log-Sigmoid activation function is shown in Fig 3.6.

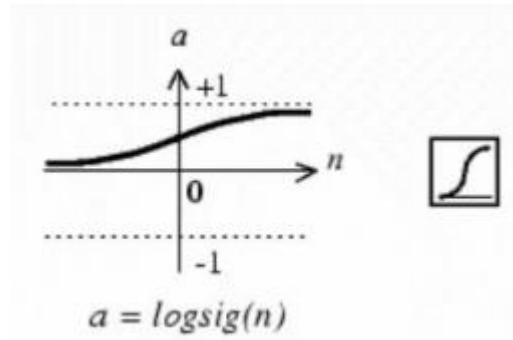


Fig 3.6 Log-sigmoid activation function (Log-sig)

3.5.5.2 Hyperbolic tangent activation function (Tansig)

$$a = \text{Tansig}(n) = \frac{2}{1+e^{-2n}} - 1$$

This transfer function is related to a bipolar sigmoid which has an output in the range of -1 to +1. Mathematically equivalent to $\tanh(n)$. For neural networks, when speed is more crucial than the precise shape of the transfer function, this function provides a good trade-off. It was observed that this transfer function was well suited in terms of better prediction results. A graphical representation of hyperbolic tangent activation function is shown in Fig 3.7.

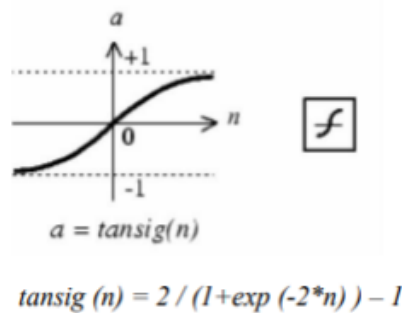


Fig 3.7 hyperbolic tangent activation function (Tansig)

3.5.5.3 Purelin Transfer function (Purelin)

$$a = \text{purlin}(n)$$

Purelin activation function specially used when, model operated with input and output parameter having liner relationship with each other. A graphical representation of Purelin activation function is shown in Fig 3.8.

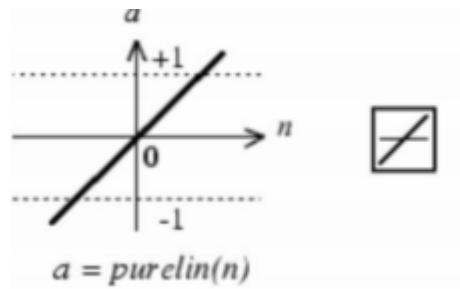


Fig 3.8 purelin transfer function (Purelin)

Among these three activation functions, hyperbolic tangent activation function (Tansig) was used in this study as it was well suited in terms of better prediction results as per literatures (Seo and Lee 2019).

3.5.6 Learning Rules in a Neural Network (Haykin, 2001)

The ability of a neural network to learn from its surroundings and to enhance performance as a result of prior experience is its key characteristic. This could be achieved by the process called as learning. Mendel and McClaren defined learning as, “Learning is the process by which the environment in which a neural network is embedded modifies the free parameters of the network through a process of simulation. The way in which the parameter changes happen determines the type of learning. There are five learning rules as follows:

1. Error-correction learning
2. Memory-based learning
3. Hebbian learning
4. Competitive learning and
5. Boltzmann learning.

In this study the most commonly used learning rule ‘error-correction learning rule’ was used based on previous research (Seo and Lee 2019).

3.5.7 Types of Learning (Haykin, 2001)

There are three major learning paradigms for the neural network; supervised learning, unsupervised learning and reinforcement learning.

3.5.7.1 Supervised Learning:

The outputs and inputs are both offered. After processing the inputs, the network compares the obtained outputs to the desired outputs. In order to modify the weights and reduce the error, the prediction error is transmitted backwards through the network. This process is continued with multiple training sets until the error is minimized across many sets

3.5.7.2 Unsupervised Learning:

Although the network is given inputs, the desired outputs are not delivered. The system must then choose for itself, through self-organization or adaptation, the features it will employ to organize the input data. May include neural cooperation, competition, or both. The training task is to classify inputs into its own categories, extract features from the independent variables, and group together patterns that are comparable in some way.

3.5.7.3 Reinforcement learning:

This kind of learning determines the neural network's parameters in situations where the data is typically generated by the interactions with the environment rather than being provided. This knowledge relates to how a neural network should behave in a given situation in order to optimise a potential long-term benefit.

Out of these three learning paradigms, the supervised learning is used in the present study because the output values for the given input vectors were provided.

3.5.8 Back propagation algorithm in ANN

A multi-layer feed-forward network trained using the error back propagation method makes up the back-propagation algorithm. It is one of the widely used neural network algorithm. It learns by applying the steepest descent approach, which modifies the network's weight values and threshold value through back propagation to get the lowest possible error sum of squares. In this approach, the

connection weight of the network is initially given a low value, and then a training sample is chosen to calculate the gradient error in relation to this training sample.

The back-propagation learning process is described as follows:

1. Forward propagation of operating signal: From the input layer via the hidden layer and onto the output layer, the input signal is propagated. The network's weight and offset values are kept constant during the forward propagation operating signal, and the status of each layer of neurons only affects the subsequent layer of neurons. The back propagation of error signal might be used if the desired output cannot be achieved in the output layer.

2. Back propagation of error signal: The difference between the network's actual output and expected output is known as an error signal. In this case, Layer by layer, the erroneous signal is transmitted from the output layer to the input layer. The error feedback that occurs during the back propagation of the error signal controls the network's weight value. Weight value and offset value are regularly modified to bring the network's actual output and expected output closer to one another.

3.5.9 Neural Network Architectures in ANN (Haykin, 2001)

There are four major types of neural network architectures. They are feed forward neural network, recurrent neural network, radial basis function network and convolutional neural network.

3.5.9.1 Feedforward Neural Network

There are no cycles in the connections between the units of an artificial neural network called a feedforward neural network. Information moves only forward in this network, passing via any potential hidden nodes along the way from the input nodes to the output nodes. There are no cycles or loops in the network (Haykin, 2001). There are two types of feedforward neural networks as:

a) Single-Layer Perceptron:

As the simplest feed forward neural network, it just has one layer of output nodes because there is no hidden layer in it. This is referred to as a single layer since

the input layer is excluded from the layer count because there are no computations performed there, the inputs are fed directly into the outputs via a set of weights. (Haykin, 2001). A single layer feed forward neural network is shown in Fig 3.9.

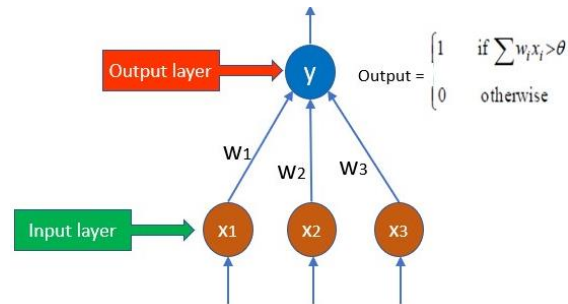


Fig 3.9 Single layer perceptron (Source: <https://cdn.educba.com/academy/wp-content/uploads/2020/02/Single-Layer-Perceptron-01.jpg>)

b) Multi-Layer Perceptron (MLP)

This class of networks consists of multiple layers of computing units that are frequently connected in a feed-forward fashion. Each neuron in a layer has direct connections with the neurons in the layer above it. A sigmoid function is widely used as an activation function in these networks' units. The ability of MLP to learn non-linear representations makes them significantly more helpful than other networks (Haykin, 2001). A Multi-layer feed forward neural network is shown in Fig 3.10.

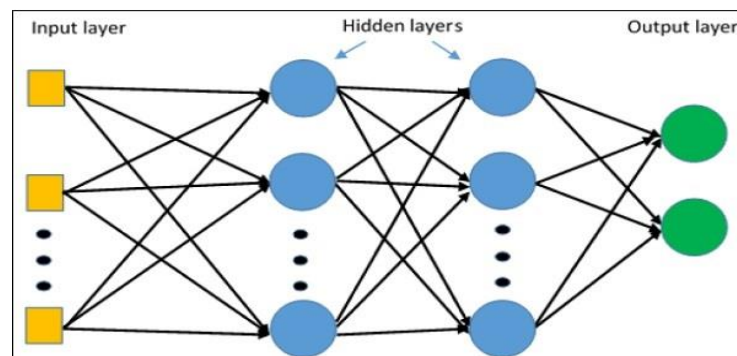


Fig 3.10 Multi-layer perceptron (MLP)

(Source: https://www.tutorialspoint.com/tensorflow/images/multi_layer_perceptron.jpg)

Among the different types of neural network architectures, the feed forward multi-layer perceptron was used in this study as it gives the best result as per literatures (Seo and Lee 2019).

3.5.10 General Procedure for Development of ANN models

It is necessary to define the data to be used and present it to the ANN as a pattern of input data with the desired outcome or target. The data are then divided into the training set and the validation set. The ANN uses only the training set in its learning process in developing the model. The validation set is used to test the model for its predictive ability and when to stop the training of the ANN. The number of hidden layers and the number of neurons for each hidden layer is to be selected. All the ANN parameters are set before starting the training process. The input data and weights are used to calculate the output during the training phase. The backpropagation algorithm is used to train the ANN by adjusting the weights to reduce the difference between the current output and the desired output. To evaluate whether the ANN has acquired the necessary skills to complete the task at hand, an evaluation procedure must be completed. Periodically pausing the training process and testing its effectiveness may be a part of this review process until a satisfactory outcome is achieved. The training of the ANN is finished, and it is prepared for usage once an acceptable result is reached. The flowchart for development of ANN model is shown in Fig 3.11.

The timing of the training process's termination is crucial for getting a decent model. If an ANN is over trained, a curve-fitting problem may occur whereby the ANN starts to fit itself to the training set instead of creating a generalized model. The test and validation data set often shows poor forecasts as a result of this. On the other side, if the ANN is not trained for a sufficient amount of time, it can settle for a local minimum solution rather than the global minimum. Usually, this results in a sub-optimal model. The number of iterations necessary to generate the optimal model can be determined by periodically testing the ANN on the test set and recording both the training and test data set results. Resetting the ANN and training the network to that number of iterations is all that is required.

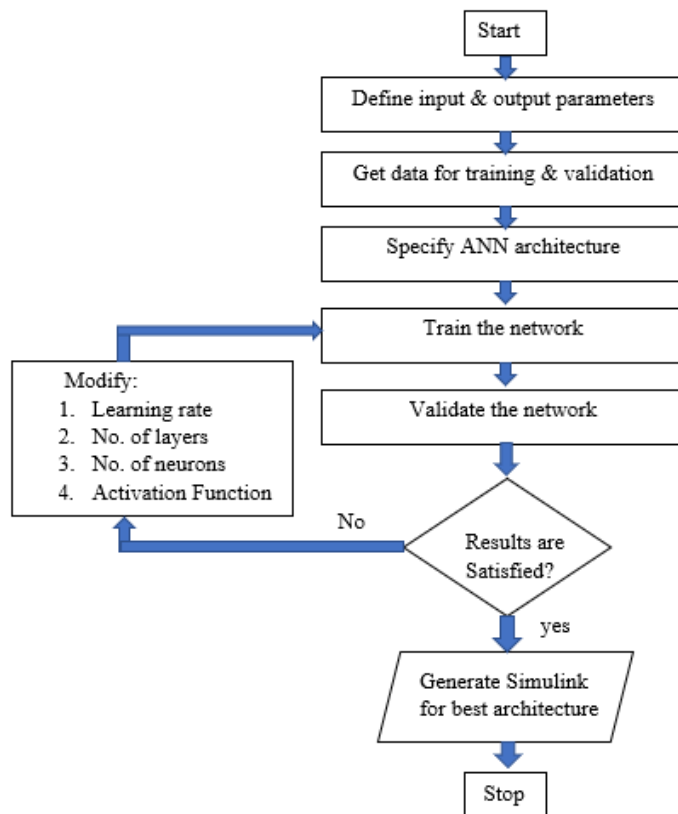


Fig 3.11 General Procedure for Development of ANN models

3.5.11 Limitations of ANN

- a) Amount of data: Typically, more data is needed for neural networks than for typical machine learning algorithms.
- b) Determination of proper network structure: When choosing the structure of Artificial Neural Networks, there is no set rule. Experience and trial and error are required to establish an appropriate network structure.
- c) Computationally expensive: Neural networks are also more computationally expensive than traditional algorithms.
- d) Difficulty in presenting the issue to the network: ANNs can handle numerical data. Before using ANN, problems must be converted into numerical values.
- e) The duration of the network is unknown: When the network's error on the sample is decreased to a specific number, the training is said to be finished. This value does not produce the best outcomes.

- f) Black-box' nature of the ANN model.
- g) These models are prone to overfitting.

When comparing its capabilities and limitations, ANN was found to give the approximate and near solutions as similar to that of physically based models which requires a lot of expensive inputs.

3.5.12 Performance Indicators of ANN Model (Haykin, 2001)

For better appreciation of model, the following performance indicators were used to evaluate the predictive efficiency of the developed ANN models.

3.5.12.1 Correlation coefficient (*r*)

The correlation coefficient is the specific measure that assesses the strength of the linear relationship between two variables in a correlation analysis. For a best model the *r* value is nearly equal to 1. The relationship between two variables is generally considered strong when their *r* value is larger than 0.7. Correlation coefficient was calculated using the equation.

$$r = \frac{\sum_{i=1}^N (X_i - \bar{X})(Y_i - \bar{Y})}{\sqrt{\sum_{i=1}^N (X_i - \bar{X})^2 \sum_{i=1}^N (Y_i - \bar{Y})^2}}$$

3.5.12.2 Coefficient of determination *R*²

The degree of accuracy with which a statistical model forecasts a result is measured by the coefficient of determination, which has a range of 0 to 1. It is the square of correlation coefficient. For a best model the coefficient of determination value is nearly equal to 1. Generally, the coefficient of determination with about 70% is considered good. 50% is considered a moderate fit for the given model.

3.5.12.3 Root Mean Square Error (RMSE)

The root mean square error is used to quantify the prediction accuracy of the created model. RMSE value should be low or nearly equal to zero for a best model. Root mean square error (RMSE) was calculated from the equation

$$RMSE = \sqrt{\frac{1}{N} \sum_{i=1}^N (X_i - Y_i)^2}$$

Where,

X_i = observed values,

Y_i = predicted values, and

N = number of observations.

3.5 APPLICATION OF ANN MODEL FOR GROUNDWATER LEVEL PREDICTION

In the present study artificial neural network (ANN) model was developed for predicting the groundwater level. The input data set used in this study involves monthly precipitation, monthly minimum temperature and maximum temperature. The development of ANN models using these input variables are supported by the researchers Javadinejad *et al.*, 2020 and Husna *et al.*, 2016. The output dataset is the monthly groundwater level data of all the selected wells. The groundwater level data collected from the department was depth to water level (below ground level) it is then converted into groundwater level with respect to mean sea level considering the elevation of each well location. The groundwater level data set of 15 years from 2007 to 2021 was used for the development of ANN model. The data set was divided into training data set and testing data set, 75 % of the total data set was assigned as training data set and the remaining 25 % as testing data set. The various steps involved in development of ANN model for predicting groundwater level are given as follows:

1. MATLAB R2016a software was used for development of ANN models
2. The data set was normalized, in order to have the same range of values for each of the inputs to the ANN model. It stabilizes convergence of network weights and biases. Data normalization was done using equation:

$$z = \frac{x - \mu}{\sigma}$$

z – Normalized value

x – each value of data to be normalised

μ - Average of data

σ – Standard deviation of data

3. A three-layer feed forward ANN model was constructed and backpropagation algorithm was used to train the network.

4. Levenberg–Marquardt (LM) algorithm was selected as learning algorithm.

5. Different combination of activation function for hidden and output layers were tried and finally the hyperbolic tangent activation function was selected.

6. The number of epochs was taken as 1000 and the max fail was altered in each iteration until the best result was obtained.

7. Although the number of hidden layers and the number of neurons in those levels are essential components of a successful ANN architecture, trial and error was employed to find the best structure because there is no unifying theory for doing so.

8. After trial and error procedure best ANN models were selected based on the several performance criteria explained above and used in this study. The overall modelling strategies used for prediction of groundwater level is shown in Table 3.3.

Table 3.3 Overall modelling strategies used for prediction of groundwater level

Components function	Type
Neural Network	Feed forward neural network
Training algorithm	Levenberg-Marquardt (LM)
Training function	TRAINLM
Learning function	LEARNGDM
Transfer function	Tan sigmoid

3.5.1 Working Environment of MATLAB Software

The ANN models were developed using MATLAB R2016a software. It has matrix-based data structures, internal data types of its own, a large collection of functions, a platform to create scripts and functions, the ability to import and export data to a variety of file kinds, and more. The network manager includes all functions for importing inputs, targets, new networks, outputs, and network problems, among others. The working environment of MATLAB software used in this study is shown in Fig 3.12.

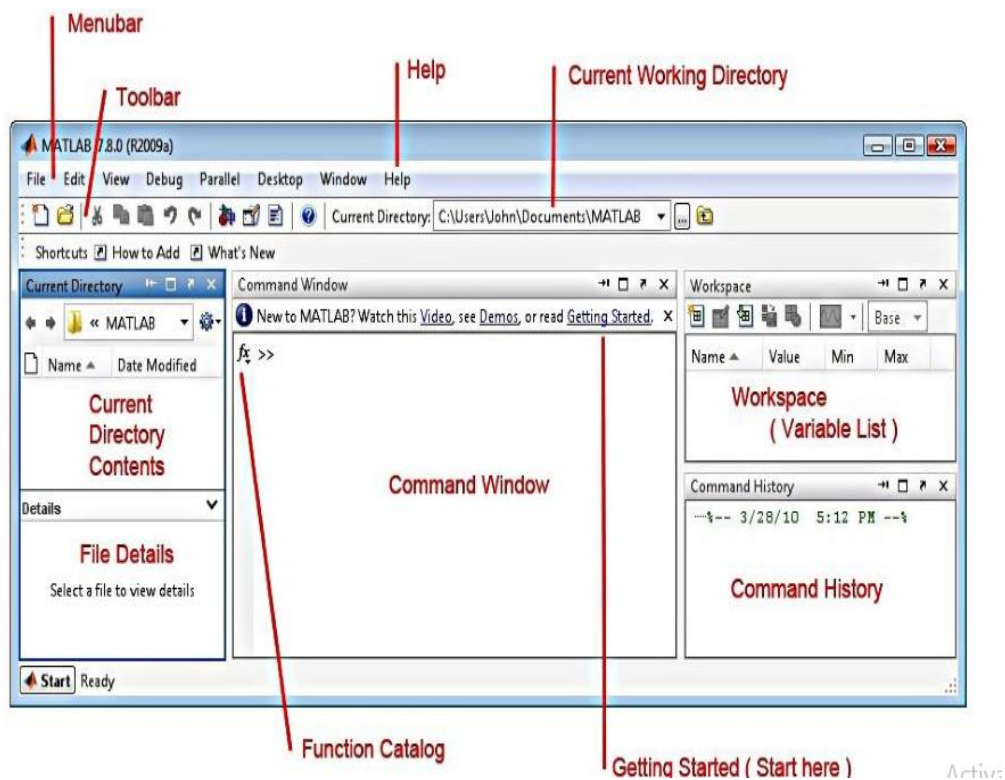


Fig 3.12 Working environment of MATLAB software

3.5.1.1 Neural network toolbox in MATLAB (nntool)

The network manager includes all functions for importing inputs, targets, new networks, outputs, and network problems, among others. The “nntool” in MATLAB is shown in Fig 3.13.

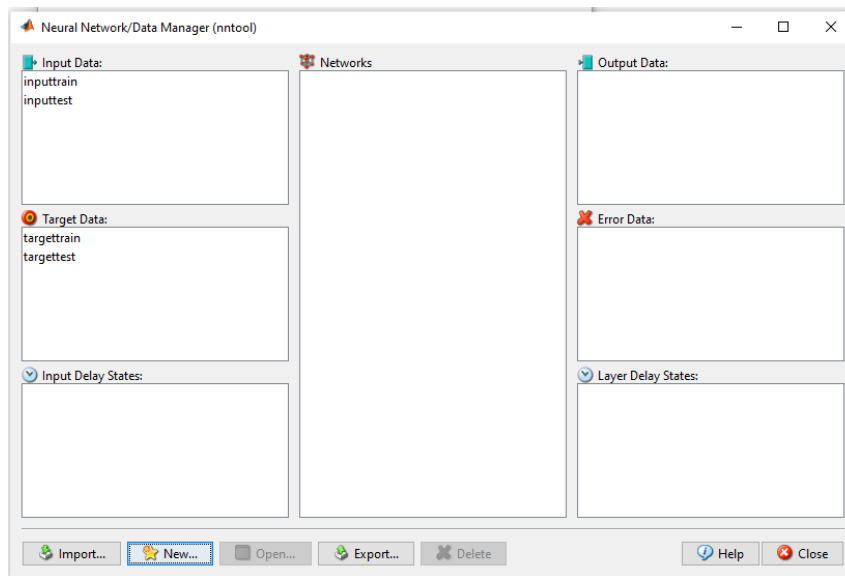


Fig 3.13 Neural network toolbox in MATLAB (nntool)

The selection of network architecture, training function, learning function, performance function, number of layers, number of neurons, and transfer function for various layers were carried out for creating new networks after importing all the input and target files from workspace to network manager. The Fig 3.14 shows the new network creation window in MATLAB

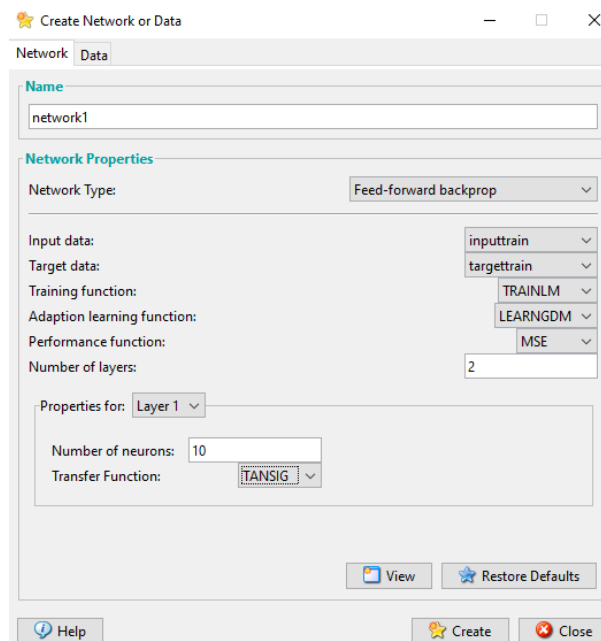


Fig 3.14 New network creation window in MATLAB

3.5.1.2 Training function

Training function is used to train the neural network to recognize a certain input and map it to an output. There are different types of training functions like TRAINGD, TRAINGDM, TRAINLM, TRAINGDX, TRAINRP etc. Among these TRAINLM is the commonly used training function in water resources studies and were used by many researchers (Seo and Lee 2019).

3.5.1.3 Learning function

Learning is the process by which a neural network adjusts its parameters appropriately in response to a stimulus, producing the desired response. There are mainly two types of learning functions LEARNGD, LEARNGDM of which LEARNGDM is commonly used as per literatures (Seo and Lee 2019) and was used in this study. A model of a neural network in MATLAB is shown in Fig 3.15.

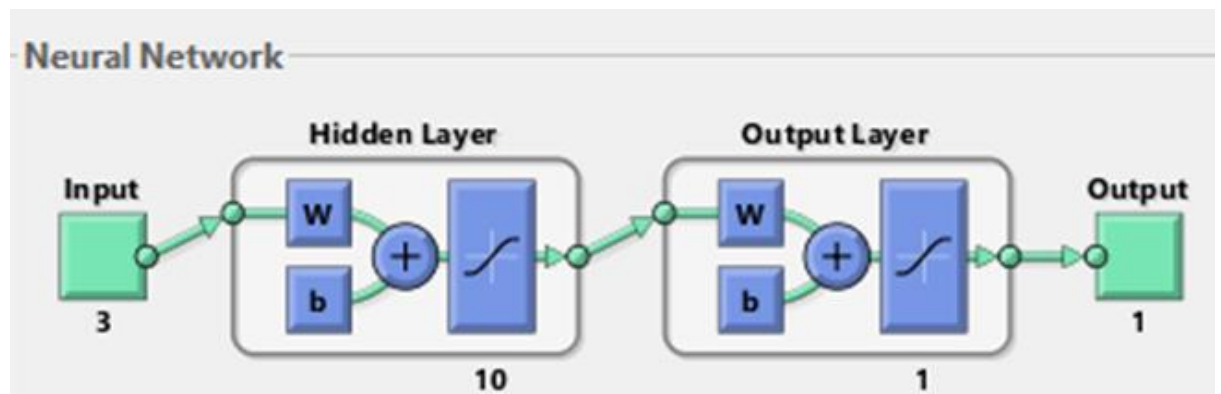


Fig 3.15 Model of a neural network in MATLAB

3.6 DETERMINATION OF DROUGHT INDEX

Standardized Groundwater level Index denoted by SGI was used for the groundwater drought assessment in this study. SGI is a quantitative method for assessing groundwater level deficits over a range of time scales, reflecting the impact of extreme drought events on the scenario for water resources. SGI for each well is estimated separately using the equation (Bloomfield and Marchant, 2013)

$$SGI = \frac{K-M}{\sigma}$$

Where,

K - groundwater level value (wrt MSL) of the respective year

M - mean value of all years

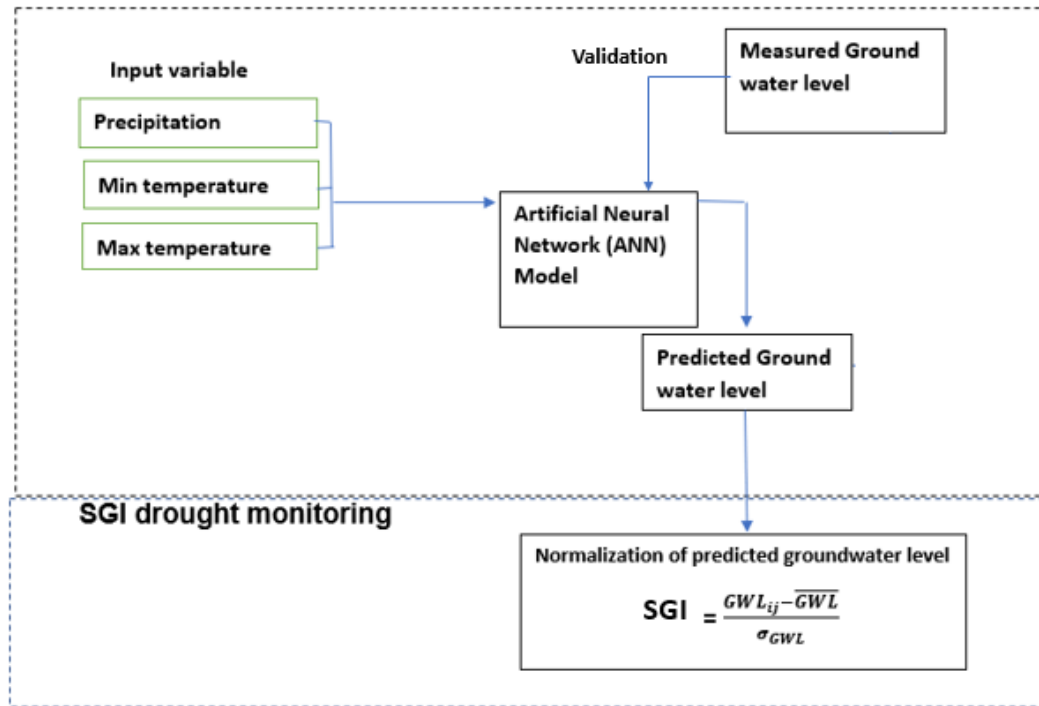
σ - standard deviation

Standardized SGI indicate the level of groundwater drought. The SGI highlights regions that are either drier or wetter than typical. The arbitrary categories of drought intensity defined for groundwater drought (Bloomfield and Marchant, 2013) is shown in the Table 3.4. Spatial distribution map of SGI for severe drought years 2013, 2016 and 2017 (April and May) months was prepared in ArcGIS using IDW interpolation technique.

Table 3.4 Drought intensity categories by Bloomfield and Marchant (2013)

SGI	DROUGHT CONDITION
$SGI \leq -1.5$	Exceptional drought
$-1.5 < SGI \leq -1.2$	Extreme drought
$-1.2 < SGI \leq -0.9$	Severe drought
$-0.9 < SGI \leq -0.6$	Moderate drought
$-0.6 < SGI \leq -0.3$	Abnormally dry condition
$SGI > -0.3$	Normal / no drought

The workflow of groundwater level modelling and drought assessment is shown in Fig 3.16.



GWL_{ij} – GWL of respective year

\overline{GWL} – Mean of GWLs of all years

σ_{GWL} – Standard deviation of GWLs of all years

Fig 3.16 Workflow of groundwater level modelling and drought assessment

3.7 FUTURE PREDICTION OF GROUNDWATER LEVEL AND STANDARDIZED GROUNDWATER LEVEL INDEX (SGI)

The developed ANN model in MATLAB was used for future prediction of monthly GWL and groundwater drought for the year 2023. MATLAB nftool was used to obtain the code for future prediction. Projected climate data of Precipitation, Max and Min temperature from CMIP6 climate model for SSP 245 scenario (medium scenario) was used for prediction. Once the network is well trained, then a relationship can be obtained between the weights and biases in a matrix format in MATLAB (MATLAB Matrix-only Function) for forecasting the GWL as shown in Fig 3.17.

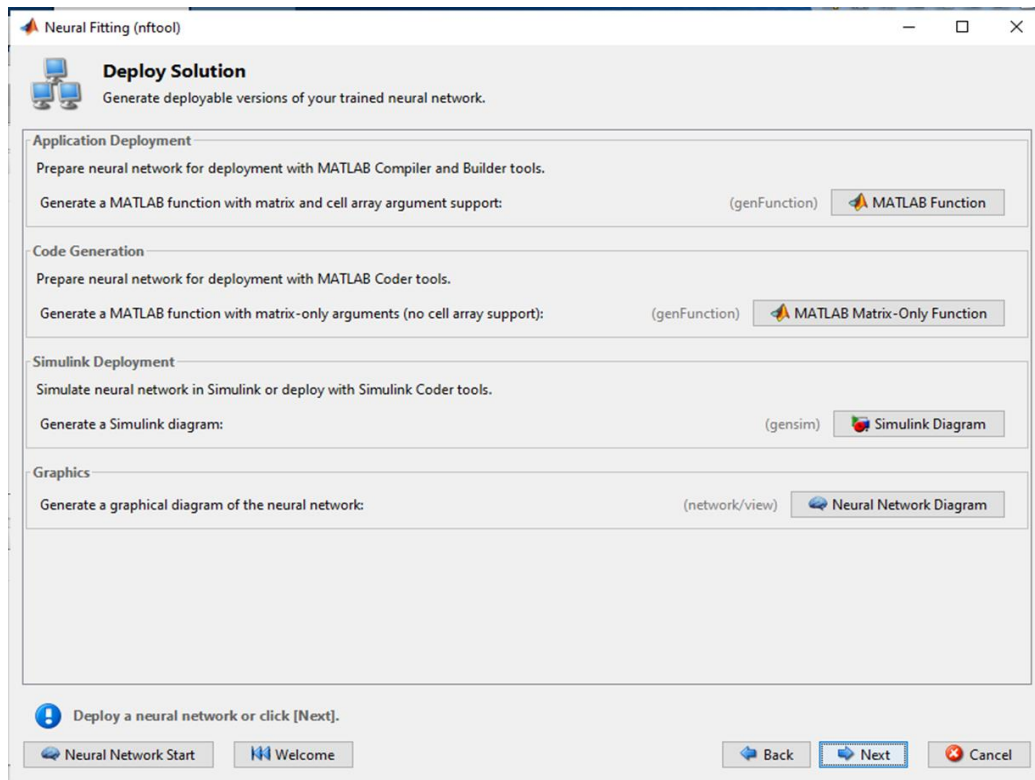


Fig 3.17 nftool window showing MATLAB Matrix-Only function

The projected climate data used for prediction of GWL for year 2023 is shown in the Table 3.4.

Table 3.5 Projected bias corrected data of 2023 from CMIP6 climate model for SSP 245 scenario

Year 2023	Precipitation (mm)	Min temp (° C)	Max temp (° C)
Jan	0.74	21.64	34.92
Feb	1.4	22.28	36.16
Mar	3.44	23.45	37.49
Apr	159.8	23.87	34.55
May	145.2	24.83	33.61
Jun	382.13	23.26	29.37
July	379.9	23.14	30.44
Aug	190.76	24.79	31.14
Sept	141.29	23.71	31.98

Oct	202.28	23.9	31.8
Nov	106.34	23.76	31.25
dec	10.12	21.89	32.8

The Fig 3.18 shows the window containing the neural network constants which can be used for the future prediction of groundwater level.

```

13 %----- NEURAL NETWORK CONSTANTS -----
14
15 % Input 1
16 xl_step1.xoffset = [-0.795;-1.975321699;-3.089388111];
17 xl_step1.gain = [0.40290088638195;0.417033789330798;0.346769772134516];
18 xl_step1.ymin = -1;
19
20 % Layer 1
21 b1 = [3.2241098264481496;-2.430325969485516;-2.211966196017319;-1.3869724863359263;1.2519442716607747;-1.03425333
22 IW1_1 = [-2.026494535315063 -0.73300794171467563 2.3172976010153818;2.4072423684356088 -2.3335084338429168 -0.33410
23
24 % Layer 2
25 b2 = -0.2861132285335199;
26 IW2_1 = [0.41327213753703573 0.04624816996834305 -0.1806047635581417 -0.01851697809763855 -0.14560670635759021 -0.3
27
28 % Output 1
29 y1_step1.ymin = -1;
30 y1_step1.gain = 0.3270666974582889;
31 y1_step1.xoffset = -3.827143059;
32
33

```

Command Window

```

>> nftool
f> >>

```

Workspace

Name	Value	Var
input	180x3 double	0.9961
target	180x1 double	1.0000

myNeuralNetworkFunction Ln 1 Col 1

Fig 3.18 MATLAB Code generated for GWL prediction

RESULTS AND DISCUSSION

CHAPTER-IV

RESULTS AND DISCUSSION

Groundwater resource is one of the most valuable and important sources of water in the world. It's essential to comprehend how both natural and man-made variables affect groundwater resources and exploitation in order to create effective management plans to address unsustainable use (Tillman and Leake, 2010). The groundwater Level is a straightforward and direct indicator of groundwater accessibility and availability (Tao et al., 2020). The understanding of groundwater level variability and trend is crucial for water resource planning in a region. Groundwater level fluctuation being a non-linear phenomenon, Artificial Neural Networks (ANN) proves to be one of the best tools for modelling non-linear relationship between input and output datasets in hydrology (Dawson and Wilby, 1999). Once the groundwater level is modelled, it is easy to assess the groundwater drought conditions of a region using Standardized Groundwater level Index (SGI). The various results of the study pertaining to variability and trend analysis of groundwater level, modelling of groundwater level using Artificial Neural Network (ANN) and assessment of groundwater drought using Standardized Groundwater level Index (SGI) were presented and discussed under the following sub-heads.

4.1 VARIABILITY OF GROUNDWATER LEVEL

The groundwater level variability of the selected wells during the period 2007 to 2021 were studied using the statistical parameters Mean, Standard Deviation (SD), Coefficient of Variation (CV), Skewness and Kurtosis.

4.1.1 Mean Monthly Groundwater level w.r.t MSL in (m) from 2007 to 2021

The mean monthly groundwater level with respect to MSL from 2007 to 2021 is shown in Table 4.1. For all the twelve wells the mean monthly groundwater level was highest in the post monsoon months (Aug and Sept) and lowest in the pre-monsoon months (Apr and May) which indicated the rise in the water level in the post-monsoon period due to recharge caused by rainfall in monsoon and lowering of the water level in the pre-monsoon period due to increased abstraction and

decreased recharge. The maximum mean monthly groundwater level of 151.3 m was seen for the well PKD S-7 in the month of September and minimum mean monthly groundwater level of 61.5 m was seen for the well 129 in the month of May.

4.1.2 Annual Mean Groundwater Level w.r.t MSL (m)

The annual mean of groundwater level with respect to MSL is shown in Table 4.2, for majority of wells, it was lowest in the year 2017 which was due to reduced rainfall and recharge in the same year. The highest annual mean groundwater level of 150.9 m was seen for the well PKD S-7 in the year 2015 and lowest of 62.1 m was seen for the well 129 in the year 2016.

4.1.3 Monthly Standard Deviation of Groundwater Level (m)

The standard deviation of monthly groundwater level is shown in Table.4.3. For majority of wells standard deviation was found higher in the month of June/July with values varied from 1 to 3.43 m than other months. The highest standard deviation of 3.81 m was found for well 142 in the month of February and the lowest was 0.17 m for well 160 PKD-12 in the month of July. More variation in the standard deviation of groundwater level is found in the June/July month which may be due to the rise in groundwater level by monsoon rainfall.

4.1.4 Monthly CV (%) of Groundwater Level

The coefficient of variation of monthly groundwater level is shown in Table 4.4. CV of majority of wells were found highly variable in the monsoon months of June and July with values varied from 21.83 to 93.30 which indicated high groundwater level fluctuation in the respective months due to arrival of monsoon. The highest CV of 93.30 was seen for the well 133 in the month of July and while lowest of 4.32 was for the well 129 in the month of February.

4.1.5 Skewness of Groundwater Level

The skewness of groundwater level of all the wells is shown in Table 4.5. It was found between -1.94 to 3.42, some wells showed a negatively skewed distribution whereas other wells showed a positively skewed distribution. The highest positive skewness of 3.42 was for the of the well PKD S-3 in the month of February and highest negative skewness of -1.94 was found for the well 129 in the

month of January. The distribution is extremely skewed which indicates that the groundwater level is highly asymmetric from the normal distribution which happens due to the rise and fall in the groundwater level due to the recharge by seasonal rainfall. The Skewness of groundwater level is represented graphically in Fig 4.1.



Fig 4.1 Skewness of groundwater level for wells a) 139 b) PKD S-7 c) 160 PKD-12 d) PKD S-3 e) PKD S-4 f) 133 g) 140 h) 142 i) PKD S-15 j) 128 k) 129 and l) 160 PKD-8

4.1.6 Kurtosis of Groundwater Level

The kurtosis of groundwater level of all the wells is shown in Table 4.6. Some wells showed a negative value of kurtosis which indicated a light peak in the distribution whereas other wells showed positive value of kurtosis which indicated a heavy peak. The highest positive kurtosis of 12.44 was seen for the well PKD S-3 in the month of February and the highest negative kurtosis of -1.7 was seen for the well 133 in November. High kurtosis indicated that the groundwater level data were more concentrated around the mean. The kurtosis of groundwater level is represented graphically in Fig 4.2.

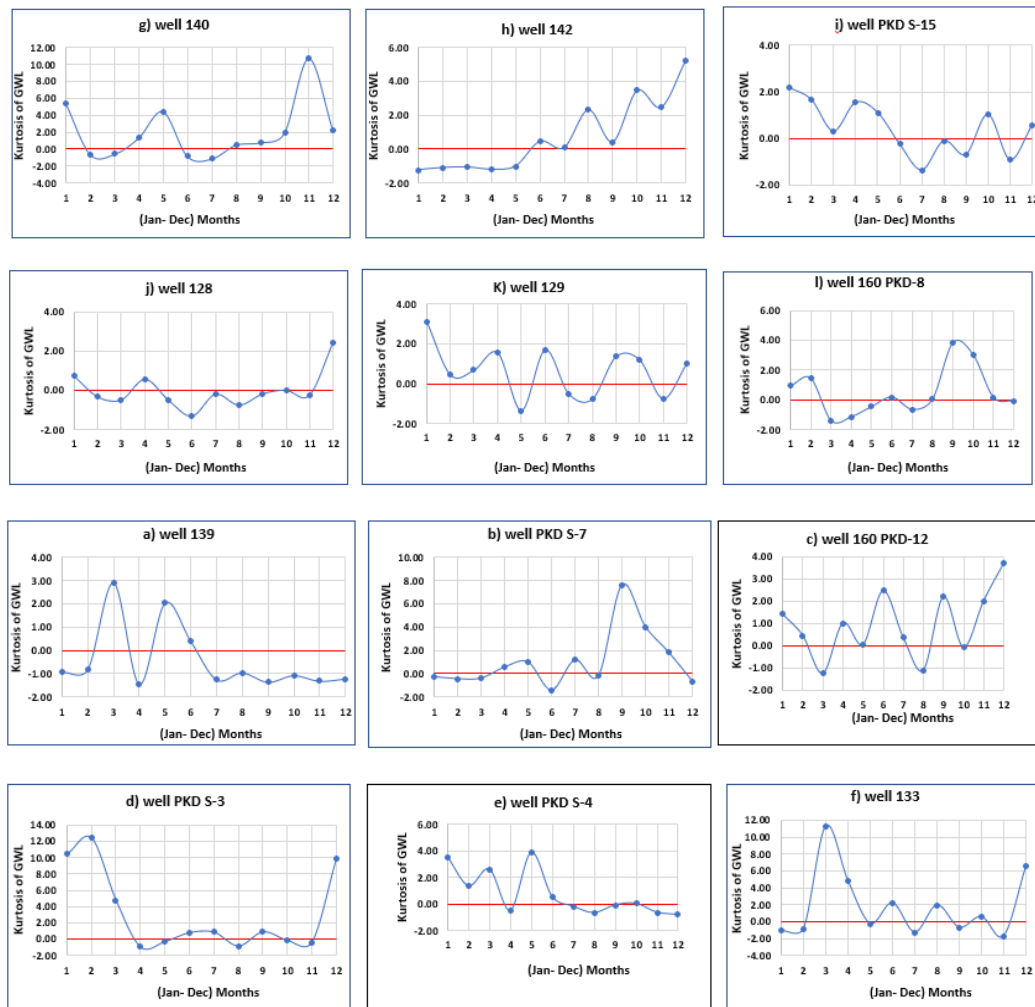


Fig 4.2 Kurtosis of groundwater level for wells a) 139 b) PKD S-7 c) 160 PKD-12 d) PKD S-3 e) PKD S-4 f) 133 g) 140 h) 142 i) PKD S-15 j) 128 k) 129 and l) 160 PKD-8

Table 4.1 Mean monthly groundwater level w.r.t MSL (m) during 2007-2021

Sl.No	Well ID	Jan	Feb	Mar	Apr	May	Jun	July	Aug	Sept	Oct	Nov	Dec
1	139	136	134.5	134.1	133.6	134.2	134.4	137.6	138.7	139.1	138.7	138	137.5
2	PKD S 7	149.7	149.2	148.9	148.6	148.8	149.5	150.7	151.2	151.3	151.1	150.9	150.4
3	160 PKD-12	68.7	68.4	67.7	67.5	67.6	68.2	68.9	68.7	68.8	68.7	68.7	68.5
4	PKD S-3	72.1	71.6	70.4	69.8	69.9	71.3	73	72.9	72.7	72.6	72.6	72.3
5	PKD S-4	63.7	63.4	62.3	62.6	63.2	64.2	64.9	64.7	64.6	64.5	64.4	64
6	133	108.5	108.1	107.7	107.8	108	108.9	111.6	112	111.7	110.9	110.8	109.4
7	140	86	85.6	84.7	84.5	84.8	85.4	86.5	86.7	86.9	86.6	86.2	86.2
8	142	101.5	100.9	100.2	100.6	100.3	101.9	104.7	105.7	106	105.3	105	103.8
9	PKD S-15	86.7	86.1	85.9	86.1	86.1	87.3	88.2	88.6	88.6	88	87.8	86.8
10	128	64.1	63.6	63	62.8	62.9	64	65.2	64.9	65	64.6	64.5	64.1
11	129	63.1	62.3	61.9	61.6	61.5	62	63.9	64.3	64.6	64	63.8	63.2
12	160PKD-8	79.9	79.1	77.5	78.9	80.2	82.4	84.4	84.5	84	83.9	83.4	81.7

Table 4.2 Annual mean groundwater level w.r.t MSL (m)

Sl. No	Well ID	2007	2008	2009	2010	2011	2012	2013	2014	2015	2016	2017	2018	2019	2020	2021
1	139	138.9	138.4	138.8	138.7	139.4	134.6	136.3	138.3	136.7	134	132.3	134.9	135.1	134.7	134.5
2	PKD S 7	150.3	150	149.8	150.2	150.7	149.9	149.6	150.1	150.9	148.9	148.2	149.8	150.1	150.6	151.4
3	160 PKD-12	68.5	68.4	68.4	68.6	68.6	68.7	68	68.5	68.4	68.3	67.9	68.5	67.8	68.2	68.4
4	PKD S-3	72.2	72.2	71.9	72.3	72.4	72	71.4	72	71.7	71.2	70.2	71.5	71.2	72	72.4
5	PKD S-4	64	64.3	63.9	63.7	64.1	63.8	63.2	63.7	64.2	63.9	63.4	63.8	63.7	64.2	64.3
6	133	110.3	109.6	110	110	110.3	109.3	108.9	109.4	109	108.9	109.1	109.6	109.9	109.6	110.4
7	140	86.1	85.9	86.1	86.1	86.4	85.7	85.8	85.6	85.5	85.3	85.3	86.1	85.6	85.9	85.9
8	142	106.5	105.2	105.4	103.9	105.3	104	103.9	103	102.4	100.5	99.4	101.3	99.5	100.6	103.5
9	PKD S-15	87.8	87.9	87.5	86.9	87.8	86.3	86.9	86.3	87.3	86.1	85.9	87.1	86.5	87.6	88.9
10	128	64	64.7	64.6	64.6	64.4	63.8	63.9	63.8	64.1	63.6	63.4	64.1	63.9	64	64.2
11	129	64.4	63.2	63.5	63.4	63.8	62.6	63.3	63	62.9	62.1	62.2	63.2	62.5	62.6	62.6
12	160PKD-8	81.2	83.2	82.6	82.4	83	81.2	80.3	79.6	81.9	80.6	80.4	82.5	81.1	82	83

Table 4.3 Monthly standard deviation of groundwater level (m)

Sl. No	Well ID	Jan	Feb	Mar	Apr	May	Jun	July	Aug	Sept	Oct	Nov	Dec
1	139	2.83	2.28	2.87	1.99	3.44	2.82	3.43	3.28	2.95	2.45	3.11	2.98
2	PKD S 7	1.02	0.99	1.15	1.37	1.39	1.77	1.17	0.59	0.66	0.78	1.04	1.22
3	160 PKD-12	0.23	0.42	0.51	0.62	0.89	1	0.17	0.26	0.19	0.26	0.37	0.39
4	PKD S-3	0.79	1.65	1.58	0.82	1.29	1.9	0.31	0.27	0.45	0.46	0.49	0.71
5	PKD S-4	0.54	0.51	1.28	1.05	0.83	0.66	0.26	0.24	0.24	0.27	0.36	0.31
6	133	0.42	0.28	0.89	0.3	0.4	1.54	1.35	0.7	1	1.48	1.25	1.95
7	140	0.34	0.38	0.39	0.53	0.68	1	0.72	0.67	0.51	0.47	1.4	0.39
8	142	4.08	3.81	3.51	3.5	2.9	3.18	2.58	1.88	1.38	2.04	2.11	2.85
9	PKD S-15	1.55	1.32	1.51	1.85	1.41	1.8	1.34	0.99	1.06	0.77	1.16	0.97
10	128	0.38	0.6	0.53	0.64	0.6	1.28	0.67	0.58	0.58	0.51	0.7	0.43
11	129	1.35	0.38	0.5	0.52	0.45	1.09	1.88	1.18	1.17	0.63	0.78	0.51
12	160PKD-8	1.94	2.21	2.63	2.76	2.57	2.09	0.55	1.36	2.35	1.66	1.41	1.81

Table 4.4 Monthly CV (%) of groundwater level

Sl. No	Wells ID	Jan	Feb	Mar	Apr	May	Jun	July	Aug	Sept	Oct	Nov	Dec
1	139	17.68	13.06	16.01	10.85	19.28	16.04	23.72	24.73	22.91	18.37	22.25	20.54
2	PKD S 7	45.4	35.22	36.76	39.82	44.04	72.05	90.47	74.8	90.1	85.66	92.04	76.79
3	160 PKD-12	17.15	26.32	22.27	24.98	37.11	55.6	15.51	20.42	16.58	19.39	27.69	26.72
4	PKD S-3	41.87	69.39	43.53	19.64	31.73	70.6	32	24.14	34.4	31.99	34.76	42.02
5	PKD S-4	16.59	14	27.04	23.84	21.9	23.49	12.16	10.26	9.85	10.85	14.03	10.64
6	133	9.25	5.77	16.76	5.72	8.09	37.45	93.3	72.5	77.4	69.56	57.16	53.94
7	140	8.55	8.69	7.33	9.58	13.03	21.85	20.49	20.48	16.16	13.89	36.59	10.23
8	142	35.63	31.49	27.38	28.36	22.86	28.67	30.98	25.83	19.81	26.51	26.46	31.03
9	PKD S-15	24.35	19.21	21.23	26.91	20.44	31.79	27.76	22.74	24	15.35	22.09	15.58
10	128	9.71	13.65	10.61	12.25	11.72	31.95	24.07	18.78	19.39	15.13	19.81	10.82
11	129	16.96	4.32	5.44	5.6	4.67	12.13	26.53	17.46	18.27	8.96	10.78	6.47
12	160PKD-8	15.98	17.12	18.15	21.11	21.81	21.83	7.34	18.17	29.47	20.49	16.37	17.6

Table 4.5 Skewness values of groundwater level

Sl. No	Wells ID	Jan	Feb	Mar	Apr	May	Jun	July	Aug	Sept	Oct	Nov	Dec
1	139	0.51	0.26	-1.36	0.58	-0.31	-0.08	-0.08	0.54	0.15	0.09	0.09	0.01
2	PKD S 7	0.72	0.43	0.41	-0.69	-0.59	0.06	1.22	0.76	2.42	2.02	1.39	0.7
3	160 PKD-12	1.42	1	0.09	0.36	0.81	1.78	0.85	0.65	1.65	0.26	1.31	1.73
4	PKD S-3	3.03	3.42	2.04	-0.07	0.5	1.2	1.24	-0.26	1.28	-0.03	0.51	2.88
5	PKD S-4	1.51	0.67	1.43	0.51	1.41	0.68	0.79	-0.55	0.1	-0.23	0.27	0.25
6	133	0.08	0.02	3.09	1.09	-0.42	-1.73	0.75	1.48	0.49	0.82	-0.05	2.13
7	140	-1.75	0.05	0.07	-0.57	-1.55	0.18	-0.23	-0.59	0.15	0.89	3.07	-0.96
8	142	0.65	0.54	0.29	0.38	0.41	0.54	0.66	1.33	-0.31	1.41	1.63	2
9	PKD S-15	-1.51	-1.44	-1.01	-1.23	-0.71	0.26	0.25	-0.01	-0.56	-0.27	-0.16	-0.88
10	128	0.63	0.48	-0.11	-1.24	-0.33	0.19	0.14	-0.18	0.39	0.69	-0.64	1.15
11	129	-1.94	0.47	-0.09	-1.13	0.19	-1.12	-0.75	-0.58	-0.83	0.73	-0.1	0.95
12	160PKD-8	-0.7	-1.35	-0.24	-0.14	0.2	0.77	0.18	0.21	1.84	1.02	0.82	0.37

Table 4.6 Kurtosis values of groundwater level

Sl. No	Wells ID	Jan	Feb	Mar	Apr	May	Jun	July	Aug	Sept	Oct	Nov	Dec
1	139	-0.92	-0.81	2.9	-1.45	2.02	0.39	-1.25	-0.95	-1.36	-1.07	-1.31	-1.22
2	PKD S 7	-0.26	-0.44	-0.39	0.55	1	-1.42	1.19	-0.19	7.6	4.02	1.82	-0.65
3	160 PKD-12	1.42	0.46	-1.25	1.02	0.05	2.48	0.38	-1.11	2.2	-0.08	2.02	3.72
4	PKD S-3	10.41	12.44	4.78	-0.97	-0.31	0.79	0.85	-0.84	0.9	-0.15	-0.4	9.9
5	PKD S-4	3.54	1.36	2.62	-0.5	3.9	0.54	-0.18	-0.68	-0.1	0.03	-0.64	-0.81
6	133	-1.07	-0.84	11.31	4.81	-0.25	2.22	-1.29	1.96	-0.7	0.58	-1.7	6.58
7	140	5.41	-0.59	-0.57	1.33	4.44	-0.8	-1.13	0.51	0.78	1.9	10.68	2.21
8	142	-1.23	-1.11	-1.07	-1.21	-1.02	0.45	0.08	2.33	0.42	3.47	2.48	5.25
9	PKD S-15	2.17	1.66	0.31	1.54	1.11	-0.24	-1.35	-0.09	-0.68	1.03	-0.9	0.56
10	128	0.72	-0.33	-0.48	0.57	-0.49	-1.31	-0.19	-0.75	-0.18	0.01	-0.24	2.43
11	129	3.13	0.44	0.7	1.57	-1.35	1.71	-0.5	-0.78	1.36	1.22	-0.75	1.01
12	160PKD-8	0.93	1.45	-1.4	-1.15	-0.45	0.19	-0.65	0.05	3.83	3.04	0.16	-0.08

4.2 TREND ANALYSIS OF GROUNDWATER LEVEL

The trend analysis of groundwater levels for all the twelve wells in the study area during the period 2007 to 2021 was done for pre-monsoon (Mar-May), post-monsoon (Sept-Nov) and annually using Mann-Kendall test and Sen's slope estimator. The trend analysis was done in the XLSTAT software. If the P value is less than the α value, there exist a trend and if the slope is negative the trend is decreasing otherwise increasing. Halder et al., (2020) used the same software XLSTAT for trend analysis of groundwater level and similar results were obtained.

4.2.1 Pre-Monsoon, Post-Monsoon and Annual Groundwater Level Trend

The Mann-Kendall trend analysis results of pre-monsoon, post-monsoon and annual groundwater level are given in Table 4.7, Table 4.8 and Table 4.9 respectively. The pre-monsoon groundwater level trend analysis results showed a decreasing trend in wells 129, 133 and 142 while all other wells showed no trend. The post-monsoon groundwater level trend analysis results showed a decreasing trend in well 139 and all other wells showed no trend. The annual groundwater level trend analysis results showed a decreasing trend in wells 129, 139 and 142 while all other wells showed no trend.

Table 4.7 Mann-Kendall trend analysis of pre-monsoon groundwater level

Sl. No	Well ID	S	VAR(S)	P	α	Slope	Trend
1	128	-31	408.333	0.138	0.05	-0.073	No
2	129	-60	407.333	0.003	0.05	-0.08	Decreasing
3	133	-43	408.333	0.038	0.05	-0.013	Decreasing
4	139	-33	408.333	0.113	0.05	-0.298	No
5	140	-21	408.333	0.322	0.05	-0.019	No
6	142	-67	408.333	0.001	0.05	-0.605	Decreasing
7	160 PKD 12	11	408.333	0.621	0.05	0.01	No

8	160 PKD S8	3	408.333	0.921	0.05	0.012	No
9	PKD S3	-11	408.333	0.621	0.05	-0.031	No
10	PKD S7	13	408.333	0.553	0.05	0.053	No
11	PKD S 15	-13	408.333	0.553	0.05	-0.003	No
12	PKD S 4	4	407.333	0.882	0.05	0.004	No

Table 4.8 Mann-Kendall trend analysis of post-monsoon groundwater level

Sl. No	Well ID	S	VAR	P	α	Slope	Trend
1	128	-23	408.333	0.276	0.05	-0.022	No
2	129	-19	408.333	0.373	0.05	-0.05	No
3	133	-11	408.333	0.621	0.05	-0.051	No
4	139	-46	407.333	0.026	0.05	-0.37	Decreasing
5	140	-29	408.333	0.166	0.05	-0.042	No
6	142	-31	408.333	0.138	0.05	-0.149	No
7	160 PKD 12	-20	407.333	0.346	0.05	-0.023	No
8	160 PKD S8	-14	407.333	0.519	0.05	-0.042	No
9	PKD S3	-39	408.333	0.06	0.05	-0.035	No
10	PKD S7	11	408.333	0.621	0.05	0.015	No
11	PKD S 15	-15	408.333	0.488	0.05	-0.044	No
12	PKD S 4	-32	407.333	0.125	0.05	-0.019	No

Table 4.9 Mann-Kendall trend analysis of annual groundwater level

Sl. No	Well ID	S	VAR	P	α	Slope	Trend
1	128	-31	408.333	0.138	0.05	-0.049	No
2	129	-59	408.333	0.004	0.05	-0.092	Decreasing
3	133	-9	408.333	0.692	0.05	-0.02	No
4	139	-61	408.333	0.003	0.05	-0.382	Decreasing
5	140	-35	408.333	0.092	0.05	-0.045	No
6	142	-73	408.333	0	0.05	-0.471	Decreasing
7	160 PKD 12	-24	407.333	0.254	0.05	-0.02	No
8	160 PKD S8	-13	408.333	0.553	0.05	-0.035	No
9	PKD S3	-29	408.333	0.166	0.05	-0.056	No
10	PKD S7	-1	408.333	1	0.05	-0.001	No
11	PKD S 15	-17	408.333	0.428	0.05	-0.063	No
12	PKD S 4	-2	407.333	0.96	0.05	-0.005	No

4.2.2 Spatial Distribution of Groundwater Level Trend in the Study Area

The spatial distribution of groundwater level trend during pre-monsoon, post-monsoon and annual is shown in Fig 4.3 (a), (b) and (c) respectively. From figure it is clear that during pre-monsoon two wells 133 and 142 of Malampuzha block and one well 129 of Palakkad block, during post-monsoon well 139 of Chittur block and during annual period well 139 of Chittur block, 142 of Malampuzha block and well 129 of Palakkad block showed a decreasing trend. The declining trend in the groundwater level was seen in the wells located in areas of increased water abstraction. The areas of Chittur, Malampuzha and Palakkad blocks are experiencing water scarcity in extreme summer due to the declining of groundwater level.

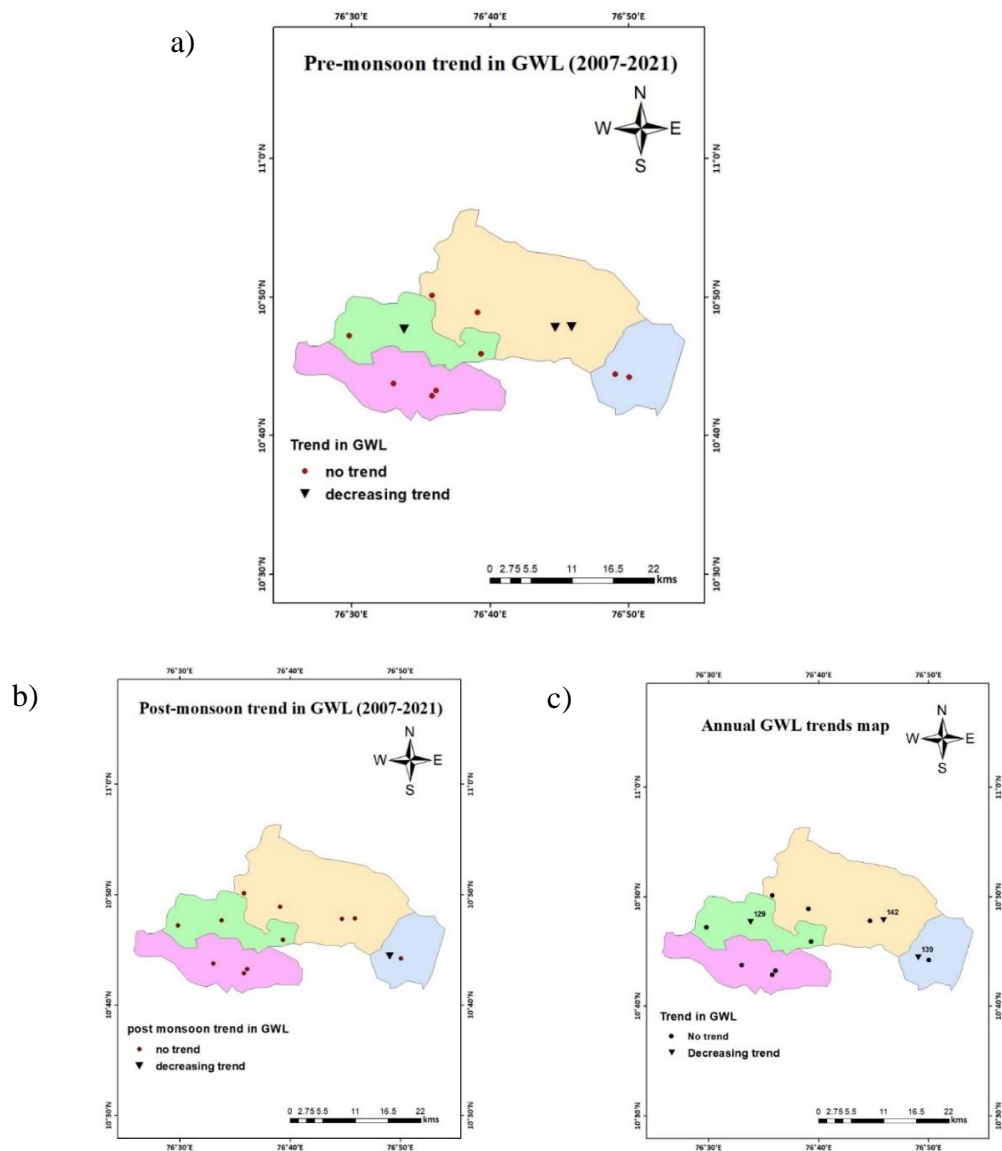


Fig 4.3 Spatial distribution of groundwater level a) pre-monsoon, b) post-monsoon and c) annual.

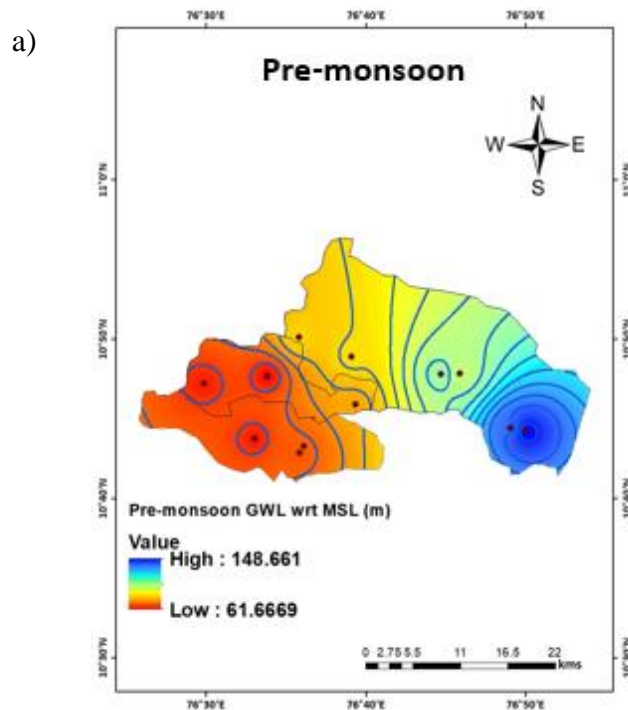
4.3 WATER TABLE CONTOUR MAP OF THE STUDY AREA

The water table contour map of the study area was generated during the study period (2007 to 2021) in Arc GIS using IDW interpolation technique. The average elevation of the well locations was about 96.25 m above MSL. The ground level elevation varied from 67 m at well PKD S-4 of Kuzhalmannam block to 152 m at wells 139 and PKD S-7 of Chittur block. The water table contour maps were

prepared for pre-monsoon (Fig 4.4 (a)), post-monsoon (Fig 4.4 (b)) and average annual (Fig 4.4 (c)) period.

4.3.1 Pre-Monsoon, Post-Monsoon and Average Annual Water Table Contour Map

The pre-monsoon water table elevation of wells varied from 148.66 m in well PKD S-7 of Chittur block to 61.66 m in well 129 of Palakkad block as shown in Fig 4.4 (a). The post-monsoon water table elevation of wells varied from 151.21 m in well PKD S-7 of Chittur block to 64.16 m in well 129 of Palakkad block as shown in Fig 4.4 (b). The average annual water table elevation of wells varied from 150.02 m in well PKD S-7 of Chittur block to 63.02 m in well 129 of Palakkad block as shown in Fig 4.4 (c).



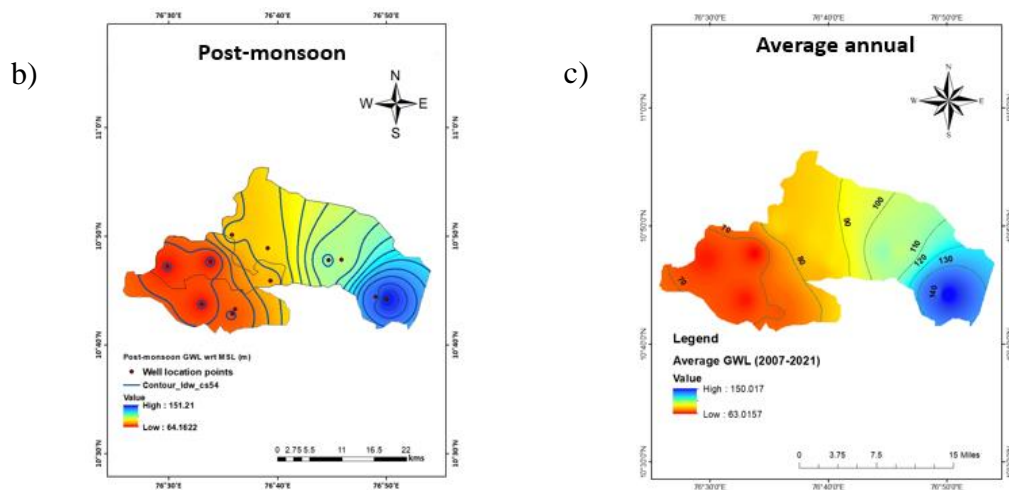


Fig 4.4 Water table contour map (a) Pre-monsoon, (b) Post-monsoon and (c) average annual

4.4 GROUNDWATER LEVEL FLUCTUATION

Groundwater level fluctuation was calculated as the difference between post- monsoon and pre-monsoon groundwater levels. The average annual seasonal fluctuation of groundwater level for the study period is shown in Fig 4.5. The average annual seasonal fluctuation of groundwater level varied from 1 to 5 m at different locations of the study area. The groundwater level fluctuation was classified into five groundwater level fluctuation zones viz; (i) 1 m to 2 m, (ii) 2 m to 3 m, (iii) 3 m to 4 m, (iv) 4 m to 5 m. The major portion of the study area was found to have a groundwater level fluctuation of 2 m to 3 m, which comprises of well PKD S-4 of Kuzhalmannam block, wells PKD S-15 and 142 of Malampuzha block. A small portion of the study area was found to have a groundwater level fluctuation of 1 m to 2 m, which comprises of wells PKD S-3 and 160 PKD-12 of Kuzhalmannam block, well 129 of Palakkad block, well 133 of Malampuzha and well 139 of Chittur block, which indicated less water abstraction in those wells. The portion with 4 m to 5 m groundwater level fluctuation included the wells 140 and 160 PKD-8 of Malampuzha block and well PKD S-7 of Chittur block, which is due to the higher elevation and excess usage of groundwater. The well 128 of Palakkad block showed a groundwater level fluctuation of 3 m to 4 m.

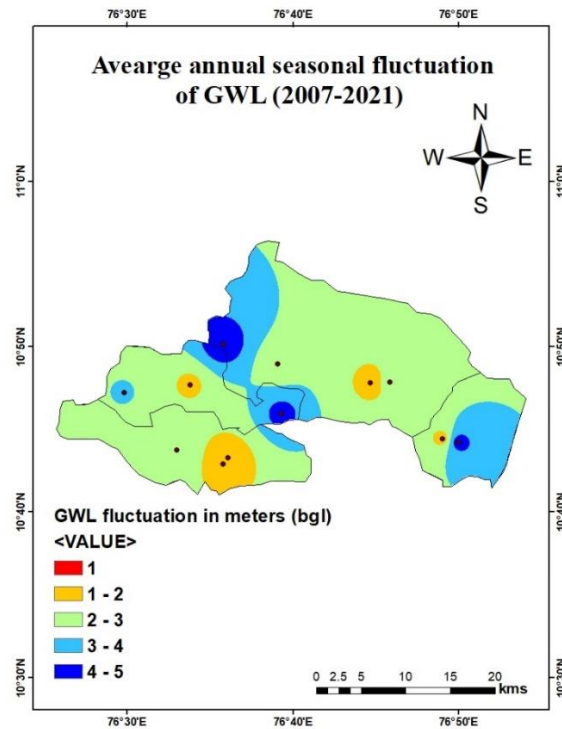


Fig 4.5 Average annual seasonal fluctuation of groundwater level

4.5 DEVELOPMENT OF ANN MODEL FOR GROUNDWATER LEVEL PREDICTION

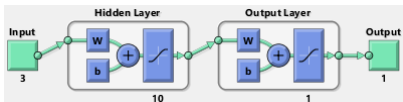

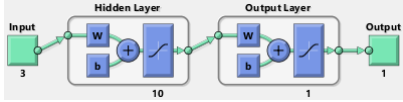
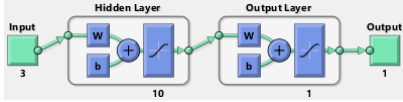
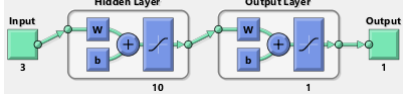
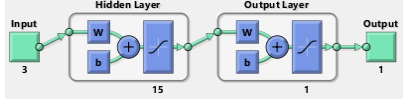
Groundwater level fluctuation is non-linear phenomenon; hence the soft computing technique ANN was used for modelling the groundwater level. Modelling was done using MATLAB R2016a software. Precipitation, minimum temperature and maximum temperature were used as the input data whereas observed groundwater level was taken as the target data for the development of ANN model. Similar input variables and target variables were used in a study conducted by Javadinejad *et al.*, (2020) and Husna *et al.*, (2016) and satisfactory results were obtained. These models offer a reasonable prediction of the future trend of the output. Models were developed separately for each individual observation wells. Thus, twelve ANN models were developed in this study.

The data were divided into two groups, viz, training dataset and testing dataset. Monthly data from 2007 to 2021 was used, which consist of 180 datasets

out of which 70% was used for training and 30% was used for testing. Using training dataset, different ANN structures were trained. Several ANN structures with feed forward back propagation algorithm, Levenberg-Marquardt learning algorithm and hyperbolic tangent as an activation function were tried and their performance in meeting the desired output were monitored. Thus, the best model for each well were selected. The study conducted by Seo and lee (2019) used feed forward back propagation algorithm, Levenberg-Marquardt learning algorithm and hyperbolic tangent as an activation function to develop ANN model for groundwater level prediction and similar results were obtained.

The performance of ANN models for the training and testing period were analysed based on values of correlation coefficient (r), coefficient of determination (R^2), Mean Square Error (MSE) and Root Mean Square Error (RMSE). The ANN structure with maximum r & R^2 and minimum RMSE & MSE was selected as the best model for each well. The most suitable configuration and ANN structure, feed forward network trained with the Levenberg–Marquardt function is shown in Table 4.10.

Table 4.10 The developed ANN configuration and its structure for groundwater level prediction.

Well ID	Training	Testing
	Best ANN structure	Best ANN structure
160 PKD-12	<p>3-10-1</p> 	<p>3-10-1</p> 
PKD S-3	<p>3-10-1</p> 	<p>3-10-1</p> 
PKD S-4	<p>3-10-1</p> 	<p>3-15-1</p> 

128	<p>3-12-1</p>	<p>3-10-1</p>
129	<p>3-10-1</p>	<p>3-14-1</p>
160 PKD-8	<p>3-10-1</p>	<p>3-10-1</p>
133	<p>3-13-1</p>	<p>3-10-1</p>
140	<p>3-12-1</p>	<p>3-12-1</p>
142	<p>3-10-1</p>	<p>3-13-1</p>
PKD S-15	<p>3-10-1</p>	<p>3-10-1</p>
139	<p>3-13-1</p>	<p>3-10-1</p>
PKD S-7	<p>3-10-1</p>	<p>3-10-1</p>

ANN structures show three layers in which 1st layer contain three neurons that indicates three input variables, 2nd layer is hidden layer and number of neurons in the hidden layer were altered in order to get the best ANN structure, 3rd layer output layer which contains only one neuron due to the single output variable as groundwater level. Hence, the model configuration for first well 160 PKD-12 is represented as 3-10-1 for training period and 3-10-1 for testing period. The number of hidden layers might vary during training and testing period; accordingly, the model configuration will also vary for example for well PKD S-4 the model during training period is represented as 3-10-1 whereas model during testing period is represented as 3-15-1. The models developed are saved in MATLAB software and can be recalled at any time for prediction.

4.5.1 Performance Evaluation of ANN Models

In order to assess the performance of the developed model, various statistical performance indicators viz, correlation coefficient (r), coefficient of determination (R^2) and Root Mean Square Error (RMSE) were assessed and the results are shown in Table 4.11.

Table 4.11 Performance indicators of ANN models developed for different wells

Well ID	Training dataset			Testing dataset		
	r	R^2	RMSE (m)	r	R^2	RMSE (m)
160 PKD-12	0.87	0.76	0.34	0.87	0.76	0.17
PKD S-3	0.83	0.69	0.43	0.88	0.77	0.17
PKD S-4	0.92	0.85	0.68	0.9	0.81	0.26
128	0.85	0.72	0.6	0.9	0.8	0.31
129	0.85	0.72	0.44	0.93	0.87	0.45
160 PKD-8	0.87	0.76	0.34	0.89	0.8	0.17
133	0.87	0.76	0.48	0.91	0.83	0.22
140	0.84	0.71	0.4	0.87	0.75	0.33

142	0.84	0.71	0.53	0.89	0.8	0.34
PKD S-15	0.84	0.71	0.42	0.89	0.79	0.35
139	0.84	0.71	0.54	0.74	0.55	0.38
PKD S-7	0.86	0.74	0.43	0.89	0.8	0.11

The value of r and R^2 highest and the values of RMSE lowest indicates that the performance indicators are in the acceptable range. The maximum r (0.92 and 0.93) and R^2 (0.85 and 0.87) were found for well PKD S-4 and 129 during training and testing period respectively. The minimum RMSE value was 0.34 m for wells 160 PKD-12 and 160 PKD-8 during training period and 0.17 m in well PKD S-7 during testing period respectively.

4.5.2 Regression Plots of Different ANN Models for Training and Testing Dataset

MATLAB plots the linear regression of targets relative to outputs and helps to visualize their linear relationships which is given by the regression plots. A high value of R (approximately equal to 1) in the regression plot indicates good correlation between output and target. The regression plots of different ANN models for training and testing dataset are shown in Fig 4.6 (a) to Fig 4.6 (l).

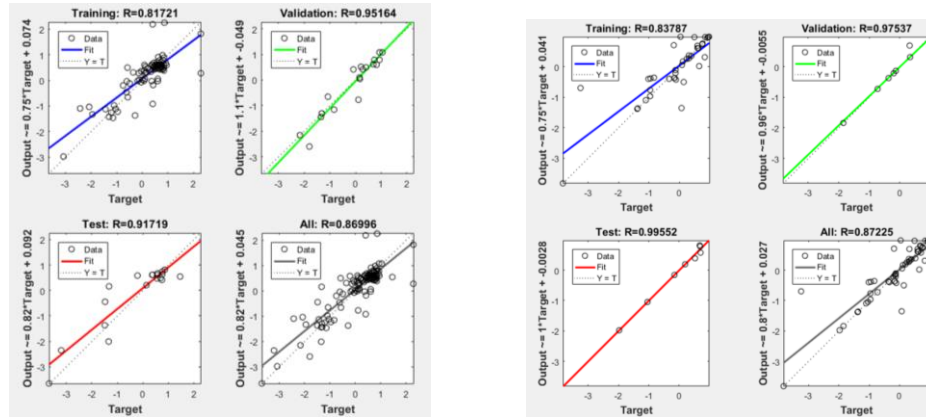


Fig 4.6 (a) Regression plot for training and testing period of well 160 PKD-12

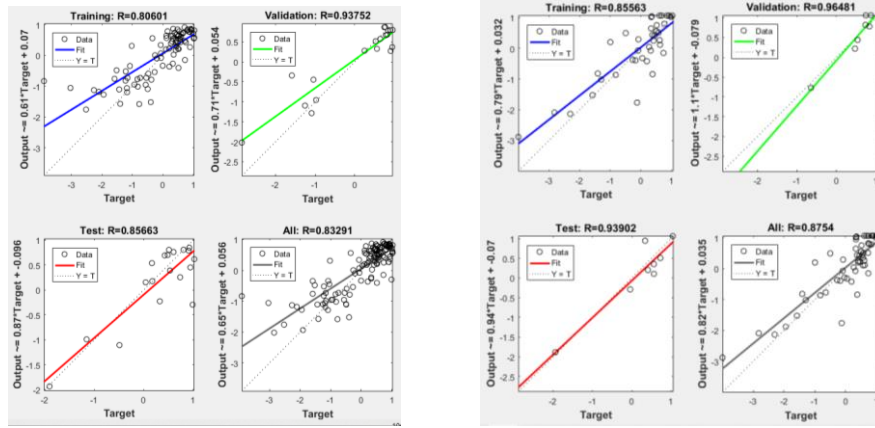


Fig 4.6 (b) Regression plot for training and testing period of well PKD S-3

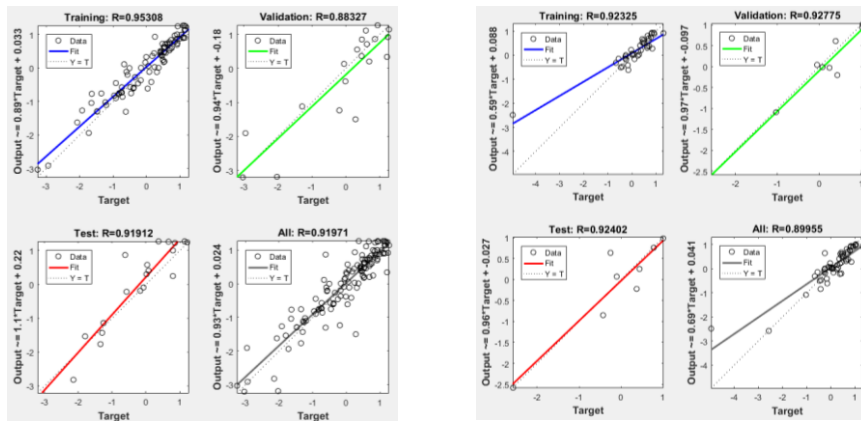


Fig 4.6 (c) Regression plot for training and testing period of well PKD S-4

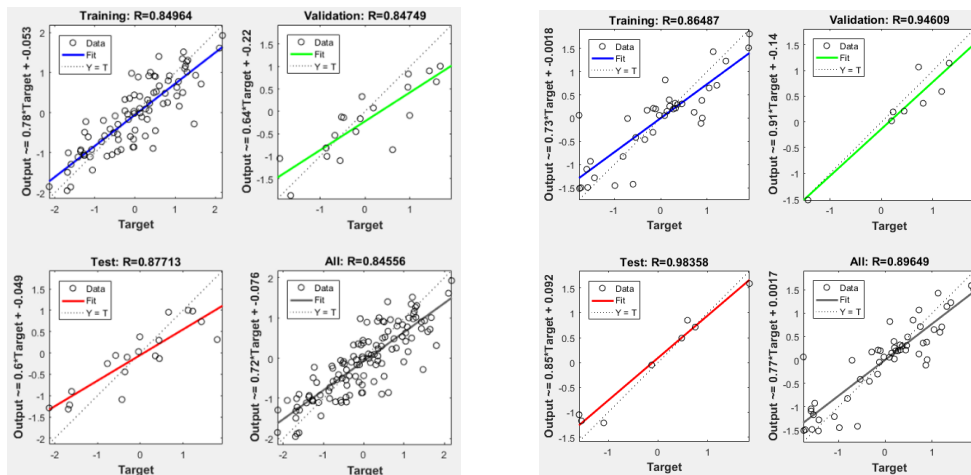


Fig 4.6 (d) Regression plot for training and testing period of well 128

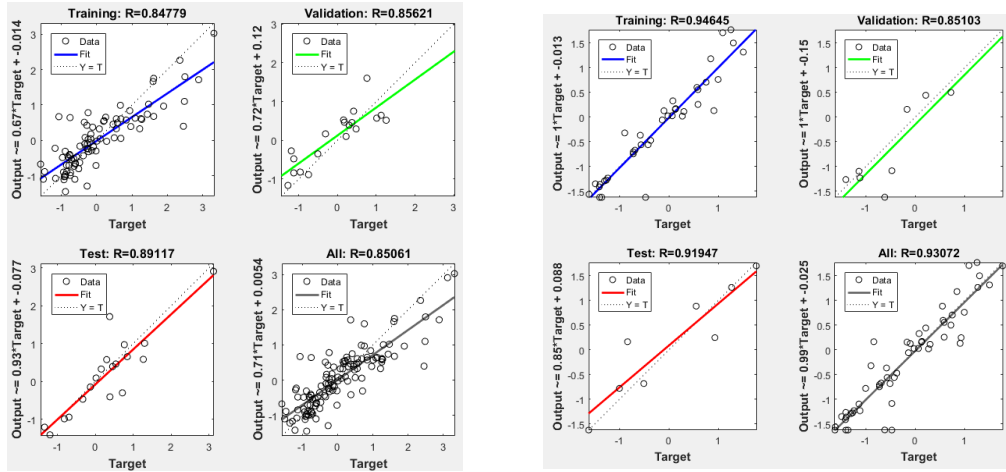


Fig 4.6 (e) Regression plot for training and testing period of well 129

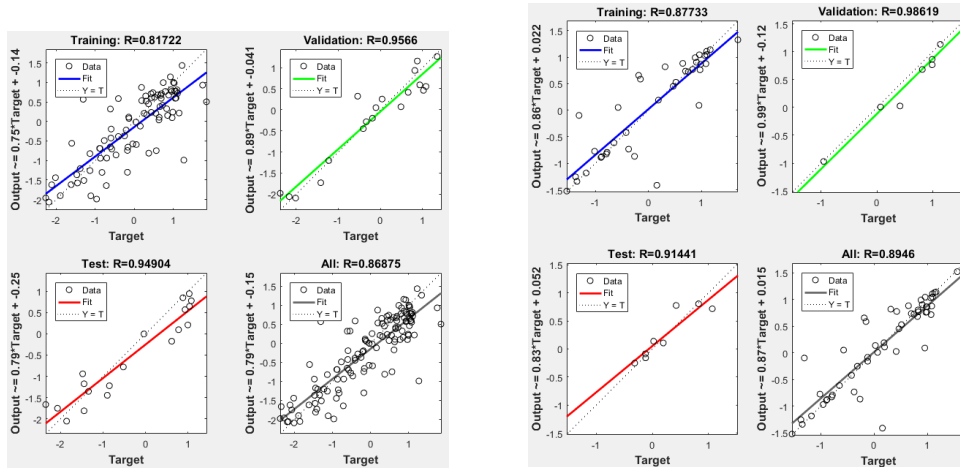


Fig 4.6 (f) Regression plot for training and testing period of well 160 PKD 8

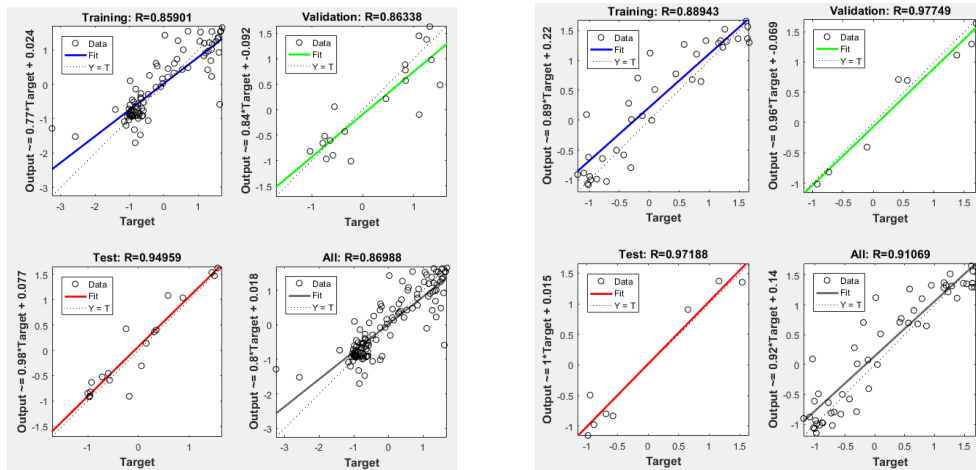


Fig 4.6 (g) Regression plot for training and testing period of well 133

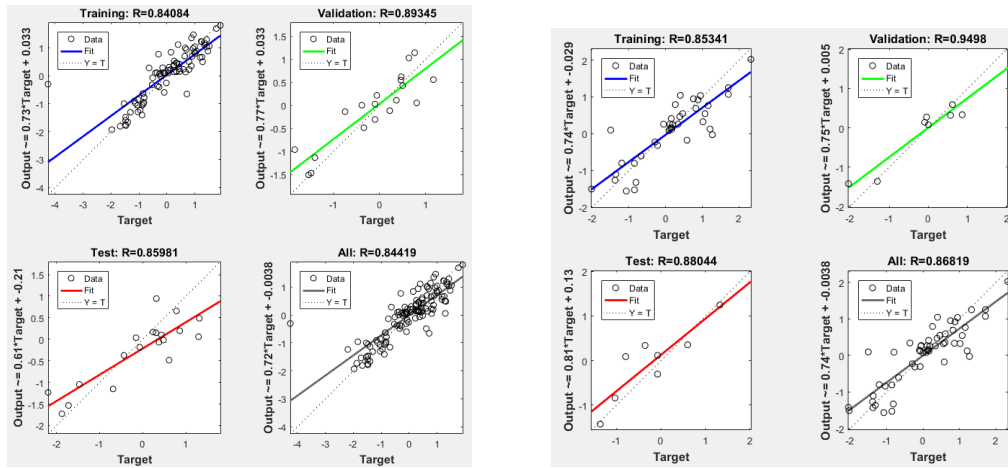


Fig 4.6 (h) Regression plot for training and testing period of well 140

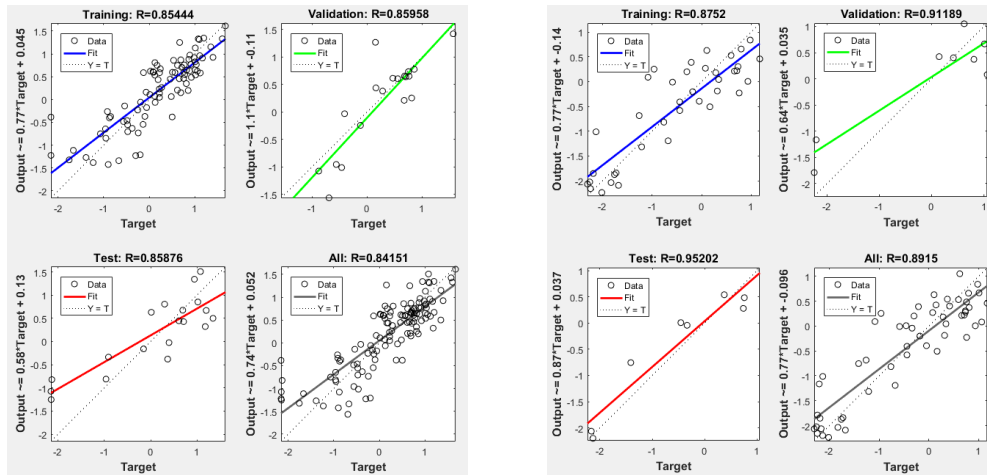


Fig 4.6 (i) Regression plot for training and testing period of well 142

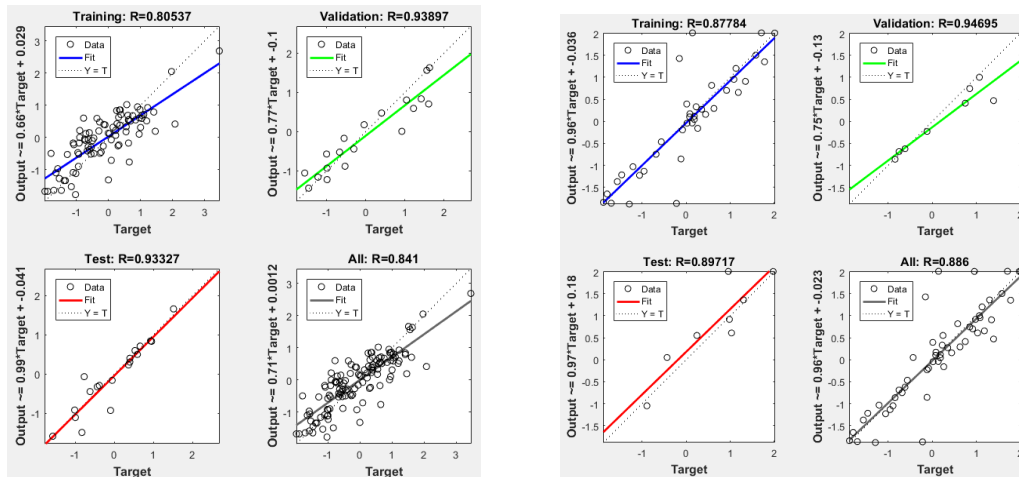


Fig 4.6 (j) Regression plot for training and testing period of well PKD S-15

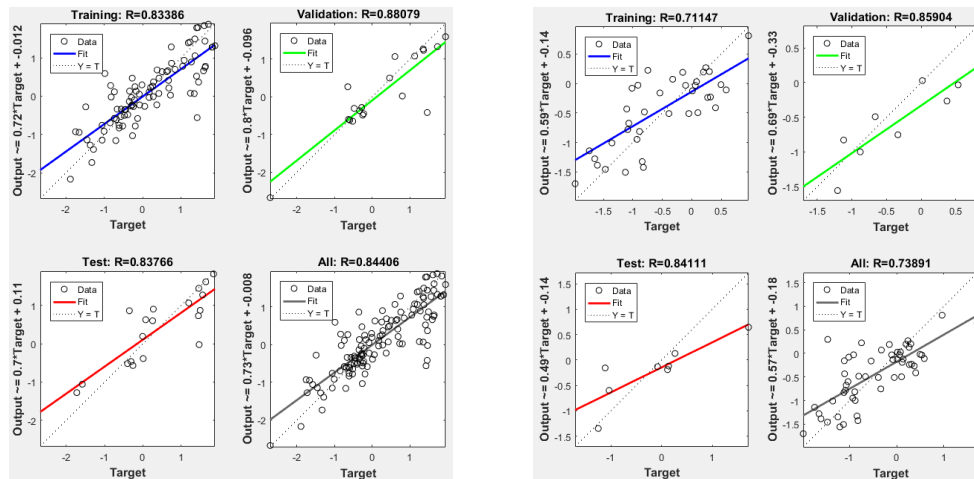


Fig 4.6 (k) Regression plot for training and testing period of well 139

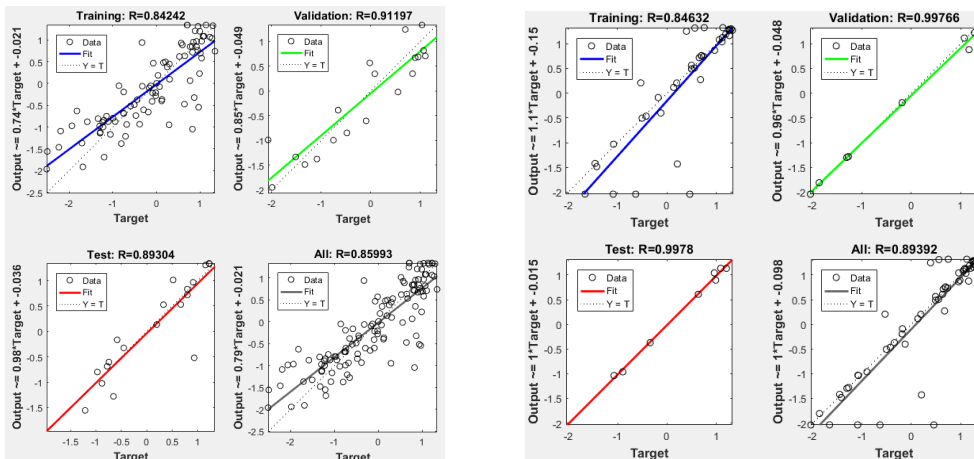


Fig 4.6 (l) Regression plot for training and testing period of well PKD S-7

4.5.3 Observed vs ANN Predicted Groundwater Level Plots of Different Wells

The observed and ANN predicted groundwater level for training and testing datasets were plotted and are shown in the Fig 4.7 (a) to Fig 4.7 (l). The observed and ANN predicted groundwater level for sample wells from each block is given in Appendix-II. It was observed that the predicted groundwater level was in good agreement with the observed groundwater level. This showed that Artificial Neural Network (ANN) had ample potential to predict the groundwater level with reasonable deviation from the observed values of groundwater level.

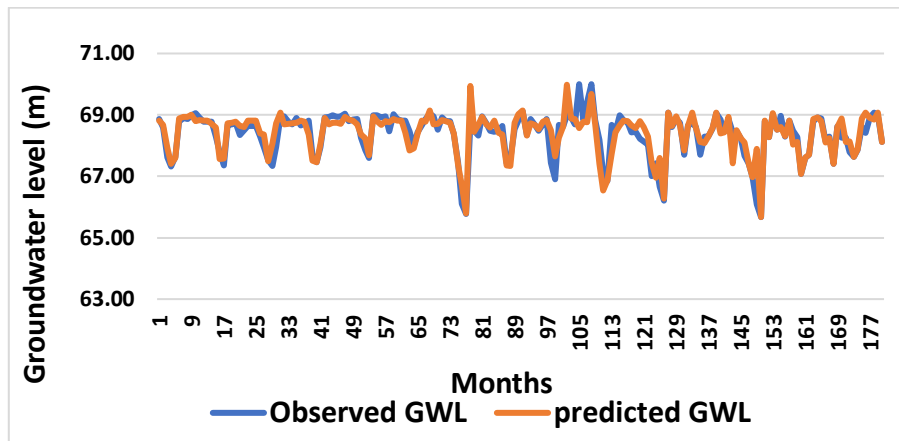


Fig. 4.7 (a) Observed vs ANN predicted groundwater level of well 160 PKD-12

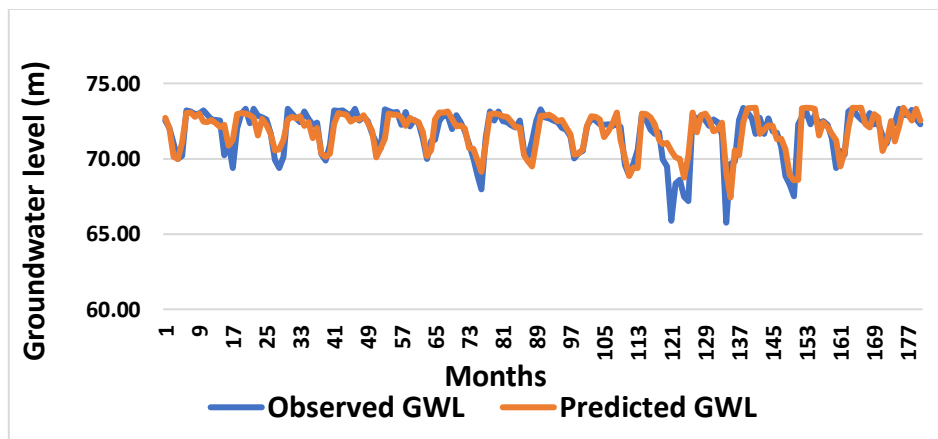


Fig. 4.7 (b) Observed vs ANN predicted groundwater level plot of well PKD S-3

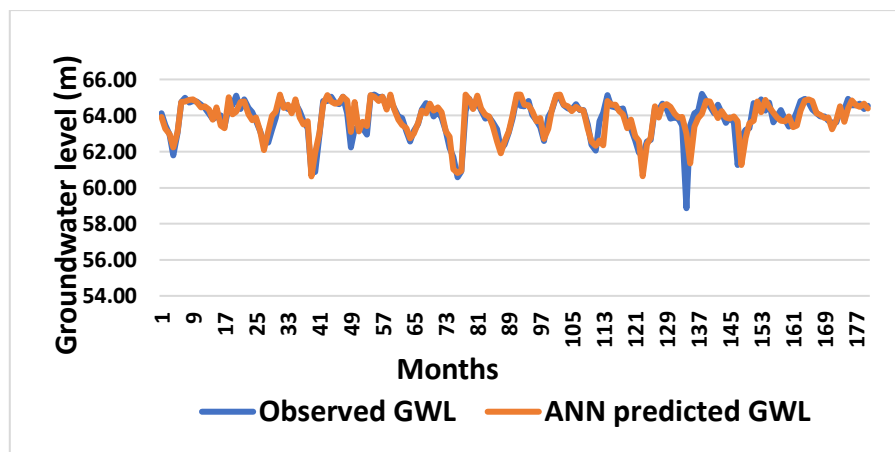


Fig. 4.7 (c) Observed vs ANN predicted groundwater level plot of well PKD S-4

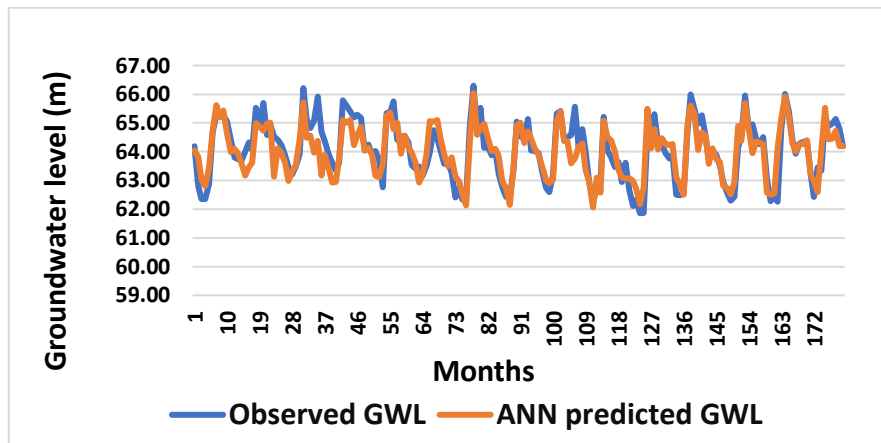


Fig. 4.7 (d) Observed vs ANN predicted groundwater level plot of well 128

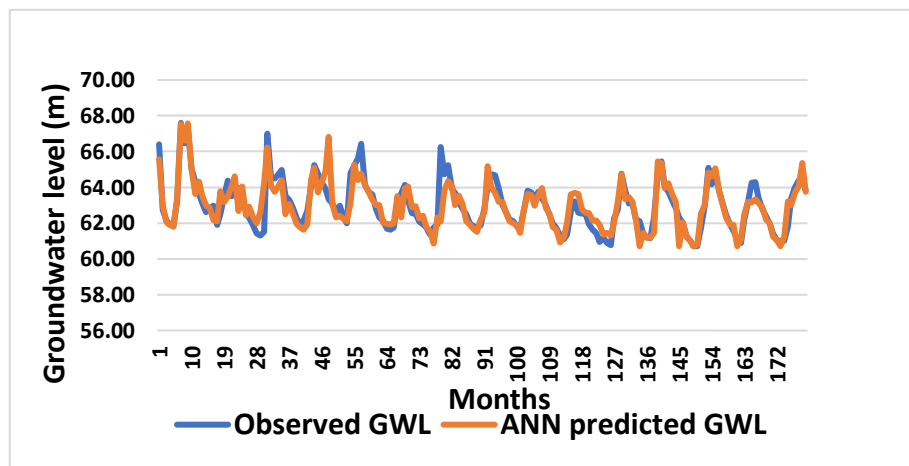


Fig. 4.7 (e) Observed vs ANN predicted groundwater level of well 129

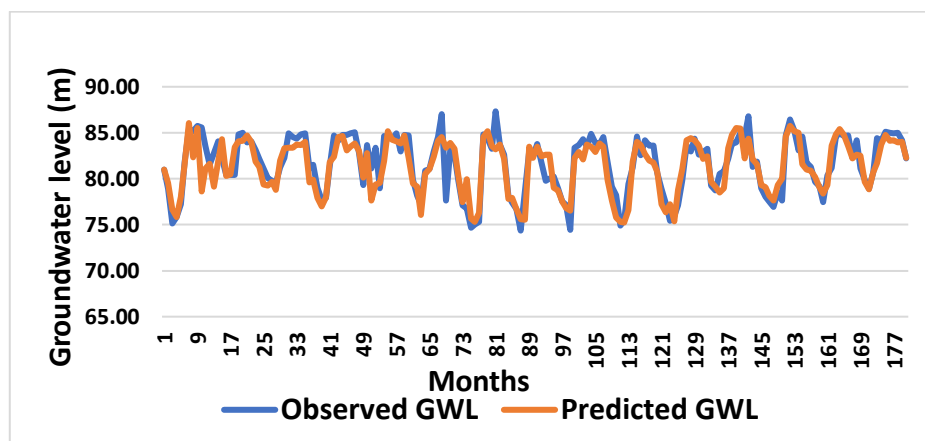


Fig. 4.7 (f) Observed vs ANN predicted groundwater level of well 160 PKD-8

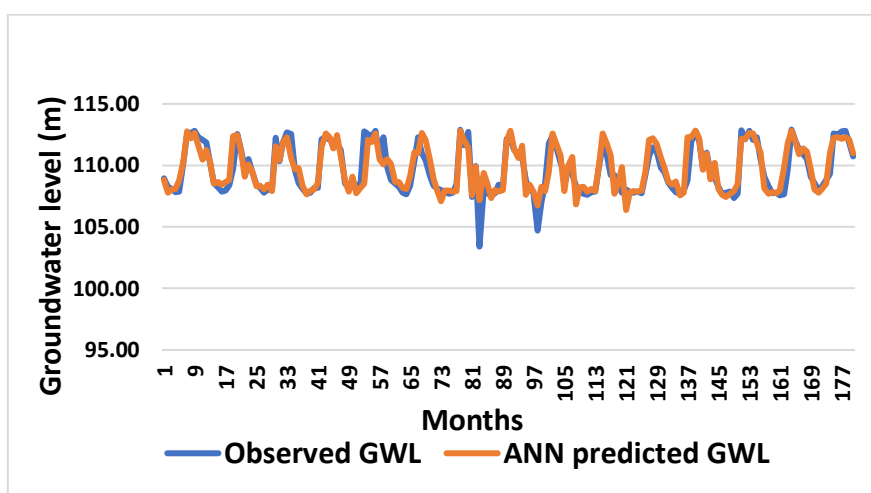


Fig. 4.7 (g) Observed vs ANN predicted groundwater level of well 133

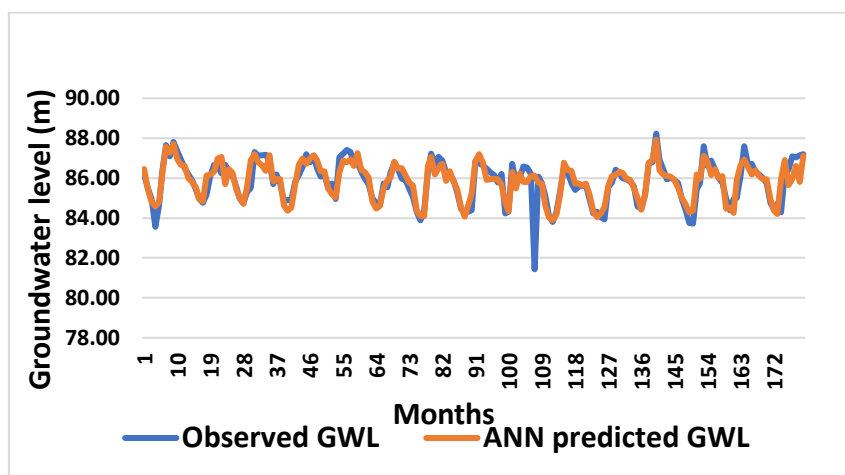


Fig. 4.7 (h) Observed vs ANN predicted groundwater level of well 140

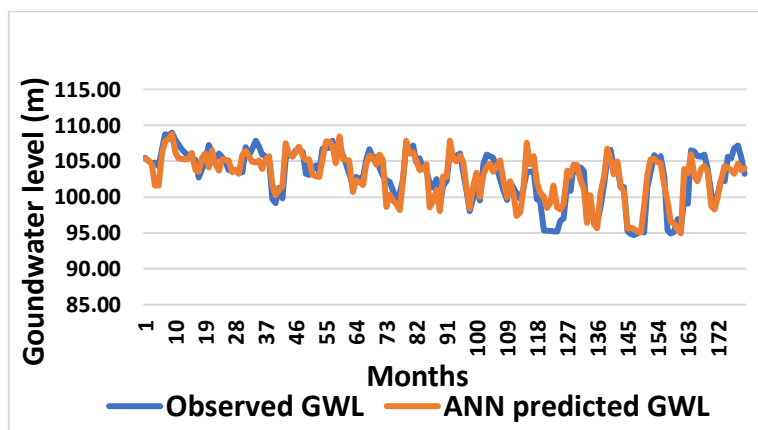


Fig. 4.7 (i) Observed vs ANN predicted groundwater level of well 142

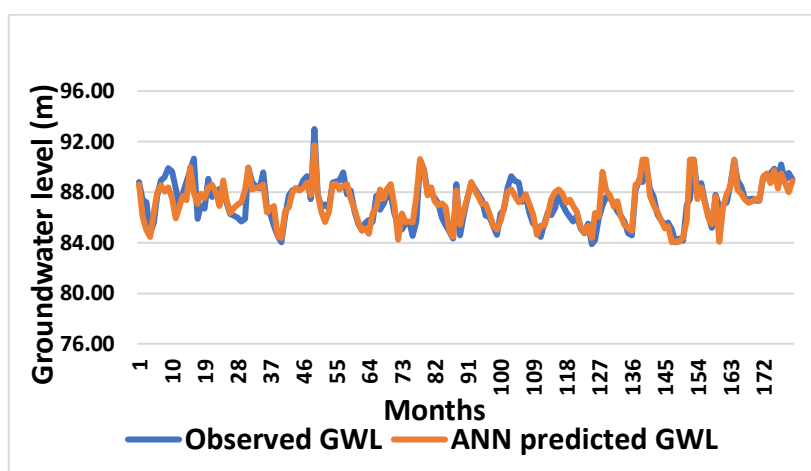


Fig. 4.7 (j) Observed vs ANN predicted groundwater level of well PKD S-15

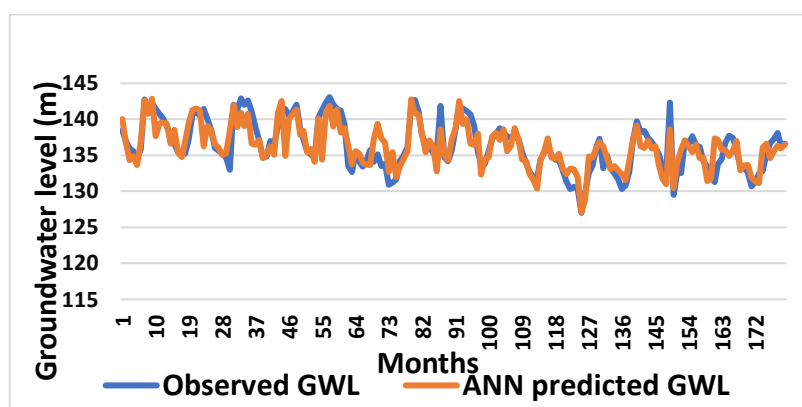


Fig. 4.7 (k) Observed vs ANN predicted groundwater level of well 139

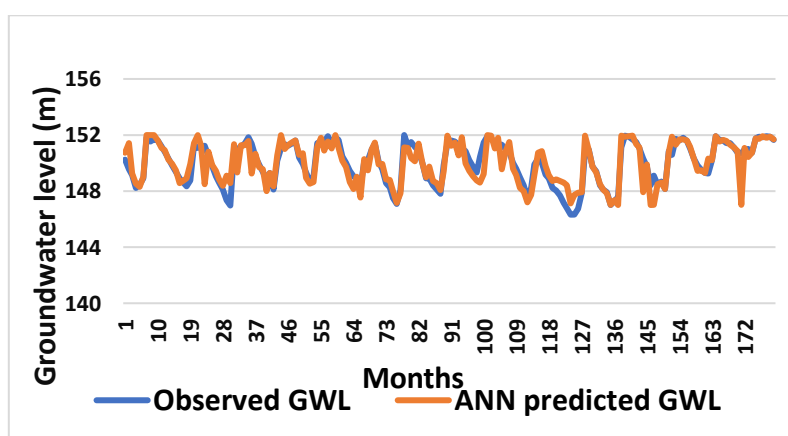


Fig. 4.7 (l) Observed vs ANN predicted groundwater level of well PKD S-7

4.6 GROUNDWATER DROUGHT ASSESSMENT

4.6.1 Estimation of SGI Values for Different Wells

Groundwater drought was assessed using Standardized Groundwater level Index (SGI). The SGI was estimated using observed groundwater level and also the ANN predicted groundwater level, and were compared. The SGI was estimated for pre-monsoon months Jan, Feb, Mar, Apr, May of the study period (2007 to 2017) for all the twelve wells as drought was more severe in these months than other months. The value of SGI indicates the drought severity, more the negative value, more the drought severity. The following tables shows the SGI values of different wells in the study area. Standardized Groundwater level Index was used by Halder *et al.*, (2020) and Seo and Lee (2019) for groundwater drought assessment and similar results were obtained.

The SGI values estimated using observed groundwater level for the wells 160 PKD-12, PKD S-3 and PKD S-4 of Kuzhalmannam block are shown in Table 4.12, Table 4.13 and Table 4.14 respectively. The SGI values estimated using the ANN predicted groundwater level is given in Appendix-VI. For well 160 PKD-12 the highest negative SGI was -3.7 found in May 2013. For well PKD S-3 the highest negative SGI was -4 found in March 2018. Similarly, for the well PKD S-4 the highest negative SGI was -3.3 found in April 2013 which indicated the highest exceptional drought condition of the respective regions.

Table 4.12 Estimated SGI values of well 160 PKD-12

Well 160 PKD-12	Jan	Feb	Mar	Apr	May
2007	0.7	0.3	-1.1	-1.5	-1.0
2008	0.6	0.6	-0.1	-0.8	-1.4
2009	0.4	-0.1	-0.6	-1.2	-1.5
2010	0.5	0.6	-1.0	-1.3	-0.6
2011	0.7	0.7	-0.2	-0.7	-1.1
2012	0.6	0.6	0.1	-0.6	0.1
2013	0.6	0.0	-1.3	-3.2	-3.7

2014	0.2	0.4	-1.3	-1.1	0.2
2015	0.7	-1.3	-2.1	0.4	0.3
2016	0.6	-0.3	-1.8	-2.2	0.4
2017	-0.4	-0.5	-1.9	-1.3	-2.4
2018	0.5	0.3	-0.9	-0.1	-0.1
2019	-0.2	-1.0	-1.4	-2.0	-3.2
2020	0.6	0.1	-0.2	-1.9	-1.1
2021	0.3	-0.2	-0.2	-0.8	-1.0

Table 4.13 Estimated SGI values of well PKD S-3

Well PKD S-3	Jan	Feb	Mar	Apr	May
2007	0.5	0.2	-0.5	-1.2	-1.0
2008	0.5	0.5	-1.0	-0.5	-1.6
2009	0.6	0.2	-0.1	-1.2	-1.6
2010	0.3	0.4	-1.0	-1.3	-0.6
2011	0.7	0.5	-0.1	-0.5	-0.7
2012	0.5	0.4	-0.3	-1.2	-0.4
2013	0.0	-0.5	-1.2	-1.9	-2.5
2014	0.2	0.5	-0.8	-1.1	-0.4
2015	0.1	-0.2	-1.2	-0.9	-0.8
2016	0.3	0.2	-1.4	-1.9	-1.4
2017	-1.5	-3.9	-2.3	-2.1	-2.9
2018	0.4	-0.1	-4.0	-1.4	-1.3
2019	0.0	0.0	-0.6	-1.9	-2.3
2020	0.5	0.3	-0.3	-1.6	-0.8
2021	0.3	0.4	-0.2	-0.5	0.2

Table 4.14 Estimated SGI values of well PKD S-4

Well PKD S-4	Jan	Feb	Mar	Apr	May
2007	0.2	-0.4	-0.9	-2.1	-0.8
2008	0.2	-0.1	0.0	0.1	-0.5
2009	-0.2	-0.8	-1.4	-1.4	-0.7
2010	-0.2	-0.6	-3.0	-3.0	-1.0
2011	-1.6	-0.6	-0.5	-0.6	-0.9
2012	0.1	0.0	-0.7	-1.3	-0.7
2013	-0.7	-1.6	-2.2	-3.3	-2.9
2014	-0.3	-0.6	-1.7	-1.5	-0.8
2015	-0.5	-1.3	0.0	0.4	1.2
2016	-0.4	-1.5	-1.8	-0.2	0.3
2017	-1.2	-1.9	-2.0	-1.3	-1.2
2018	-0.4	-0.5	-0.4	0.2	0.4
2019	0.0	-0.2	-2.6	-1.0	-0.7
2020	0.1	0.4	-0.1	-0.5	-0.2
2021	0.1	-0.2	-0.3	-0.3	0.4

The SGI values estimated using observed groundwater level for the wells 128, 129 and 160 PKD-8 of Palakkad block are shown in Table 4.15, Table 4.16 and Table 4.17 respectively. For well 128, the highest negative SGI was -2.1 found in April 2017. For well 129, the highest negative SGI was -1.6 found in May 2019. Similarly, for well 160 PKD-8, the highest negative SGI was -2.4 found in March 2014 which indicated the highest exceptional drought condition of the respective regions.

Table 4.15 Estimated SGI values of well 128

Well 128	Jan	Feb	Mar	Apr	May
2007	0.1	-1.2	-1.7	-1.7	-1.2
2008	-0.3	-0.4	-0.1	0.3	0.0

2009	0.2	-0.2	-0.6	-0.8	-0.5
2010	0.3	-0.1	-0.4	-0.7	-0.4
2011	0.2	-0.2	0.0	-0.4	-1.3
2012	-0.5	-0.6	-0.6	-0.9	-0.5
2013	-1.6	-1.3	-1.7	-1.7	0.8
2014	-0.8	-1.3	-1.6	-1.6	-0.7
2015	-0.8	-1.3	-1.4	-0.8	1.2
2016	0.0	-1.1	-1.7	-1.4	-1.1
2017	-1.4	-1.9	-1.7	-2.1	-2.1
2018	-0.2	-1.5	-1.5	-1.4	0.6
2019	-0.2	-0.5	-1.1	-1.4	-1.7
2020	0.2	0.4	-1.0	-1.7	-1.6
2021	0.3	0.3	-0.8	-1.6	-0.6

Table 4.16 Estimated SGI values of well 129

Well 129	Jan	Feb	Mar	Apr	May
2007	2.5	-0.2	-0.6	-0.7	-0.8
2008	0.1	-0.3	-0.1	0.0	-0.8
2009	-0.2	-0.5	-0.8	-1.1	-1.2
2010	0.2	-0.1	-0.5	-0.7	-0.6
2011	0.1	-0.3	0.0	-0.5	-0.7
2012	-0.2	-0.5	-0.6	-0.9	-1.0
2013	-0.6	-0.8	-0.9	-1.2	-0.9
2014	-0.1	-0.3	-0.7	-0.8	-0.9
2015	-0.2	-0.6	-0.6	-0.8	-0.9
2016	-0.4	-0.7	-0.9	-1.2	-1.3
2017	-1.0	-1.1	-1.5	-1.3	-1.5
2018	-0.6	-0.6	-1.1	-1.3	-1.3

2019	-0.5	-0.7	-1.2	-1.4	-1.6
2020	0.1	-0.4	-0.7	-1.0	-1.4
2021	-0.4	-0.7	-1.1	-1.4	-1.4

Table 4.17 Estimated SGI values of well 160 PKD-8

Well 160 PKD-8	Jan	Feb	Mar	Apr	May
2007	-0.2	-0.9	-2.1	-1.9	-1.4
2008	0.4	0.8	0.2	-0.4	-0.4
2009	-0.2	-0.5	-0.6	-0.7	-0.1
2010	0.0	-0.9	-1.3	-1.2	-0.1
2011	-0.8	0.7	-0.2	0.6	-0.9
2012	-0.6	-1.1	-1.4	-0.3	-0.2
2013	-1.5	-1.6	-2.3	-2.2	-2.1
2014	-1.4	-1.6	-2.4	-1.0	0.4
2015	-1.3	-1.5	-2.3	0.6	0.7
2016	-0.8	-1.1	-2.2	-2.0	-0.7
2017	-0.9	-1.4	-2.0	-1.9	-1.5
2018	-0.8	-1.0	-0.4	-0.3	0.2
2019	-0.9	-1.2	-1.3	-1.5	-1.0
2020	-0.1	-0.7	-0.8	-1.4	-0.4
2021	-0.2	-0.6	-0.9	-0.3	0.9

The SGI values estimated using observed groundwater level for the wells 133, 140, 142 and PKD S-15 are shown in Table 4.18, Table 4.19, Table 4.20 and Table 4.21 respectively. For well 133, the highest negative SGI was -2.6 found in February 2015. For well 140, the highest negative SGI was -2.2 found in April 2007. For well 142, the highest negative SGI was -2.3 found in February and March 2019. For well PKD S-15, the highest negative SGI was -2 found in May 2017 which indicated the highest exceptional drought conditions of the respective regions.

Table 4.18 Estimated SGI values of well 133

Well1 133	Jan	Feb	Mar	Apr	May
2007	-0.4	-0.7	-0.8	-1.0	-0.9
2008	0.3	-0.6	-0.7	-0.9	-0.9
2009	-0.6	-0.8	-1.0	-0.8	-0.8
2010	-0.8	-1.0	-1.0	-0.8	-0.8
2011	-0.7	-0.5	-0.8	-0.6	1.6
2012	-0.6	-0.7	-1.0	-1.0	-0.7
2013	-0.9	-0.9	-1.0	-1.0	-0.6
2014	-1.0	-1.1	-1.0	-0.6	-0.7
2015	-0.9	-2.6	-1.4	-0.6	1.1
2016	-0.9	-1.0	-1.1	-0.9	-0.9
2017	-0.8	-0.9	-1.0	-0.9	-1.0
2018	-0.8	-0.9	-1.0	-0.9	-0.5
2019	-0.7	-1.0	-1.0	-0.9	-1.2
2020	-0.3	-0.7	-1.0	-1.0	-1.1
2021	-0.3	-0.6	-0.9	-0.7	-0.4

Table 4.19 Estimated SGI values of well 140

Well 140	Jan	Feb	Mar	Apr	May
2007	0.3	-0.3	-0.8	-2.2	-1.2
2008	0.3	0.0	-0.4	-0.8	-1.0
2009	0.3	-0.3	-0.8	-1.0	-0.5
2010	0.3	-0.1	-1.0	-0.9	-0.9
2011	0.2	0.4	-0.3	-0.1	-0.9
2012	0.1	-0.2	-0.8	-1.0	-1.1
2013	-0.4	-0.7	-1.5	-1.9	-1.4

2014	0.0	-0.5	-1.3	-1.5	-1.5
2015	-0.1	0.4	-1.5	-1.5	0.9
2016	-0.1	-0.7	-1.7	-2.0	-1.5
2017	-0.2	-0.9	-1.5	-1.5	-1.7
2018	0.0	-0.2	-1.2	-1.3	-0.7
2019	0.1	-0.1	-0.9	-1.4	-2.0
2020	0.2	0.0	-0.8	-1.4	-0.9
2021	0.2	-0.1	-1.0	-1.4	-1.1

Table 4.20 Estimated SGI values of well 142

Well 142	Jan	Feb	Mar	Apr	May
2007	0.7	0.6	0.5	0.5	0.4
2008	0.9	0.8	0.7	0.6	-0.1
2009	0.6	0.2	0.2	0.2	0.1
2010	0.8	0.6	-0.9	-1.1	-0.5
2011	0.1	0.0	0.2	0.4	0.1
2012	0.5	0.1	-0.4	-0.1	-0.1
2013	-0.2	-0.2	-0.6	-0.9	-0.7
2014	0.2	-0.3	-0.5	-0.1	-1.2
2015	-0.6	-1.4	-0.8	0.0	-1.0
2016	-1.0	-0.3	-0.5	-0.7	-0.9
2017	-2.1	-2.1	-2.2	-2.2	-1.8
2018	-1.7	-1.4	-1.8	-1.8	-1.3
2019	-2.2	-2.3	-2.3	-2.2	-2.1
2020	-2.1	-2.2	-2.2	-1.7	-2.0
2021	0.3	-0.7	-1.2	-0.8	-0.2

Table 4.21 Estimated SGI values of well PKD S-15

Well PKD S-15	Jan	Feb	Mar	Apr	May
2007	1.0	0.1	0.0	-1.5	-1.0
2008	0.4	1.0	1.5	2.1	-0.8
2009	0.0	-0.5	-0.6	-0.7	-0.9
2010	-0.5	-1.1	-1.6	-1.9	-0.7
2011	3.5	0.4	-0.2	-0.1	-0.3
2012	-1.0	-1.3	-1.0	-0.8	-0.9
2013	-1.3	-1.0	-0.9	-1.6	-0.9
2014	-1.1	-1.4	-1.7	0.8	-1.6
2015	-0.7	-1.1	-1.5	-0.5	-0.4
2016	-1.0	-1.2	-1.6	-1.0	-0.5
2017	-0.6	-1.2	-1.5	-1.0	-2.0
2018	-0.6	-0.9	-1.5	-1.6	0.6
2019	-1.1	-1.0	-1.3	-1.9	-1.7
2020	-0.7	-1.2	0.4	-0.2	-0.1
2021	0.2	0.1	0.1	1.1	1.3

The SGI values estimated using observed groundwater level for the wells 139 and PKD S-7 are shown in Table 4.22 and Table 4.23 respectively. For well 139, the highest negative SGI was -2.7 found in May 2017. For well PKD S-7, the highest negative SGI was -2.5 found in April and May 2017 which indicated the highest exceptional drought condition of the respective regions.

Table 4.22 Estimated SGI values of well 139

Well 139	Jan	Feb	Mar	Apr	May
2007	0.6	0.2	-0.1	-0.2	-0.5

2008	0.8	0.4	0.1	-0.3	-0.3
2009	0.6	-0.1	-0.2	-0.3	-0.5
2010	0.7	0.2	-0.5	-0.4	0.2
2011	0.7	0.3	-0.2	-0.4	-0.5
2012	0.8	-0.8	-1.1	-0.3	-0.7
2013	-1.6	-1.5	-1.4	-0.6	-0.4
2014	-0.3	-0.3	1.6	-0.5	-0.6
2015	-0.3	-0.7	-0.7	-0.3	0.3
2016	-0.3	-0.7	-1.1	-1.3	-1.3
2017	-1.5	-1.8	-1.7	-1.7	-2.7
2018	-0.9	-1.1	-1.4	-1.7	-1.6
2019	-0.1	-0.3	-0.8	-1.2	1.7
2020	0.0	-0.7	-0.8	-1.2	-1.5
2021	-0.9	-1.1	-1.6	-1.5	-1.1

Table 4.23 Estimated SGI values of well PKD S-7

PKD S-7	Jan	Feb	Mar	Apr	May
2007	0.2	-0.3	-0.6	-1.2	-1.1
2008	0.2	-0.1	-0.4	-0.8	-0.9
2009	-0.2	-0.7	-1.0	-1.3	-1.8
2010	0.3	-0.1	-0.5	-0.8	-0.5
2011	0.2	-0.1	-0.5	-0.9	-0.7
2012	0.3	0.0	-0.4	-0.7	-0.8
2013	-1.0	-1.2	-1.7	-2.0	-1.3
2014	-0.8	-1.1	-1.3	-1.5	-0.1
2015	-0.2	-0.5	0.3	1.0	1.3

2016	-0.3	-0.7	-1.1	-1.7	-1.2
2017	-1.6	-1.9	-2.2	-2.5	-2.5
2018	-1.3	-1.4	-2.0	-1.9	-1.7
2019	-0.2	-1.1	-0.6	-1.1	-0.9
2020	0.7	0.2	-0.1	-0.3	-0.5
2021	0.7	0.5	0.5	0.6	0.7

4.6.2 Variation of SGI in the Pre-Monsoon Months

The variation of SGI in the pre-monsoon months of Jan, Feb, Mar, Apr and May for all wells of the study area are shown graphically in the Fig 4.8 (a) to Fig 4.8 (l). It was found that SGI values were more negative in the Mar, Apr and May months which indicated severe drought in these months compared to other months, it is due to the excess usage and reduced recharge.

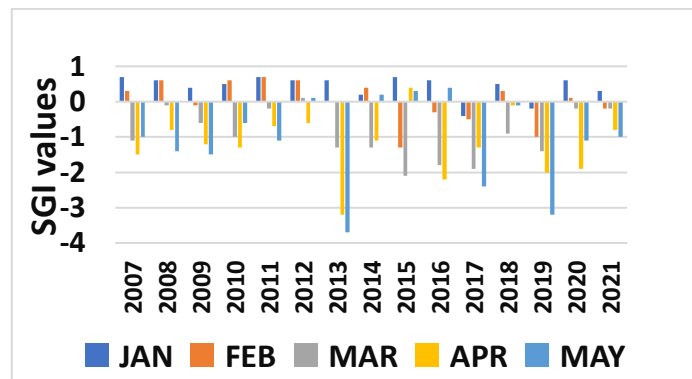


Fig 4.8 (a) SGI values of well 160 PKD-12

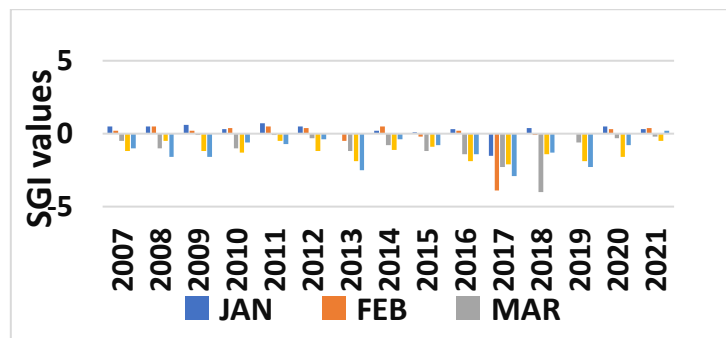


Fig 4.8 (b) SGI values of well PKD S-3

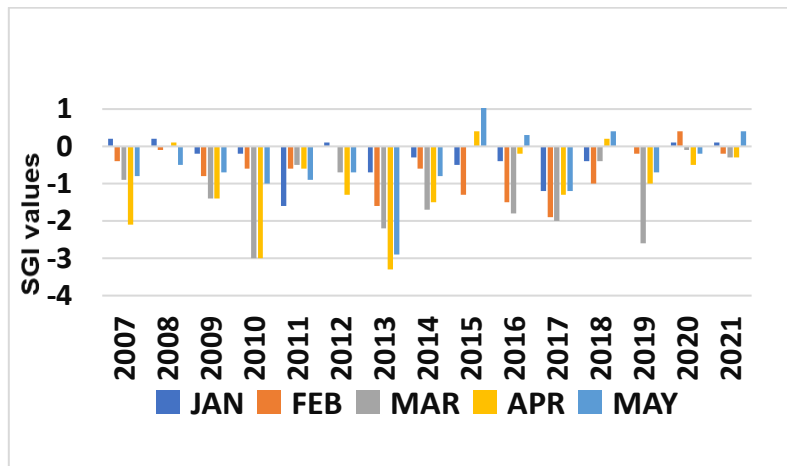


Fig 4.8 (c) SGI values of well PKD S-4

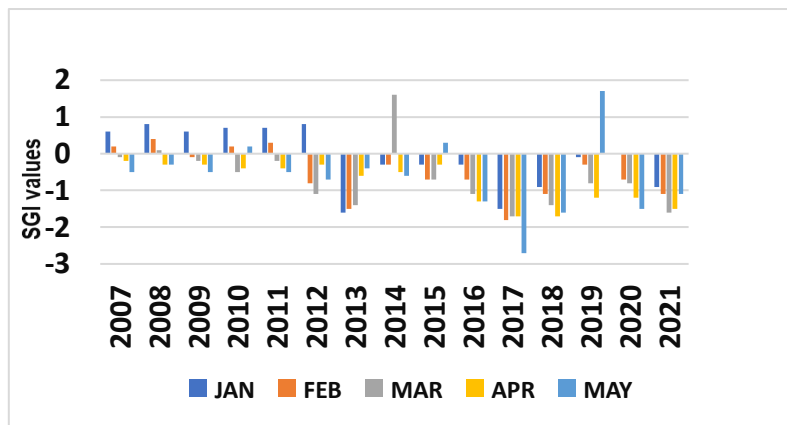


Fig 4.8 (d) SGI values of well 139

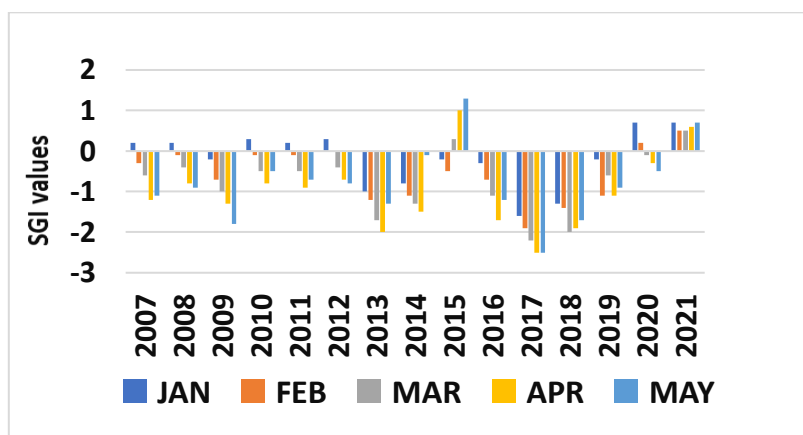


Fig 4.8 (e) SGI values of well PKD S-7

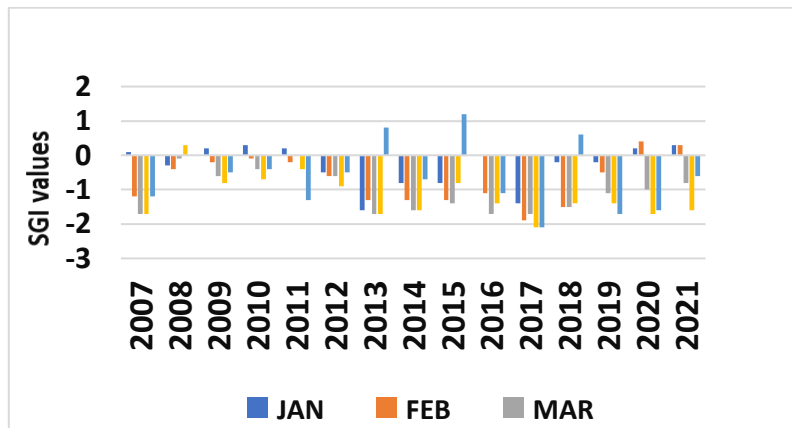


Fig 4.8 (f) SGI values of well 128

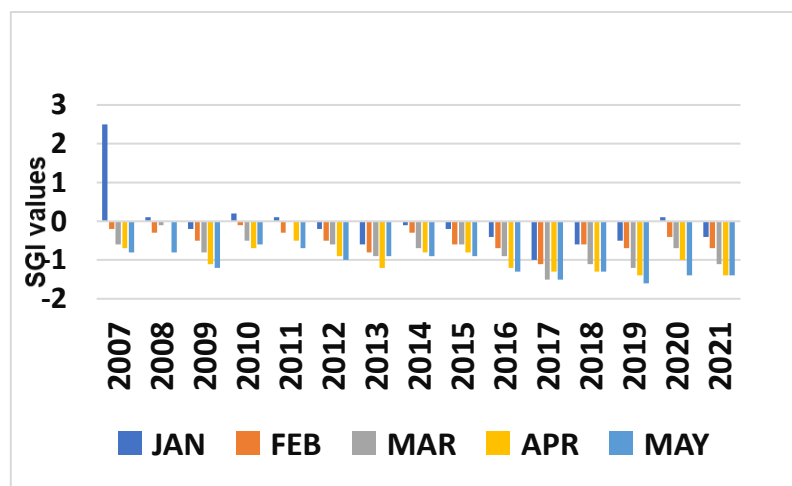


Fig 4.8 (g) SGI values of well 129

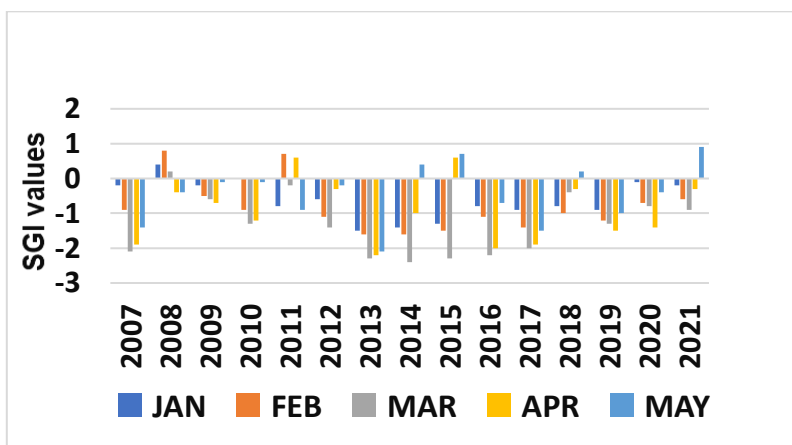


Fig 4.8 (h) SGI values of well 160 PKD-8

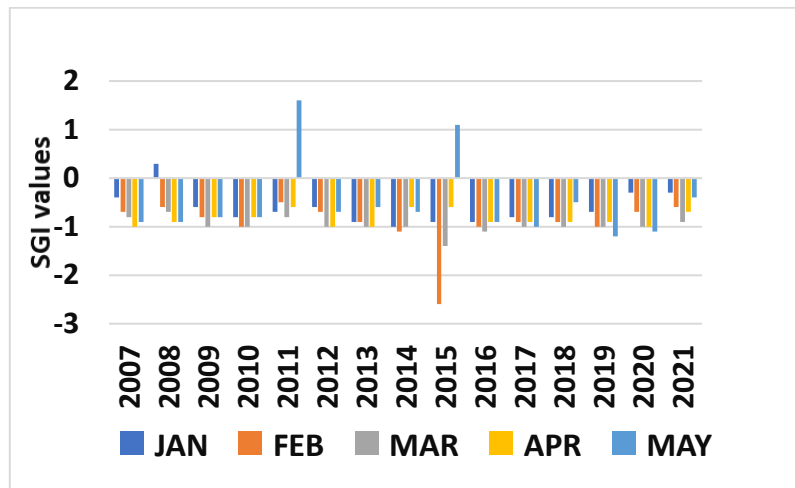


Fig 4.8 (i) SGI values of well 128

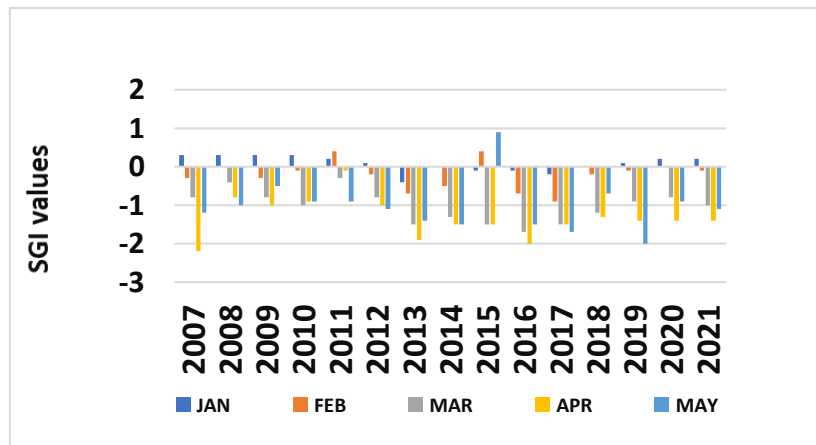


Fig 4.8 (j) SGI values of well 140

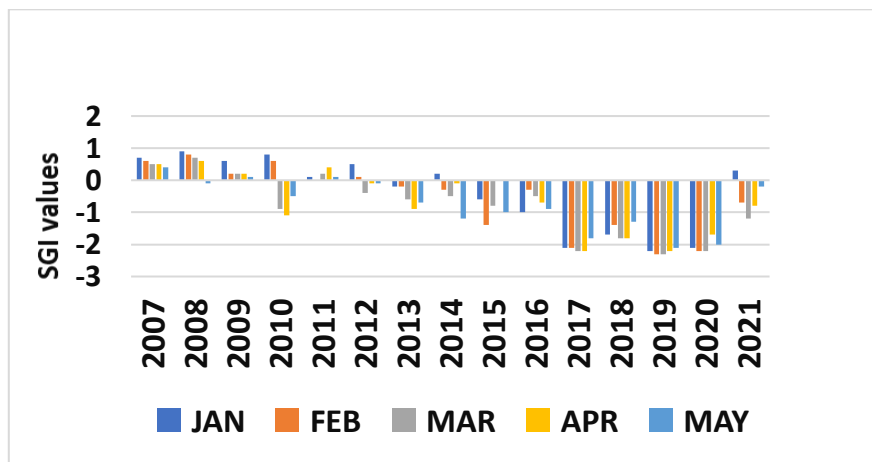


Fig 4.8 (k) SGI values of well 141

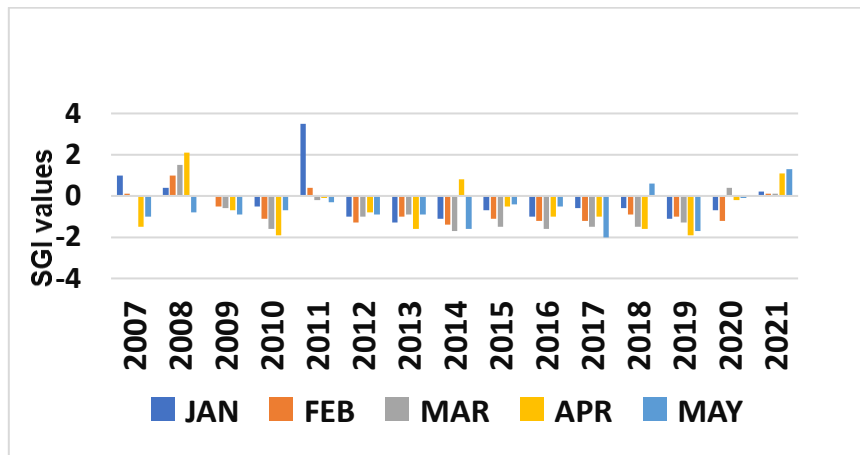


Fig 4.8 (I) SGI values of well PKD S-15

4.6.3 Comparison of SGI Values Estimated by ANN Model and Observed Groundwater Level Data

The graphical representation of SGI values estimated by observed groundwater level data vs ANN predicted groundwater level data is shown in Fig 4.9, Fig 4.10, Fig 4.11 and Fig 4.12. From the figures it is clear that the SGI values estimated by ANN predicted groundwater level data were in good agreement with the SGI values estimated by observed groundwater level data which indicated the effectiveness of ANN modelling.

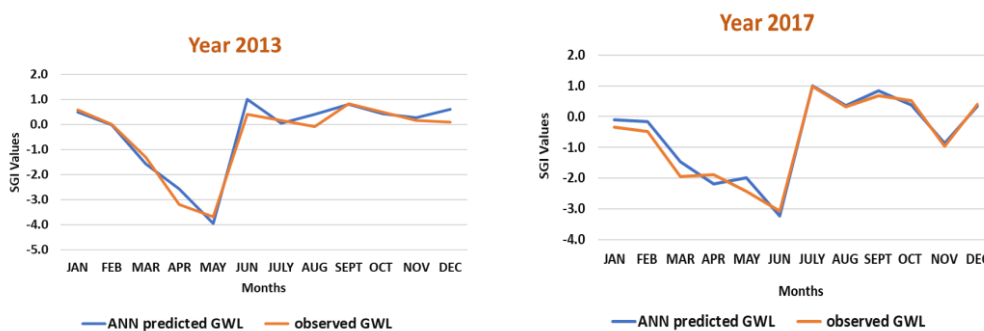


Fig 4.9 SGI values estimated by ANN model and observed groundwater level data of well 160 PKD-12 of Kuzhalmannam block

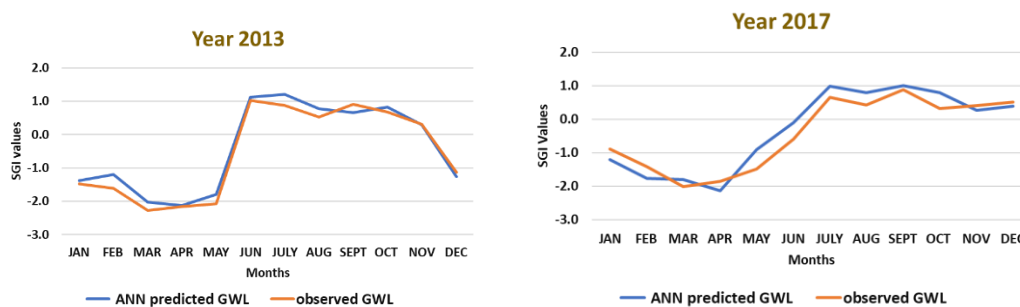


Fig 4.10 SGI values estimated by ANN model and observed groundwater level data of well 160 PKD-8 Palakkad block

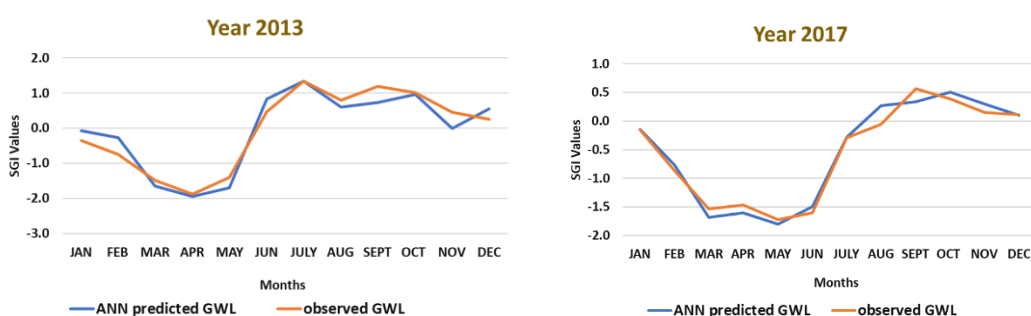


Fig 4.11 SGI values estimated by ANN model and observed groundwater level data of well 140 of Malampuzha block

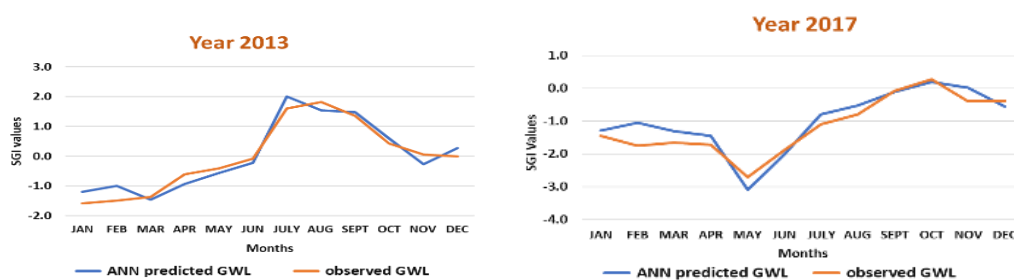


Fig 4.12 SGI values estimated by ANN model and observed groundwater level data of well 139 of Chittur block

4.6.4 Spatial Distribution of SGI Values in the Study Area

Estimated SGI values indicated that the years 2013, 2016 and 2017 were severe drought years since the SGI values of those years were more negative for almost all the wells. So, the spatial distribution map of SGI values of the study area

was made for April and May months of those three years. The spatial distribution map was created in ArcGIS using IDW interpolation technique.

The Fig 4.13 shows the spatial distribution of SGI values during April 2013. It was found that the SGI value ranged from -3.29 to -0.6, that is from exceptional to moderate drought condition in the area. Exceptional drought was seen in the wells 160 PKD-12, PKD S-3 and PKD S-4 of Kuzhalmannam block, well 128 and 160 PKD -8 of Palakkad block, wells 140 and PKD S-15 of Malampuzha block and well PKD S-7 of Chittur block. The Fig 4.14 shows the spatial distribution of SGI values during May 2013. It was found that the SGI value ranges from -3.69 to 0.79, that is from exceptional to no drought condition in the area. Exceptional drought was seen in the wells 160 PKD-12, PKD S-3 and PKD S-4 of Kuzhalmannam block and well 160 PKD -8 of Palakkad block.

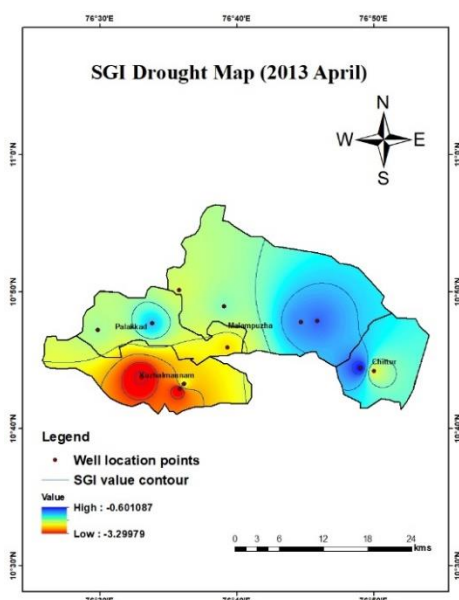


Fig 4.13 Spatial distribution of SGI during April 2013

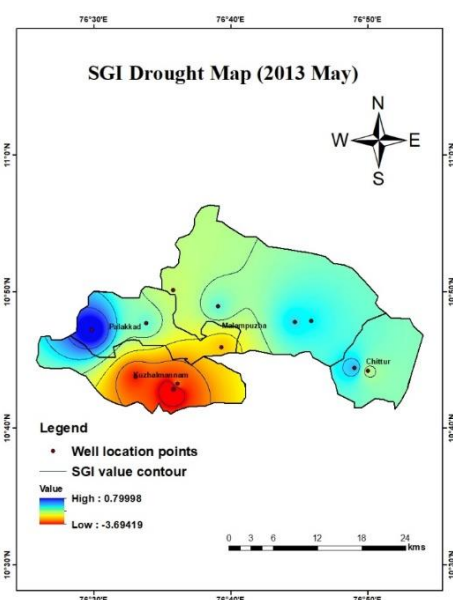


Fig 4.14 Spatial distribution of SGI during May 2013

The Fig 4.15 shows the spatial distribution of SGI values during April 2016. It was found that the SGI value ranges from -2.19 to -0.20, that is from exceptional to no drought condition in the area. Exceptional drought was seen in the wells 160 PKD-12 and PKD S-3 of Kuzhalmannam block and well PKD S-7 of Chittur block.

The Fig 4.16 shows the spatial distribution of SGI values during May 2016. It was found that the SGI value ranges from -1.49 to 0.39, that is from exceptional to no drought condition in the area. Exceptional drought was seen in the well 140 of Malampuzha block and extreme drought was seen in the well PKD S-3 of Kuzhalmannam block and wells 139 and PKD S-7 of Chittur Block.

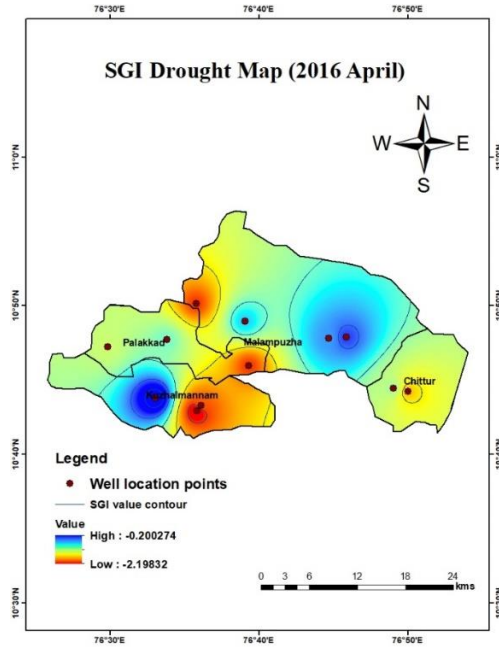


Fig 4.15 Spatial distribution of SGI during April 2016

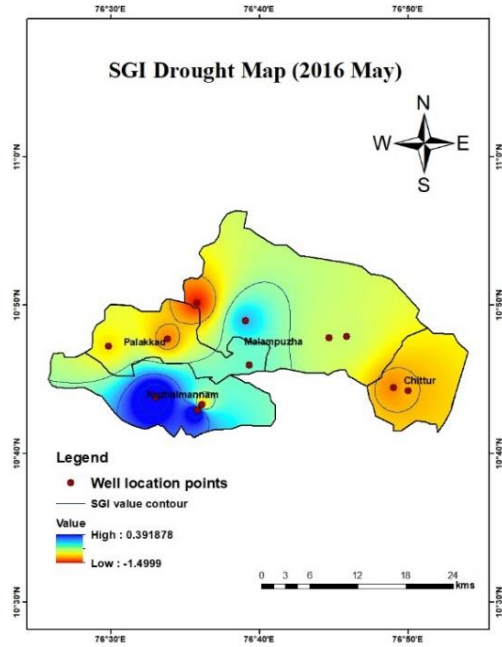


Fig 4.16 Spatial distribution of SGI during May 2016

The Fig 4.17 shows the spatial distribution of SGI values during April 2017. It was found that the SGI value ranges from -2.49 to -0.90, that is from exceptional to severe drought condition in the area. Exceptional drought was seen in the well PKD S-3 of Kuzhalmannam block, wells 140 and 142 of Malampuzha block, wells 128 and 160 PKD-8 of Palakkad block and wells 139 and PKD S-7 of Chittur block. The Fig 4.18 shows the spatial distribution of SGI values during May 2017. It was found that the SGI value ranges from -2.89 to -1.00, that is from exceptional to severe drought condition in the area. From the figure it is clear that exceptional drought was seen in the wells PKD S-3 and 160 PKD-12 of Kuzhalmannam block, wells 140, 142, PKD S-15 of Malampuzha block, wells 128, 129 and 160 PKD-8 of Palakkad block and wells 139 and PKD S-7 of Chittur block.

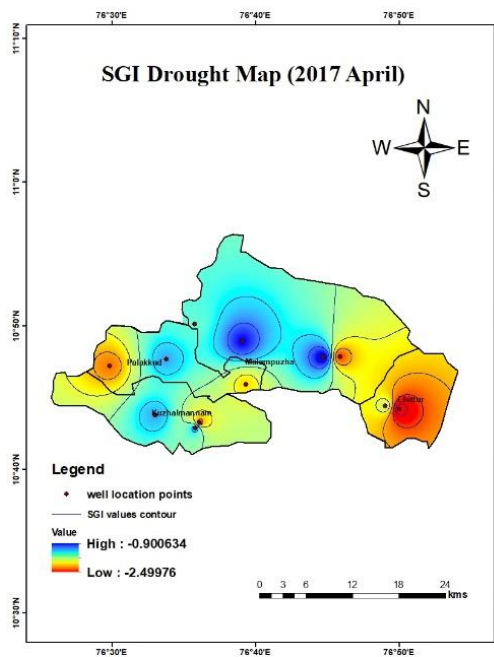


Fig 4.17 Spatial distribution of SGI during April 2017

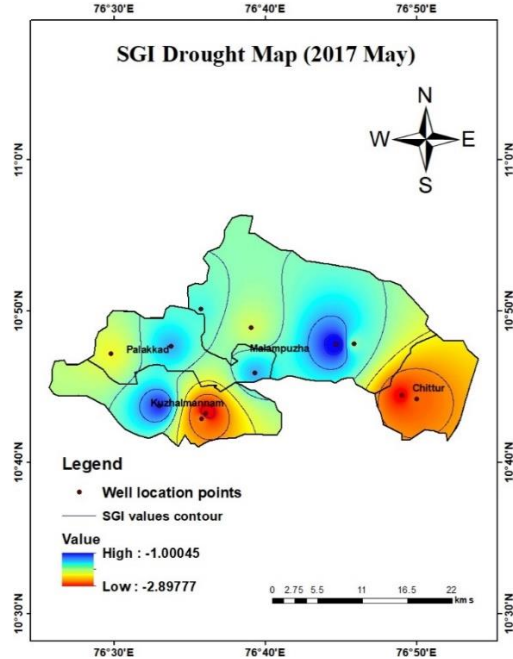


Fig 4.18 Spatial distribution of SGI during May 2017

4.7 FUTURE PREDICTION OF GROUNDWATER LEVEL AND FORECAST OF GROUNDWATER DROUGHT FOR THE YEAR 2023

Future prediction of groundwater level was done for the year 2023 for two drought effected wells, well 142 of Malampuzha block and well 160 PKD-12 of Kuzhalmannam block. The forecasted groundwater drought index was also estimated for the same wells 142 and 160 PKD-12 for the year 2023.

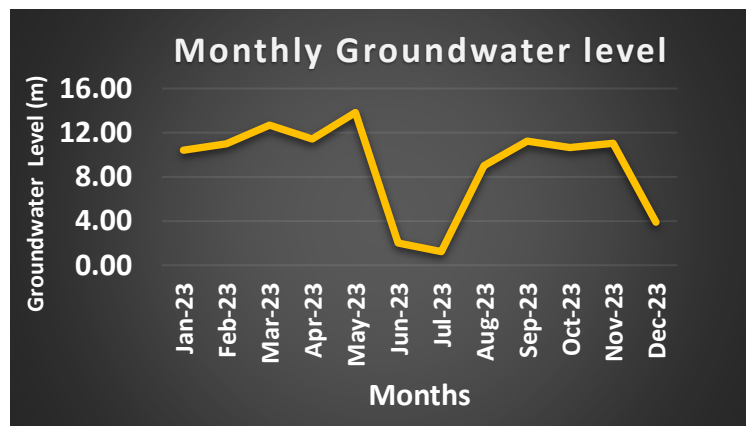


Fig 4.19 Monthly predicted groundwater level (bgl) of well 142

The Fig 4.19 shows the monthly groundwater level (bgl) of well 142 of Malampuzha block for the year 2023. The groundwater level (bgl) was lowest in the monsoon period of June and July which indicated that the water table is raised due to recharge during the period. But in the pre-monsoon and post-monsoon months, the groundwater level (bgl) was high which indicated a lowered water table during the period due to lack of recharge by precipitation.

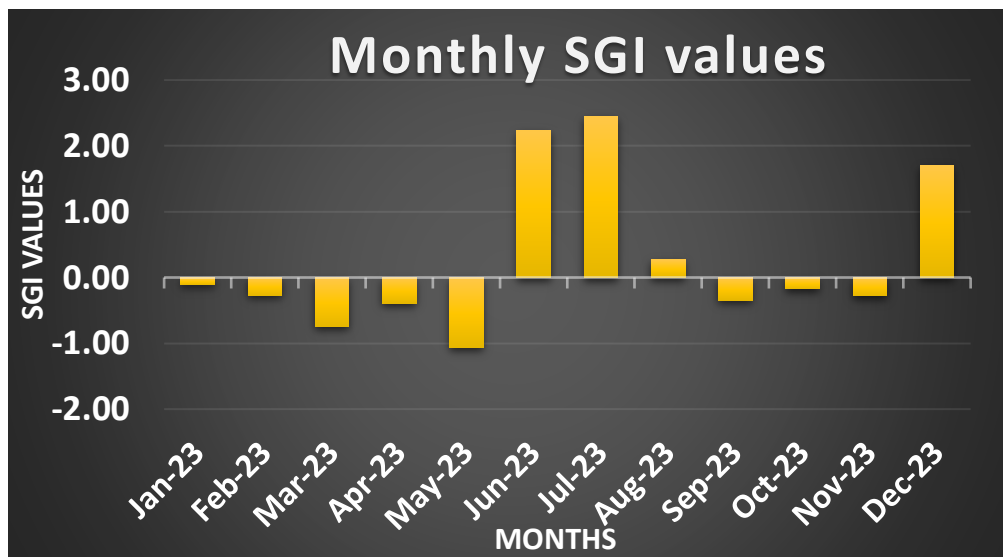


Fig 4.20 Monthly forecasted SGI values of well 142 for the year 2023

The Fig 4.20 shows the monthly SGI values of well 142 for the year 2023. It was found that the SGI value was more negative in the March, April and May months which indicated that the drought severity is more in those months. But in monsoon months June and July, the SGI value showed more positive value indicated no drought condition in those periods.

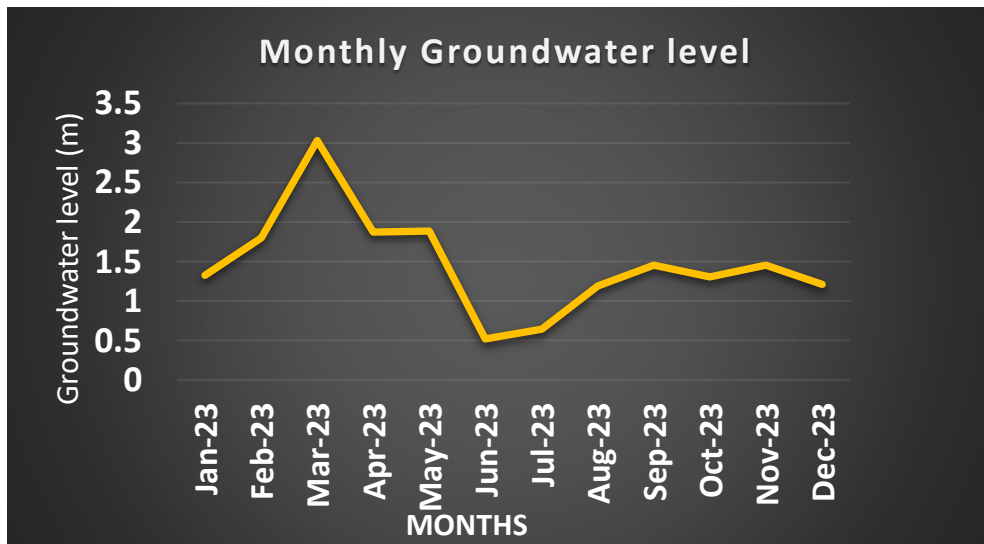


Fig 4.21 Monthly predicted groundwater level (bgl) of well 160 PKD-12

The Fig 4.21 shows the monthly groundwater level (bgl) of well 160 PKD-12 of Kuzhalmannam block for the year 2023. The groundwater level (bgl) was lowest in the monsoon period of June and July which indicated that the water table is raised due to recharge during the period and in the pre-monsoon and post-monsoon months, the groundwater level (bgl) was high which indicated a lowered water table during the period due to lack of recharge by precipitation.

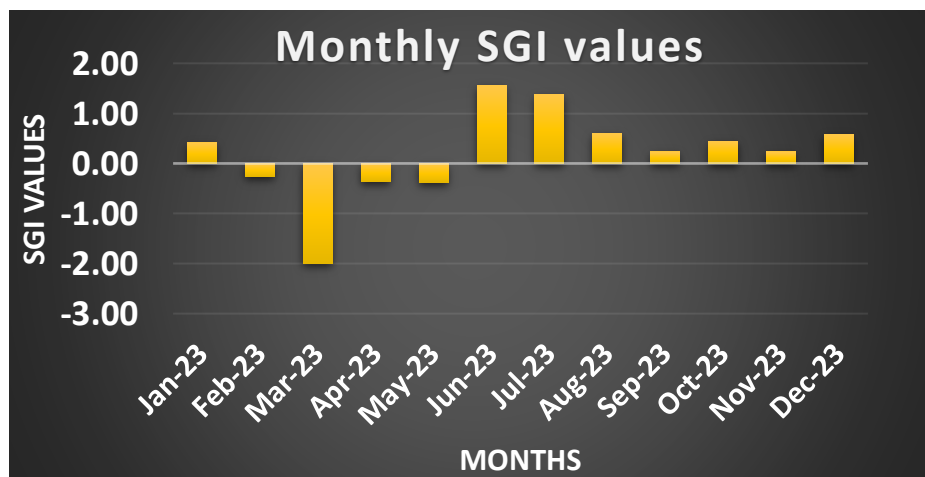


Fig 4.22 Monthly forecasted SGI values of well 160 PKD-12 for the year 2023

The Fig 4.22 shows the monthly SGI values of well 160 PKD-12 for the year 2023. It was found that the SGI value was more negative in the March, April

and May months which indicated that the drought severity is more in those months. But in monsoon months June and July, the SGI value showed more positive value indicated no drought condition in those periods.

From the above results, it could be concluded that variability and trend analysis of groundwater level is essential for water resource planning and management. It also gives an overall idea about the groundwater level status of the region. Modelling of groundwater level makes a better and easier understanding of the groundwater level. ANN is a best soft computing technique which can model non-linear relationship between input and output. Hence, groundwater level can be best modelled by ANN. Drought intensity can be well quantified by drought indices. SGI is found to be a proven communication tool to quantify the groundwater drought of the area. Using SGI, the areas that are more drought effected or drought prone could be identified and appropriate management practices could be applied in the region.

SUMMARY AND CONCLUSIONS

CHAPTER-V

SUMMARY AND CONCLUSIONS

Groundwater is one of the most precious and significant sources of water in the world and is essential to many aspects of human life, including agriculture, the growth of industry, and the provision of drinking water. The study entitled “Spatio-Temporal Groundwater Drought Assessment Based on ANN Model and GIS for a Sub-basin of Bharathapuzha” was focussed to study the variability and trend analysis of groundwater level, to model groundwater level using ANN and to assess the groundwater drought using Standardised Groundwater level Index (SGI).

The study was conducted in Kalpathypuzha sub-basin of Bharathapuzha. Twelve observation wells, evenly distributed in Kuzhalmannam, Palakkad, Malampuzha and Chittur blocks of Palakkad district were selected for the study. The data on precipitation, maximum and minimum temperature, and groundwater level were acquired for a period of 15 years from 2007 to 2021. The groundwater level variability was analyzed by various descriptive statistics like mean, standard deviation, coefficient of variation, skewness and kurtosis. The groundwater level trend was estimated by Mann- Kendall test and Sens slope estimator. ANN models were developed separately for each observation well to predict the groundwater level using MATLAB software. SGI was estimated for both observed and predicted groundwater level data to assess the groundwater drought scenario and to develop spatio-temporal groundwater drought map of the study area. Groundwater level and drought conditions were predicted for the year 2023 using the projected climate data obtained from CMIP6 climate model for two representative wells in the area.

The results of variability analysis showed that, the highest mean monthly groundwater level of 139.1 m was found for the well 139 of Chittur block in the month of September and the lowest mean monthly groundwater level of 61.5 m was found for the well 129 of Palakkad block in the month of September. Highest mean annual groundwater level was 138.9 m in the year 2007 for the well 139 of Chittur block and lowest was 62.1 m in the year 2016 for the well 129 of Palakkad block. Results of trend analysis showed a decreasing pre-monsoon groundwater level trend

in three wells 129 (Palakkad block), 133 and 142 (Malampuzha block) and decreasing post-monsoon groundwater level trend in well 139 (Chittur block), while no trend in all other wells for both seasons. The annual groundwater level trend showed a decreasing trend in wells 129 (Palakkad Block), 139 (Chittur block) and 142 (Malampuzha block).

The water table contour map of the study area was generated for the study period in Arc GIS using IDW interpolation technique. The average elevation of the well locations was about 96.25 m above MSL. The ground level elevation varied from 67 m at well PKD S-4 of Kuzhalmannam block to 152 m at wells 139 and PKD S-7 of Chittur block. The water table contour maps were prepared for pre-monsoon, post-monsoon and annual. The average seasonal groundwater level fluctuation varied from 1 to 2 m in some portions of Kuzhalmannam and Palakkad block, and 4 to 5 m in some portions of Chittur and Malampuzha blocks. Majority of the area showed 2 to 3 m groundwater level fluctuation.

Groundwater level fluctuation being a non-linear phenomenon, the soft computing technique ANN was used for modelling the groundwater level. Modelling was done using MATLAB R2016a software. Precipitation, minimum temperature and maximum temperature were used as the input data whereas observed groundwater level was taken as the target data for the development of ANN model. The data were divided into two groups, viz, training dataset and testing dataset. The monthly data from 2007 to 2021 consist of 180 datasets, out of which 70% was used for training and 30% was used for testing. Several ANN structures with feed forward back propagation algorithm, Levenberg-Marquardt learning algorithm and hyperbolic tangent as an activation function were tried and their performance in meeting the desired output were monitored. Feed forward ANN models were developed for all the 12 wells in the study area and the performance indicators correlation coefficient (r) ranged from 0.93 to 0.74, Root Mean Square (RMSE) ranged from 0.11 to 0.45 m, and Coefficient of determination (R^2) ranged from 0.87 to 0.69 all of which were in the acceptable range. The best model performance for training was for the well PKD S-4 with model configuration 3-10-

1 and $r = 0.92$ whereas, during testing it was found for the well 129 with model configuration 3-14-1 and $r = 0.93$.

Groundwater drought conditions were assessed by SGI using observed groundwater level data and ANN predicted groundwater level data for all the wells. The SGI was estimated for pre-monsoon months Jan, Feb, Mar, Apr and May of the study period from 2007 to 2021 for all the twelve wells as drought was more severe during these months. The value of SGI indicates the drought severity, more the negative value more is the drought severity. SGI values ranged from -3.7 to 1.1 indicated exceptional to no drought condition in the study area. The computed SGI values indicated that the years 2013, 2016, 2017 were the severe drought years of the study area.

According to Spatial distribution of SGI for 2013, 2016 and 2017 April and May months, Chittur and Malampuzha block were the most drought affected areas followed by Kuzhalmannam and Palakkad block. Exceptional drought was seen in well PKD S-4 of Kuzhalmannam block, and moderate drought was seen in well 139 of Chittur block in April 2013. During May 2013, exceptional drought was seen in well 160 PKD-12 of Kuzhalmannam block and moderate drought was seen in well 133 of Palakkad block. Well 160 PKD-12 of Kuzhalmannam block showed exceptional drought and well 142 of Malampuzha block showed moderate drought in April 2016. Exceptional drought was seen in well 140 of Malampuzha block, and moderate drought was seen in well 160 PKD-8 of Palakkad block during May 2016. During April 2017, exceptional drought was seen in well PKD S-7 of Chittur block and in May 2017 Well PKD S-3 of Kuzhalmannam block showed exceptional drought, and well 133 of Malampuzha block showed moderate drought. SGI estimated by ANN predicted groundwater level data showed good agreement with the SGI calculated by the observed groundwater level data for the study area which convey the effectiveness of ANN modelling in this study.

Future prediction of groundwater level and drought of the year 2023 were assessed for two representative wells in drought affected region viz, well 142 of Malampuzha block and well 160 PKD-12 of Kuzhalmannam block using the

developed ANN models. The results showed low groundwater level (bgl) of 0.5 m in well 160 PKD-12 and 2 m in well 142 in the months Jun and July. But high groundwater level (bgl) of 2 m in 160 PKD-12 and 14 m in well 142 in April and May months was seen due to recharge by rainfall. Forecasted drought for the same wells showed that severe drought was observed in well 142 and 160 PKD-12 in May and March months respectively.

Hence, it is concluded from the study that:

1. ANN predicted groundwater level was in close agreement with that of the observed groundwater level in this study. Hence the model developed could be safely and effectively applied in the study area.
2. ANN was found as a simple soft computing technique for modelling groundwater level and can be considered as a viable alternative for physically based model.
3. SGI estimated by ANN predicted groundwater level data showed good agreement with the SGI calculated by the observed groundwater level data for the study area.
4. SGI were found proven communication tools to quantify the groundwater drought of the area.
5. As per the estimated SGI, Chittur and Malampuzha blocks were more drought affected followed by Palakkad and Kuzhalmannam blocks.

Suggestions and recommendations

- Further abstraction of ground water should immediately be stopped in the blocks Chittur and Malampuzha block which are under over-exploited category.
- Groundwater recharge structures are recommended to implement in drought affected area to recharge groundwater.
- The input data like net groundwater recharge, net groundwater discharge, recharge due to rainfall, return flow of irrigation, canal seepage and seepage from tanks and ponds, draft from minor irrigation structure can also be

incorporated in ANN model if possible, to model the groundwater level and can check the efficiency of the model to predict groundwater level.

- Further studies should be done in the study area with the application of other soft computing machine learning techniques and physically based groundwater flow models to check the credibility of ANN models.

REFERENCES

REFERENCES

- Adamowski, J. and Chan, H. F. 2011. A wavelet neural network conjunction model for groundwater level forecasting. *J. Hydrol.* 407(4): 28-40.
- Ahmadi, S.H. and Sedghamiz, A. 2007. Geostatistical Analysis of Spatial and Temporal Variations of Groundwater Level. *Environ. Monit. Assess.* 129: 277–294.
- Ali, S., Liu, D., Fu, Q., Cheema, M.J.M., Pal, S.C., Arshad, A., Pham, Q.B., and Zhang, L. 2022. Constructing high-resolution groundwater drought at spatio-temporal scale using GRACE satellite data based on machine learning in the Indus Basin. *J. Hydrol.* 612: 1-17.
- American Meteorological Society (AMS). 2004. *Statement on meteorological Drought* [on- line]. Bulletin of the American Meteorological Society. 85, 771–773.
- Bak, G.M. and Bae, Y.C. 2019. Groundwater level prediction using ANFIS algorithm. *J. Korea Inst. Electron. Commun. Sci.* 14(6): 1235–1240.
- Balavalikar, V., Nayak, P., Shenoy, N., and Nayak, K. 2018. Particle swarm optimization based artificial neural network model for forecasting groundwater level in Udupi district. In: AIP Conference Proceedings, Vol. 1952, AIP Publishing LLC. p. 020021.
- Bierkens, M.F.P. 1998. Modeling water table fluctuations by means of a stochastic differential equation. *Water Resour. Res.* 34(10): 2485-2499.
- Bloomfield, J.P. and Marchant, B.P. 2013. Analysis of groundwater drought building on the standardised precipitation index approach. *Hydrol. Earth Syst. Sci.* 17: 4769–4787.
- Bui, D.D., Kawamura, A., Tong, T., Amaguchi, H., and Nakagawa, N. 2012. Spatio-temporal analysis of recent groundwater-level trends in the Red River Delta, Vietnam. *Hydrogeol. J.* 20
- CGWB [Central Ground Water Board]. 2013. *Ground Water Information Booklet of Palakkad District*- 2013.

- Chang, F.J., Chang, L.C., Huang, C.W., and Kao, I.F. 2016. Prediction of monthly regional groundwater levels through hybrid soft-computing techniques. *J. Hydrol.* 541: 965–976.
- Chen, Z., Grasby, S.E., and Osadetz, K.G. 2002. Predicting average annual groundwater levels from climatic variables: an empirical model. *J. Hydrol.* 260: 102-117.
- Chitsazan, M., Rahmani, G and Neyamadpour, A. 2015. Forecasting groundwater level by artificial neural networks as an alternative approach to groundwater modelling. *J. Geol. Soc. India.* 85: 98-106.
- Daliakopoulos, I.N., Coulibaly P., and Tsanis, I.K. 2004. Groundwater level forecasting using artificial neural networks. *J. Hydrol.* 309(2005): 229–240.
- Dawson, C. and Wilby, R. 1999. A comparison of artificial neural networks used for river forecasting. *Hydrol. Earth Syst.* 3: 529–540.
- Derbela, M. and Nouiri, I. 2020. Intelligent approach to predict future groundwater level based on artificial neural networks (ANN). *Euro-Mediterranean J. Environ. Integration.* 5(3): 1–11.
- Devarajan, K. and Sindhu, G. 2015. Application of numerical and empirical models for groundwater level forecasting. *Int. J. Res. Eng. Technol.* 4(11): 127-133.
- Djurovic, N., Domazet, M., Stricevic, R., Pocuca, V., Spalevic, V., Pivic, R., and Domazet, U. 2015. Comparison of groundwater level models based on artificial neural networks and ANFIS. *Sci.* 12:1-14.
- Drisya, J., Sathish Kumar, D., and Roshni, T. 2020. Hydrological drought assessment through streamflow forecasting using wavelet enabled artificial neural networks. *Environ. Dev. Sustainability.* 3: 1-20.
- Emamgholizadeh, S., Moslemi, K., and Karami, G. 2014. Prediction the groundwater level of bastam plain (Iran) by artificial neural network (ANN) and adaptive

- neuro-fuzzy inference system (ANFIS). *Water Resour. Manag.* 28(15): 5433-5446.
- Fu, G., Rojas, R., and Gonzales, D. 2022. Trends in groundwater levels in alluvial aquifers of the Murray–Darling basin and their attributions. *Water*. 14: 1-25.
- Gautam, V.K., Kothari, M., Singh, P.K., Bhakar, S.R., and Yadav, K.K. 2021. Analysis of groundwater level trend in Jakham River Basin of Southern Rajasthan. *J. Groundw. Sci. and Eng.* 10(1): 1-9.
- Gibrilla, A., Anornu, G., and Adomako, D. 2017. Trend analysis and ARIMA modelling of recent groundwater levels in the White Volta River basin of Ghana. *Groundw. Sustain. Dev.* 3: 1-33.
- Gleeson, T., Wada, Y., and Bierkens, M. 2012. Water balance of global aquifers revealed by groundwater footprint. *Nature*. 488: 197–200.
- Guo, M., Yue, W., Wang, T., Zheng, N., and Wu, L. 2021. Assessing the use of standardized groundwater index for quantifying groundwater drought over the conterminous US. *J. Hydrol.* 4: 598-60.
- Guzman, S.M., Paz, J.O., Tagert, M.L.M., and Mercer, A.E. 2019. Evaluation of seasonally classified inputs for the prediction of daily groundwater levels: Narx networks vs support vector machines. *Environ. Model. Assess.* 24(2): 223–234.
- Halder, S., Roy, M. B., and Roy, P. K., 2020. Analysis of groundwater level trend and groundwater drought using standard groundwater level index: a case study of an eastern river basin of West Bengal, India. *SN appl.Sci.* 2(5): 507-527.
- Han, Z., Huang, S., Huang, Q., Leng, G., Liu, Y., Bai, Q., He, P., Liang, H., and Shi, W. 2021. GRACE-based high-resolution propagation threshold from meteorological to groundwater drought. *Agric. For. Meteorol.* 307: 1-12.
- Hasda, R., Rahaman, M., Jahan, C., Molla, M.K., and Mazumder, Q. 2020. Climatic data analysis for groundwater level simulation in drought prone Barind Tract,

- Bangladesh: Modelling approach using artificial neural network. *Groundw. Sustain. Dev.* 10: 235-243.
- Haykin, S. 2001. *Neural Networks A Comprehensive Foundation* (2nd Ed.). Addison Wesley Longman Pte. Ltd. Publishers, Delhi.
- Hong, Y.M. 2017. Feasibility of using artificial neural networks to forecast groundwater levels in real time. *Landslides*. 14(5): 1815–1826.
- Husna, N.E.A., Bari, S.H., Hussain, M.M., Ur-rahman, M.T., and Rahman, M. 2016. Ground water level prediction using artificial neural network. *Int. J. Hydrol. Sci. Technol.* 6(4): 371-381.
- India. Ministry of Water Resources, River Development and Ganga Rejuvenation. 2015. *Annual Report 2014-15*. Ground Water Resource Estimation Committee, New Delhi, 142 p.
- Jothiprakash, V. and Suhasini, S. 2008. Ground Water Level Fluctuations using Artificial Neural Network. In: 12th International Conference on Computer Methods and Advances in Geomechanics. p.3.
- Kerala State Drought Monitoring Cell. 2017. *Drought - Situation Assessment Report, 2017*, Thiruvananthapuram.
- Khaki, M., Yusoff, I., and Islami, N. 2015. Simulation of groundwater level through artificial intelligence system. *Environ. Earth Sci.* 73(12): 8357–8367.
- Kombo, O.H., Kumaran, S., Sheikh, Y.H., Bovim, A., and Jayavel, K. 2020. Long-term groundwater level prediction model based on hybrid KNN-RF technique. *Hydrology*. 7(3): 59.
- Kumar, K.S. and Rathnam, E.V. 2019. Analysis and prediction of groundwater level trends using four variations of Mann Kendall tests and ARIMA modelling. *J. Geol. Soc. India*. 94: 281-289.

- Kumar, P., Chandniha, S.K., Lohani, A.K, Krishan, G., and Nema, A.K. 2018. Trend analysis of groundwater level using non-parametric tests in alluvial aquifers of Uttar Pradesh, India. *Curr. World Environ.* 13(1): 44-54.
- Lanen, H.A.J. and Peters, E. 2000. Definition, effects and assessment of groundwater droughts [on-line]. Available: <https://research.wur.nl/en/publications/definition-effects-and-assessment-of-groundwater-drought> [15 May 2022].
- Lee, J.M., Park, J.H., Chung, E., and Woo, N.C. 2018. Assessment of groundwater drought in the Mangyeong river basin, Korea. *Sustainability*. 10: 831-857.
- Li, B. and Rodell, M. 2015. Evaluation of a model-based groundwater drought indicator in the conterminous U.S. *J. Hydrol.* 526: 78–88.
- Lohani, A.K. and Krishan, G. 2015. Groundwater level simulation using Artificial Neural Network in Southeast, Punjab, India. *J. Geol. Geosciences*. 4(3): 206-213.
- Marchant, B.P. and Bloomfield, J.P. 2018. Spatio-temporal modelling of the status of groundwater droughts. *J. Hydrol.* 564: 397–413.
- Mayilvaganan, M. K. and Naidu, K. B. 2011. Application of artificial neural network for the prediction of groundwater level in hard rock region. In: Proceedings of International Conference on Computational Science, Engineering and Information Technology, Berlin, Heidelberg, September 23- 25, 2011, pp. 673-682.
- Mishra, A.K. and Singh, V.P. 2010. A review of drought concepts. *J. Hydrol.* 391(2): 202–216.
- Mohanty, S., Jha, M.K., Kumar, A., and Panda, D.K. 2013. Comparative evaluation of numerical model and artificial neural network for simulating groundwater flow in Kathajodi–Surua Inter-basin of Odisha, India. *J. Hydrol.* 495: 38-51.

- Moravej, M., Amani, P., and Hosseini-Moghari, S.M. 2020. Groundwater level simulation and forecasting using interior search algorithm-least square support vector regression (isa-lssvr). *Groundw. Sustain. Dev.* 11: 124-135.
- Nair, S.S. and Sindhu, G. 2016. Groundwater level forecasting using artificial neural network. *Int. J. Sci. Res. Publ.* 6(1): 2250–315.
- Nayak, P. C., Rao, Y. S., and Sudheer, K. P. 2006. Groundwater level forecasting in a shallow aquifer using artificial neural network approach. *Water Resour. Manag.* 20(1): 77-90.
- Ndlovu, M.S. and Demlie, M. 2018. Statistical analysis of groundwater level variability across KwaZulu-Natal Province, South Africa. *Environ. Earth Sciences.* 77: 739.
- NIDIS [National Integrated Drought Information System]. 2021. NIDIS homepage [online]. Available: <https://www.drought.gov/what-is-drought/monitoring-drought>. [06 Nov. 2021].
- Nie, S., Bian, J., Wan, H., Sun, X., and Zhang, B. 2017. Simulation and uncertainty analysis for groundwater levels using radial basis function neural network and support vector machine models. *J. Water Supply: Res. Technol.* 66(1): 15–24.
- Noori, A.R. and Singh, S.K. 2021. Spatial and temporal trend analysis of groundwater levels and regional groundwater drought assessment of Kabul, Afghanistan. *Environ. Earth Sci.* 80: 698-714.
- Nourani, V. and Mousavi, S. 2016. Spatiotemporal groundwater level modeling using hybrid artificial intelligence-meshless method. *J. Hydrol.* 536: 10–25.
- Nygren, M., Giese, M., and Barthel, R. 2021. Recent trends in hydroclimate and groundwater levels in a region with seasonal frost cover. *J. Hydrol.* 602: 1-13.
- Pathak, A.A. and Dodamani, B.M. 2018. Trend analysis of groundwater levels and assessment of regional groundwater drought: Ghataprabha River Basin, India. *Nat. Resour. Res.* 28(3): 631-643.

- Patle, G. T., Singh, D. K., Sarangi, A., Rai, A., Khanna, M., and Sahoo, R. N. 2015. Time series analysis of groundwater levels and projection of future trend. *J. Geol. Soc. India*. 85: 232–242.
- Qadir, M., Sharma, B.R., Bruggeman, A., Choukr-Allah, R., and Karajeh, F. 2007 Non-conventional water resources and opportunities for water augmentation to achieve food security in water scarce countries. *Agric. Water Manag.* 87 (1): 2–22.
- Raghavendra, N.S and Deka, P.C. 2016. Multistep ahead groundwater level time-series forecasting using gaussian process regression and anfis. *Advanced Computing and Syst. Security*. 396: 289–302.
- Rose, M.A.J. and Chithra, N.R. 2020. Evaluation of temporal drought variation and projection in a tropical river basin of Kerala. *J. Water and Clim. Change*. 11: 115-13.
- Roshni, T., Jha, M.K., and Drisya, J. 2020. Neural network modeling for groundwater-level forecasting in coastal aquifers. *Neural Comput. Appl.* 1–18.
- Sattari, M.T., Mirabbasi, R., Sushab, R.S., and Abraham, J. 2018. Prediction of groundwater level in ardebil plain using support vector regression and M5 tree model. *Groundw.* 56(4): 636–646.
- Seo, J. Y. and Lee, S. 2019. Spatio-temporal groundwater drought monitoring using multi-satellite data based on an artificial neural network. *Water*. 11(1953): 1-19.
- Shahid, S. and Hazarika, M.K. 2010. Groundwater drought in the north western districts of Bangladesh. *Water Resour. Manage.* 24:1989–2006.
- Shamsuddin, M. K. N., Kusin, F.M., Sulaiman, W. N. A. and Ramli, M. F. 2017. Forecasting of groundwater level using artificial neural network by incorporating river recharge and riverbank infiltration. Available: <https://www.researchgate.net/publication/315968773>.

- Shamsudduha, M., Chandler, R.E., Taylor, R.G., and Ahmed, K.M. 2009. Recent trends in groundwater levels in a highly seasonal hydrological system: the Ganges-Brahmaputra-Meghna Delta. *Hydrol. Earth Syst. Sci.* 13(12): 2373-2385.
- Sreekanth. P.D., Geethanjali, N., Sreedevi, P.D., Ahmed, S., Kumar, N.R., and Jayanthi, P.D.K., 2009. Forecasting groundwater level using artificial neural networks. *Curr. Sci.* 96(7): 933-939.
- Swain, S., Sahoo, S., Taloor, A.J, Mishra, S.K., and Pandey, A. 2022. Exploring recent groundwater level changes using Innovative Trend Analysis (ITA) technique over three districts of Jharkhand, India. *Groundw. Sustain. Dev.* 18: 234-248.
- Tao, B., Yang, Y., Yang, J., Smith, R., Fox, J., Liu, J., Ruane, A.C., and Ren, W. 2020. Recent shrinkage and fragmentation of bluegrass landscape in Kentucky. *Remote Sens.* 12: 1815-1826.
- Tawfik, M., Ibrahim, A., and Fahmy, H. 1997. Hysteresis sensitive neural network for modelling rating curves. *J. Comput. Civ. Eng.* 11(3): 206-211.
- Thomas, B.F., Famiglietti, J.S., Landerer, F.W., Wiese, D.N., Molotch, N.P., and Argus, D.F. 2017. GRACE Groundwater Drought Index: Evaluation of California Central Valley groundwater drought. *Remote Sensing Environ.* 198: 384–392.
- Thompson, L., Scaria, T., and Raveendran, P. 2021. Precepts for groundwater drought index in Kerala: a case study from Chaliyar river basin. *J. Geol. Soc. India.* 10:106-117.
- Tillman, F. and Leake, S. 2010. Trends in groundwater levels in wells in the active management areas of Arizona, USA. *Hydrogeology J.* 18: 1515-1524.
- Wang, F., Lai, H., Li, Y., Feng, K., Zhang, Z., Tian, Q., Zhu, X., and Yang, H. 2022. Identifying the status of groundwater drought from a GRACE mascon model perspective across China during 2003–2018. *Agric. Water Manag.* 260: 1-15.

- Wei, Z.L., Wang, D.F., Sun, H.Y., and Yan, X. 2020. Comparison of a physical model and phenomenological model to forecast groundwater levels in a rainfall-induced deep-seated landslide. *J. Hydrol.* 586:1-9.
- Yadav, B., Ch, S., Mathur, S., and Adamowski, J. 2017. Assessing the suitability of extreme learning machines (elm) for groundwater level prediction. *J. Water Land Develop.* 32 (1): 103–112.
- Yang, Z.P., Lu, W, X., Long, Y.Q., and Li, P. 2009. Application and comparison of two prediction models for groundwater levels: A case study in Western Jilin Province, China. *J. Arid Environ.* 73 (4–5): 487-492.
- Yin, W., Fan, Z., Tangdanrongsub, N., Hu, L., and Zhang, M. 2021. Comparison of physical and data-driven models to forecast groundwater level changes with the inclusion of GRACE – A case study over the state of Victoria, Australia. *J. Hydrol.* 602:1-13.
- Zhang, N., Xiao, C., Liu, B., and X. Liang. 2017. Groundwater depth predictions by GSM, RBF, and ANFIS models: a comparative assessment. *Arab. J. Geosci.* 10(8): 189.
- Zhao, A., Xiang, K., Zhang, A., and Zhang, X. 2022. Spatial-temporal evolution of meteorological and groundwater droughts and their relationship in the North China Plain. *J. Hydrol.* 610: 1-11.
- Zhu, Q. and Zhang, H. 2022. Groundwater drought characteristics and its influencing factors with corresponding quantitative contribution over the two largest catchments in China. *J. Hydrol.* 609: 1-20.

APPENDICES

APPENDIX-I
Monthly depth to water table

Table A-1: Monthly depth to water table (m) of well 139

Well 139	2007	2008	2009	2010	2011	2012	2013	2014	2015	2016	2017	2018	2019	2020	2021
Jan	13.56	13.03	13.46	13.12	13.30	12.71	21.10	16.65	16.58	16.54	20.67	18.86	16.00	15.81	18.71
Feb	15.04	14.17	15.95	14.92	14.76	18.48	20.78	16.55	18.06	18.01	21.70	19.51	16.80	17.93	19.40
Mar	16.09	15.39	16.37	17.28	16.48	19.30	20.37	10.13	18.20	19.30	21.38	20.33	18.55	18.48	21.34
Apr	16.42	16.60	16.80	17.17	16.85	16.58	17.76	17.26	16.51	20.08	21.60	21.66	19.81	19.95	20.72
May	17.44	16.71	17.29	15.05	17.42	17.94	17.03	17.81	14.66	20.23	24.99	21.19	9.71	20.70	19.54
Jun	16.23	16.82	19.05	15.61	11.75	18.58	15.91	16.33	14.05	17.70	22.17	19.21	22.49	18.22	19.15
Jul	9.27	14.70	9.97	13.05	10.71	17.76	10.07	13.36	13.27	16.67	19.46	14.81	19.34	17.51	16.76
Aug	10.25	11.35	10.64	10.75	9.66	16.30	9.32	10.64	13.88	15.70	18.42	12.30	19.48	15.23	15.28
Sept	9.69	10.92	9.10	10.60	8.92	17.88	10.93	10.48	14.36	16.98	15.91	13.79	14.95	14.24	14.70
Oct	10.58	11.51	9.96	11.51	10.00	16.86	14.16	10.90	14.68	17.60	14.72	13.61	15.43	14.54	13.92
Nov	11.23	10.57	9.36	10.97	10.60	18.53	15.45	11.32	14.33	17.58	18.80	14.60	14.35	16.17	15.60
Dec	11.88	12.02	10.97	10.00	10.76	18.19	15.66	12.88	14.73	19.12	16.98	15.16	15.58	18.68	15.36

Table A- 2: Monthly depth to water table (m) of well PKD S-7

Well PKD S-7	2007	2008	2009	2010	2011	2012	2013	2014	2015	2016	2017	2018	2019	2020	2021
Jan	1.74	1.69	2.22	1.54	1.61	1.53	3.44	3.08	2.25	2.41	4.31	3.90	2.24	0.95	0.89
Feb	2.46	2.17	2.94	2.10	2.08	2.00	3.75	3.60	2.68	3.02	4.83	4.07	3.58	1.69	1.25
Mar	2.85	2.63	3.41	2.64	2.67	2.54	4.49	3.89	1.55	3.57	5.21	4.98	2.91	2.16	1.30
Apr	3.78	3.08	3.87	3.16	3.27	2.94	4.90	4.20	0.55	4.46	5.68	4.72	3.56	2.48	1.02
May	3.53	3.37	4.66	2.72	2.98	3.12	3.93	2.12	0.07	3.76	5.66	4.42	3.30	2.72	0.98
Jun	3.09	3.66	5.02	3.88	0.58	3.74	0.00	0.57	0.27	2.11	5.27	0.87	3.85	2.76	1.25
Jul	0.17	3.24	1.10	1.85	0.52	1.92	0.76	0.40	0.49	1.67	4.12	0.03	1.16	1.78	0.23
Aug	0.45	0.73	1.03	0.94	0.45	1.79	0.52	0.45	0.67	2.00	1.15	0.11	1.40	0.07	0.12
Sept	0.30	0.93	0.80	0.65	0.10	1.02	0.84	0.73	0.70	2.83	1.04	0.32	0.26	0.34	0.15
Oct	0.40	0.84	0.62	0.77	0.56	0.63	1.14	0.95	0.99	3.07	2.25	0.52	0.37	0.40	0.10
Nov	0.80	0.76	0.17	0.62	0.16	1.87	1.97	1.16	1.21	3.79	2.60	0.96	0.20	0.56	0.11
Dec	1.20	1.49	0.60	0.37	0.35	2.45	3.08	1.80	2.00	3.95	3.57	1.67	0.42	0.56	0.33

Table A- 3 Monthly depth to water table (m) of well 128

Well 128	2007	2008	2009	2010	2011	2012	2013	2014	2015	2016	2017	2018	2019	2020	2021
Jan	3.81	4.5	3.77	3.63	3.75	3.67	4.73	3.97	4.05	3.22	4.39	4.24	4.11	3.74	3.66
Feb	5.20	4.4	4	4.06	4.11	4.45	5.59	4.75	4.72	3.98	5.34	4.10	4.49	3.49	3.62
Mar	5.65	4.31	4.53	4.38	3.97	4.58	5.25	5.23	5.25	5.09	5.89	5.49	5.06	4.95	4.77
Apr	5.64	3.68	4.80	4.66	4.30	4.51	5.67	5.58	5.40	5.68	5.67	5.52	5.40	5.73	5.57
May	5.14	3.94	4.49	4.38	5.23	4.83	5.64	5.59	4.81	5.33	6.14	5.41	5.70	5.55	4.55
Jun	3.32	2.47	4.08	2.22	2.65	4.48	3.11	4.63	2.68	5.03	6.13	3.33	5.57	5.74	4.67
Jul	2.70	3.09	1.78	2.39	2.64	4.03	1.70	2.95	2.59	2.79	3.33	2.50	3.84	3.20	2.78
Aug	2.67	2.31	2.87	2.61	2.62	3.26	3.40	3.45	3.62	3.96	3.85	3.02	3.47	1.98	3.11
Sept	2.73	3.42	3.17	2.81	2.25	3.55	2.47	3.57	3.49	4.20	2.70	2.74	2.05	2.59	3.03
Oct	2.96	3.06	2.92	2.72	3.59	4.01	3.86	2.87	3.42	4.53	3.74	3.45	3.17	3.61	2.87
Nov	3.50	3.48	2.09	2.83	3.48	4.43	3.82	3.95	2.43	4.37	3.75	4.29	3.05	4.07	3.20
Dec	4.20	3.58	3.31	3.96	3.46	4.39	4.13	3.98	3.82	5.05	4.05	3.97	3.57	3.71	3.80

Table A-4 : Monthly depth to water table (m) of well 129

Well 129	2007	2008	2009	2010	2011	2012	2013	2014	2015	2016	2017	2018	2019	2020	2021
Jan	4.60	4.5	8.35	7.71	7.91	8.24	8.91	8.21	8.35	8.54	9.36	8.81	8.68	7.93	8.61
Feb	8.25	8.38	9.00	8.14	8.39	8.67	9.00	8.49	8.80	9.00	9.59	8.88	8.98	8.54	9.03
Mar	8.85	8.65	9.10	8.72	8.04	8.85	9.25	9.04	8.90	9.29	10.06	9.61	9.75	9.03	9.58
Apr	9.06	8.04	9.59	9.06	8.68	9.32	9.63	9.17	9.19	9.70	9.80	9.79	9.99	9.42	9.97
May	9.20	9.10	9.68	8.87	9.00	9.36	9.24	9.25	9.30	9.90	10.11	9.84	10.29	9.92	9.98
Jun	7.77	8.50	9.50	8.33	8.00	9.25	9.06	9.14	8.28	9.65	10.22	8.68	10.28	10.10	9.98
Jul	3.40	7.50	4.00	6.96	6.21	7.74	4.74	8.17	7.20	8.35	8.73	6.27	9.27	8.83	9.19
Aug	4.54	6.61	6.45	5.77	5.38	7.35	6.27	6.96	7.27	7.80	8.25	5.55	8.05	7.84	7.64
Sept	3.67	7.50	6.50	6.24	4.56	6.85	5.77	6.27	7.62	8.40	6.25	6.97	5.92	6.75	7.01
Oct	5.97	7.44	6.26	6.71	6.85	7.72	7.06	6.32	7.24	8.48	7.20	7.25	6.84	6.72	6.63
Nov	6.00	7.03	6.02	7.08	7.24	8.45	7.32	7.06	7.61	8.40	7.91	7.72	6.20	7.60	6.50
Dec	7.37	7.60	7.49	7.66	7.39	8.47	7.81	8.00	8.00	9.06	7.83	8.16	7.23	8.21	7.20

Table A-5 : Monthly depth to water table (m) of well 160 PKD-8

Well 160 PKD-8	2007	2008	2009	2010	2011	2012	2013	2014	2015	2016	2017	2018	2019	2020	2021
Jan	10.99	8	10.89	10.47	12.71	12.12	14.87	14.61	14.47	12.89	13.11	12.75	13.06	10.73	10.92
Feb	13.08	7.96	11.95	12.96	8.33	13.84	15.27	15.32	14.82	13.77	14.69	13.29	13.96	12.35	12.11
Mar	16.85	9	12	14.32	10.89	14.79	17.32	17.64	17.56	17.07	16.55	11.50	14.49	12.79	13.10
Apr	16.17	11.60	12.52	14.11	8.62	11.12	16.99	8.99	8.65	16.52	16.05	11.16	15.08	14.57	11.32
May	14.79	11.6	10.79	10.68	13.05	10.93	16.71	8.50	8.33	12.55	14.89	9.87	13.47	11.65	7.58
Jun	10.22	11.60	9.76	7.32	7.37	9.01	7.19	7.00	7.73	10.77	12.17	8.21	14.37	10.82	7.85
Jul	6.59	7.17	7.04	7.85	7.65	7.46	7.67	8.00	8.49	7.41	8.37	8.05	7.31	7.41	6.86
Aug	6.82	6.98	7.49	7.21	7.30	4.97	8.75	9.58	7.12	9.45	9.05	6.99	5.56	7.09	7.03
Sept	6.23	8.07	7.64	7.22	7.04	14.37	4.67	8.23	8.13	7.80	7.65	7.69	6.78	7.34	7.07
Oct	6.45	7.91	7.17	7.07	9.03	8.88	8.27	12.23	8.21	8.39	9.39	5.18	8.92	7.31	6.99
Nov	8.00	8.86	7.07	6.95	7.26	9.42	9.37	11.79	7.49	8.41	9.08	10.72	7.43	9.75	7.82
Dec	10.46	10.00	10.85	9.23	7.29	12.19	13.84	13.02	9.00	11.38	8.77	10.15	10.28	7.80	9.78

Table A-6: Monthly depth to water table (m) of well 160 PKD-12

Well 160 PKD-12	2007	2008	2009	2010	2011	2012	2013	2014	2015	2016	2017	2018	2019	2020	2021
Jan	1.13	1.10	1.36	1.29	1.15	1.19	1.20	1.50	1.13	1.17	1.87	1.27	1.76	1.18	1.38
Feb	1.66	1.22	1.70	1.19	1.13	1.19	1.62	1.36	2.56	1.82	1.97	1.40	2.34	1.52	1.75
Mar	1.42	2.00	2.05	2.30	1.75	1.54	2.54	2.57	3.09	2.89	3.00	2.29	2.60	1.73	1.74
Apr	2.38	2.21	2.48	2.55	2.15	2.02	3.89	2.43	1.32	3.15	2.57	1.70	3.02	2.93	2.21
May	2.68	2.64	2.67	2.06	2.40	1.57	4.23	1.47	1.38	1.33	3.34	1.71	3.92	2.40	2.36
Jun	2.36	1.33	2.03	1.08	1.01	1.13	1.33	1.18	1.01	1.55	3.80	1.45	4.33	2.30	2.13
Jul	1.22	1.31	1.06	1.06	1.02	0.96	1.51	0.88	1.09	1.02	0.93	0.95	1.20	1.20	1.39
Aug	1.10	1.25	1.05	1.02	1.09	1.05	1.68	1.65	1.30	1.17	1.40	1.16	1.73	1.08	1.59
Sept	1.14	1.65	1.23	1.07	1.04	1.48	1.04	1.13	0.00	1.25	1.14	1.56	0.97	1.12	1.09
Oct	1.02	1.50	1.30	1.05	1.53	1.08	1.51	1.52	1.17	1.57	1.25	1.13	1.48	1.86	0.92
Nov	0.95	1.36	1.10	0.96	0.97	1.21	1.56	1.51	0.00	1.55	2.30	1.57	1.03	1.71	1.02
Dec	1.23	1.20	1.34	1.21	1.14	1.20	1.30	1.50	1.00	1.77	1.34	1.54	1.71	2.59	1.88

Table A-7: Monthly depth to water table (m) of well PKD S-3

Well PKD S-3	2007	2008	2009	2010	2011	2012	2013	2014	2015	2016	2017	2018	2019	2020	2021
Jan	1.47	1.5	1.39	1.74	1.23	1.44	2.17	1.92	2.08	1.72	4.52	1.56	2.16	1.52	1.73
Feb	1.97	1.48	2.00	1.60	1.50	1.60	3.05	1.45	2.54	1.91	8.11	2.42	2.29	1.75	1.66
Mar	2.98	3.8	2.32	3.70	2.33	2.62	3.98	3.47	3.97	4.39	5.64	8.25	3.20	2.64	2.49
Apr	4.00	2.95	4.08	4.12	2.97	4.01	5.16	3.87	3.64	5.10	5.40	4.35	5.16	4.61	2.98
May	3.80	4.62	4.62	3.08	3.35	2.80	6.03	2.83	3.49	4.34	6.52	4.18	5.70	3.47	1.94
Jun	0.81	2.00	3.86	0.81	0.74	2.75	2.64	1.46	1.86	3.40	6.80	1.42	6.48	3.73	1.61
Jul	0.85	1.01	0.70	0.84	0.83	1.51	0.88	0.72	1.32	1.04	1.08	0.63	1.70	0.85	0.69
Aug	1.05	0.68	1.00	0.79	0.95	1.11	1.46	1.24	1.45	1.42	1.45	1.32	1.21	0.66	1.08
Sept	1.02	1.65	1.33	0.97	0.90	1.16	0.86	1.32	1.73	2.06	1.12	2.37	0.91	1.11	1.13
Oct	0.81	0.69	1.59	1.16	1.75	2.05	1.50	1.58	1.74	2.34	1.47	1.29	1.72	1.38	0.76
Nov	1.00	1.14	0.87	0.68	0.89	1.12	1.56	1.98	1.70	2.24	1.83	2.35	1.12	1.61	1.36
Dec	1.38	1.40	1.36	1.45	1.84	1.56	1.77	1.90	1.83	4.07	1.38	1.31	1.67	0.97	1.72

Table A-8: Monthly depth to water table (m) of well PKD S-4

Well PKD S-4	2007	2008	2009	2010	2011	2012	2013	2014	2015	2016	2017	2018	2019	2020	2021
Jan	2.88	3	3.29	3.30	4.78	3.04	3.87	3.38	3.30	2.70	3.73	3.18	3.12	3.02	3.04
Feb	3.52	3.20	4.00	3.70	3.75	3.14	4.79	3.75	3.64	3.51	4.37	3.56	3.37	2.69	3.28
Mar	4.05	3	4.49	6.20	3.59	3.87	5.30	4.87	4.40	4.62	5.07	8.14	5.73	3.23	3.41
Apr	5.22	2.98	4.49	6.12	3.71	4.43	6.42	4.62	3.09	4.95	5.18	3.54	4.17	3.60	3.38
May	3.97	3.62	3.80	4.10	4.05	3.85	6.10	3.95	2.70	3.32	4.44	2.88	3.80	3.30	2.75
Jun	2.26	2.53	3.13	2.19	1.89	3.47	2.75	3.18	1.94	2.84	4.34	2.75	3.69	2.78	2.68
Jul	2.02	2.43	1.97	2.18	1.84	2.66	2.07	1.98	2.02	1.87	2.57	1.80	2.31	2.20	2.09
Aug	2.27	1.90	2.43	1.96	2.00	2.32	2.60	2.45	2.42	2.50	2.69	2.48	2.49	2.08	2.43
Sept	2.20	2.65	2.64	2.27	1.97	2.44	2.26	2.50	2.60	2.55	2.33	2.88	2.11	2.29	2.42
Oct	2.21	2.12	2.63	2.38	2.54	3.05	2.70	2.20	2.66	2.66	2.65	2.40	2.73	2.68	2.34
Nov	2.30	2.58	2.32	1.95	2.18	2.79	3.16	2.95	2.36	2.60	3.16	2.83	2.27	2.86	2.63
Dec	2.59	2.81	2.76	2.87	2.59	3.11	3.07	3.00	2.70	3.51	3.10	3.40	3.38	3.05	2.47

Table A-9: Monthly depth to water table (m) of well 133

Well PKD 133	2007	2008	2009	2010	2011	2012	2013	2014	2015	2016	2017	2018	2019	2020	2021
Jan	4.03	4	4.58	4.42	4.50	4.16	4.87	4.93	4.94	4.67	5.24	4.40	4.76	3.94	3.92
Feb	4.73	4.45	4.81	4.86	4.77	4.48	5.00	5.25	5.17	5.14	4.96	4.85	5.33	4.72	4.45
Mar	4.90	5	5	5.32	4.23	4.73	5.29	5.46	8.30	5.30	5.16	5.17	5.24	5.26	5.03
Apr	5.18	5.13	5.23	5.23	4.80	5.20	5.22	5.28	6.06	5.39	5.20	5.30	5.13	5.23	4.67
May	5.13	5.03	4.95	4.81	4.50	5.34	4.53	4.58	4.48	5.17	5.12	5.05	5.65	5.45	4.17
Jun	2.75	4.63	4.96	4.82	0.24	4.64	0.10	4.72	1.22	5.14	5.25	4.23	5.30	5.36	3.72
Jul	0.35	3.30	0.76	0.87	0.65	2.62	1.35	0.82	0.57	3.13	3.80	1.12	0.14	3.32	0.39
Aug	0.35	0.47	2.68	0.68	0.20	0.73	0.28	0.82	2.77	1.31	2.23	1.06	0.87	0.09	0.50
Sept	0.17	1.74	1.10	0.94	2.33	2.01	5.57	1.75	3.70	2.23	1.53	3.27	0.19	0.99	0.23
Oct	0.69	3.24	0.33	1.03	0.69	2.57	3.06	2.27	3.44	3.79	1.83	1.97	0.92	1.69	0.20
Nov	1.00	2.48	0.43	1.23	3.12	3.82	9.60	4.23	3.73	3.80	3.17	3.55	0.70	2.05	1.13
Dec	1.13	3.80	3.41	1.73	3.50	4.66	8.00	4.50	4.00	4.59	3.57	4.01	2.55	2.50	2.27

Table A-10: Monthly depth to water table (m) of well 140

Well PKD 140	2007	2008	2009	2010	2011	2012	2013	2014	2015	2016	2017	2018	2019	2020	2021
Jan	3.82	4	3.91	3.82	3.92	4.03	4.54	4.12	4.23	4.27	4.33	4.17	4.08	4.01	4.00
Feb	4.52	4.12	4.00	4.27	3.80	4.33	4.94	4.72	3.78	4.88	5.06	4.40	4.25	4.22	4.25
Mar	5.04	4.3	4.5	5.16	4.52	5.02	5.70	5.52	5.76	5.90	5.76	5.41	5.05	5.01	5.24
Apr	6.44	5.01	5.01	5.09	4.27	5.24	6.11	5.71	5.70	6.21	5.69	5.52	5.58	5.60	5.58
May	5.38	5.24	5.25	5.09	5.05	5.34	5.62	5.69	3.28	5.70	5.95	4.86	6.26	5.05	5.28
Jun	3.67	4.83	4.70	4.19	2.96	4.27	3.68	5.62	4.24	4.62	6.07	3.26	6.28	4.99	5.72
Jul	2.34	3.90	4.48	3.84	2.60	4.45	2.78	3.15	3.94	3.51	4.47	3.19	4.54	3.90	3.76
Aug	2.90	3.35	2.70	3.45	2.70	3.72	3.35	3.26	3.43	3.72	4.23	1.77	4.27	2.40	3.57
Sept	2.19	3.38	2.87	2.81	3.27	3.24	2.94	3.36	3.48	4.24	3.59	3.63	2.40	3.32	2.92
Oct	2.65	3.76	2.83	3.20	3.19	3.56	3.13	3.71	3.79	4.60	3.77	3.55	3.39	3.28	2.97
Nov	3.00	3.34	3.14	2.88	3.69	4.02	3.70	3.85	8.57	4.40	4.01	4.05	3.12	3.69	2.85
Dec	3.51	3.65	4.30	3.49	3.80	4.09	3.91	4.00	3.92	4.41	4.05	3.98	3.54	3.82	2.80

Table A-11: Monthly depth to water table (m) of well 142

Well PKD 142	2007	2008	2009	2010	2011	2012	2013	2014	2015	2016	2017	2018	2019	2020	2021
Jan	7.56	8	8.01	7.30	9.73	8.33	10.74	9.33	12.05	13.44	17.73	16.22	17.80	17.68	8.99
Feb	8.00	7.27	9.21	7.80	9.93	9.69	10.89	11.09	15.00	10.93	17.75	15.09	18.14	18.07	12.45
Mar	8.37	7.5	9.23	13.29	9.22	11.37	11.00	11.68	13.06	11.00	17.76	16.34	18.30	17.88	14.37
Apr	8.22	7.81	9.59	13.87	8.60	10.23	13.18	10.51	9.98	12.51	17.76	16.59	18.08	16.05	12.76
May	8.70	10.27	9.58	11.73	9.56	10.45	12.42	14.44	13.48	13.25	16.33	14.55	17.69	17.26	10.67
Jun	6.42	9.15	6.05	13.16	6.24	10.37	10.57	11.49	8.29	11.77	16.00	11.23	17.94	13.47	10.77
Jul	4.28	8.11	7.26	7.63	6.09	7.83	5.73	10.71	7.11	9.47	11.09	7.78	11.66	13.91	7.38
Aug	4.38	5.79	6.38	6.91	6.00	6.32	6.36	6.63	7.54	9.44	12.13	6.39	9.64	6.49	7.64
Sept	4.03	6.83	5.19	7.31	5.18	7.46	5.84	7.53	8.00	9.41	8.52	6.84	7.15	6.66	6.20
Oct	5.01	7.66	6.01	6.50	6.71	7.47	8.20	7.00	9.00	13.32	9.50	8.78	7.88	7.29	5.80
Nov	5.50	6.96	7.10	6.40	6.16	8.94	7.59	6.93	9.50	13.47	8.88	8.68	7.30	7.37	7.46
Dec	6.42	8.00	7.50	6.74	7.09	9.97	9.05	9.59	10.00	17.68	9.42	11.60	10.19	7.11	9.74

Table A-12: Monthly depth to water table (m) of well PKD S-15

Well PKD S-15	2007	2008	2009	2010	2011	2012	2013	2014	2015	2016	2017	2018	2019	2020	2021
Jan	4.20	5	5.81	6.70	7.00	7.50	7.95	7.61	6.92	7.48	6.84	6.84	7.58	6.95	5.49
Feb	5.65	4	6.71	7.64	5.13	8.05	7.46	8.12	7.00	7.74	7.85	7.30	7.41	7.83	5.66
Mar	5.80	3.4	7.01	8.44	6.18	7.46	7.37	8.66	8.37	8.55	8.25	8.26	7.97	5.21	5.67
Apr	8.26	2.32	7.30	8.98	5.96	7.19	8.45	4.38	6.69	7.50	7.47	8.43	8.96	6.17	3.90
May	7.40	7.09	7.10	6.91	6.31	7.35	7.30	7.72	6.44	6.56	9.12	4.83	8.66	6.00	3.61
Jun	5.35	6.04	3.06	5.25	4.24	5.30	2.50	8.42	4.66	6.80	8.80	3.98	8.82	5.78	3.54
Jul	4.05	6.30	4.18	4.81	4.06	6.40	3.18	6.79	3.75	6.26	7.07	4.19	6.00	4.37	3.14
Aug	3.80	3.95	4.53	4.76	3.43	5.87	4.87	5.42	4.12	4.91	6.06	2.93	5.56	2.48	3.81
Sept	3.10	5.37	4.69	4.05	5.18	5.27	5.42	4.28	4.25	5.98	5.39	5.85	2.42	4.07	2.81
Oct	3.35	5.12	3.42	3.75	4.88	5.22	5.89	5.65	5.74	6.56	5.42	5.36	5.06	4.54	4.15
Nov	5.00	4.75	6.24	5.56	6.53	6.73	7.04	6.85	5.20	6.98	5.94	6.75	4.26	5.49	3.46
Dec	6.07	4.84	6.50	6.00	6.90	7.52	7.80	7.00	6.64	7.33	6.53	7.22	5.77	5.57	4.00

APPENDIX-II

Observed and ANN predicted groundwater level of sample wells from each block

Table A-13: Observed and ANN predicted groundwater level of sample wells 139 (Chittur block), well PKD S-3 (Kuzhalmannam block), well 129 (Palakkad block) and well 133 (Malampuzha block)

Well 139- Observed GWL	Well 139-ANN predicted GWL	Well PKD S-3 Observed GWL	Well PKD S-3 ANN predicted GWL	Well 129 – Observed GWL	Well 129- ANN predicted GWL	Well 133- Observed GWL	Well 133- ANN predicted GWL
138.44	140.04	72.53	72.71	66.40	65.57	108.97	108.82
136.96	136.74	72.03	72.03	62.75	62.98	108.27	107.78
135.91	134.34	71.02	70.12	62.15	62.06	108.10	108.06
135.58	134.81	70.00	69.97	61.94	61.92	107.82	108.07
134.56	133.66	70.20	71.10	61.80	61.81	107.87	108.78
135.78	136.81	73.19	73.04	63.23	63.42	110.25	110.35
142.73	142.65	73.15	73.07	67.60	67.53	112.65	112.78
141.75	140.75	72.95	72.77	66.46	66.60	112.65	112.20
142.31	142.86	72.98	72.98	67.33	67.57	112.83	112.63
141.42	137.63	73.19	72.45	65.03	64.99	112.31	111.59
140.77	139.45	72.91	72.41	64.33	63.63	112.09	110.46
140.12	139.61	72.62	72.57	63.63	64.30	111.87	111.24
138.98	139.33	72.57	72.36	63.13	63.54	110.21	110.28
137.83	136.61	72.52	72.11	62.62	62.99	108.55	108.51
136.62	138.52	70.23	72.24	62.79	62.86	108.21	108.64
135.40	135.39	71.05	70.88	62.96	62.17	107.87	108.43
135.29	134.75	69.38	71.25	61.90	62.11	107.97	108.66

135.18	136.82	72.00	72.95	62.50	63.77	108.37	108.83
137.30	139.47	72.99	73.05	63.50	63.17	109.70	112.39
140.65	141.25	73.32	73.00	64.39	63.47	112.53	112.48
141.08	141.53	72.35	72.88	63.50	64.05	111.26	111.15
140.49	141.18	73.31	72.70	63.56	64.60	109.76	109.06
141.43	136.27	72.86	71.55	63.97	62.67	110.52	110.06
139.99	139.06	72.74	72.63	63.40	64.04	109.47	109.51
138.54	138.57	72.61	72.26	62.65	62.44	108.42	108.29
136.06	136.54	71.68	71.65	62.28	62.92	108.19	108.34
135.63	136.02	69.92	70.53	61.90	62.35	107.77	108.03
135.20	135.09	69.38	70.63	61.41	61.98	108.05	108.42
134.71	135.30	70.14	71.25	61.32	62.61	108.04	107.89
132.95	138.41	73.30	72.60	61.50	64.23	112.24	111.54
142.03	141.94	73.00	72.79	67.00	66.22	110.32	110.42
141.36	138.88	72.67	72.69	64.55	64.07	111.90	111.94
142.90	140.92	72.41	72.81	64.50	63.76	112.67	112.27
142.04	139.07	73.13	72.17	64.74	64.08	112.57	110.58
142.64	140.79	72.64	72.42	64.98	64.40	109.59	109.70
141.03	136.59	72.26	71.37	63.51	62.51	108.58	109.76
138.88	136.45	72.40	72.04	63.29	63.06	108.14	108.38
137.08	137.14	70.30	70.33	62.86	62.54	107.68	107.64
134.72	134.63	69.88	70.12	62.28	61.97	107.77	107.96
134.83	135.16	70.92	70.33	61.94	61.77	108.19	108.04
136.95	136.24	73.19	72.32	62.13	61.65	108.18	108.56
136.39	135.02	73.16	73.05	62.67	61.94	112.13	111.51
138.95	140.81	73.21	72.96	64.04	64.41	112.32	112.60
141.25	142.54	73.03	72.94	65.23	65.10	112.06	112.31
141.40	134.92	72.84	72.48	64.76	63.71	111.97	111.39
140.49	140.04	73.32	72.64	64.29	64.24	111.77	112.45

141.03	140.74	72.55	72.59	63.92	64.89	111.27	110.75
142.00	141.34	72.77	72.89	63.34	66.82	108.50	108.77
138.70	137.79	72.50	72.39	63.09	63.06	108.23	107.89
137.24	138.43	71.67	71.87	62.61	62.32	108.77	109.09
135.52	135.42	71.03	70.10	62.96	62.41	108.20	107.74
135.15	135.89	70.65	70.67	62.32	62.24	108.50	108.16
134.58	134.12	73.26	71.32	62.00	62.11	112.76	108.52
140.25	140.09	73.17	73.00	64.79	63.12	112.56	112.06
141.30	134.42	73.05	72.94	65.21	65.26	112.35	111.89
142.34	140.96	73.10	72.92	65.62	64.40	112.80	112.59
143.08	141.86	72.25	72.75	66.44	64.78	110.67	110.47
142.00	138.95	73.11	72.18	64.15	64.13	112.31	110.09
141.40	141.35	72.16	72.72	63.76	63.74	109.88	110.53
141.24	138.17	72.56	72.55	63.61	63.31	108.84	110.14
139.29	138.79	72.40	72.42	62.76	63.00	108.52	108.64
133.52	136.28	71.38	71.78	62.33	63.01	108.27	108.64
132.70	133.74	69.99	70.17	62.15	62.03	107.80	108.16
135.42	135.58	71.20	70.58	61.68	61.97	107.66	108.07
134.06	135.19	71.25	72.61	61.64	61.94	108.36	109.13
133.42	133.96	72.49	73.05	61.75	61.98	110.38	111.06
134.24	133.73	72.89	73.07	63.26	63.50	112.27	110.97
135.70	133.66	72.84	73.15	63.65	62.33	110.99	112.62
134.12	137.28	71.95	72.62	64.15	63.92	110.43	112.09
135.14	139.33	72.88	72.15	63.28	64.05	109.18	110.47
133.47	137.32	72.44	72.21	62.55	62.89	108.34	108.90
133.81	136.75	71.83	72.00	62.53	62.96	108.13	107.90
130.90	132.71	70.95	70.68	62.09	62.25	108.00	107.10
131.22	135.39	70.02	70.67	61.92	62.42	107.86	107.95
131.63	131.93	68.84	69.85	61.75	61.79	107.71	107.95

134.24	133.48	67.97	69.12	61.37	61.55	107.78	107.88
134.97	134.57	71.36	70.96	61.76	60.87	108.47	107.90
136.09	135.57	73.12	72.96	61.94	62.31	112.90	112.82
141.93	142.74	72.54	72.98	66.26	62.08	111.65	112.05
142.68	140.80	73.14	72.95	64.73	63.83	112.72	111.43
141.07	140.61	72.50	72.82	65.23	64.36	107.43	107.56
137.84	137.99	72.44	72.79	63.94	64.08	109.94	109.91
136.55	135.44	72.23	72.45	63.68	63.00	103.40	107.18
136.34	137.02	72.08	72.11	63.19	63.54	108.07	109.38
135.35	136.24	72.55	72.08	62.79	63.06	107.75	108.49
135.45	132.79	70.53	70.24	62.51	62.10	107.54	107.34
141.87	138.65	70.13	69.83	61.96	61.89	107.72	108.01
134.74	135.14	71.17	69.48	61.83	61.69	108.42	107.86
134.19	134.29	72.54	71.16	61.75	61.51	108.28	107.99
135.67	137.22	73.28	72.85	61.86	62.18	112.18	111.98
138.64	138.66	72.76	72.86	62.83	62.59	112.18	112.79
141.36	142.56	72.68	72.91	64.04	65.18	111.25	111.35
141.52	139.36	72.55	72.73	64.73	63.99	110.99	110.58
141.10	140.01	72.42	72.51	64.68	63.69	110.73	111.59
140.68	136.63	72.02	72.58	63.94	63.17	108.77	107.62
139.12	136.43	71.92	72.07	63.00	63.20	108.06	108.41
135.42	137.99	71.46	71.63	62.65	62.62	107.83	107.85
133.94	132.35	70.03	70.28	62.20	62.12	104.70	106.72
133.80	134.35	70.36	70.34	62.10	61.99	106.94	108.24
135.49	134.68	70.51	70.61	61.81	61.87	108.52	107.92
137.34	137.64	72.14	72.19	61.70	61.45	111.78	109.46
137.95	138.08	72.68	72.82	62.72	62.76	112.43	112.61
138.73	137.10	72.55	72.76	63.80	63.62	111.33	111.65
138.12	138.58	72.27	72.59	63.73	63.58	110.23	110.82

137.64	135.58	72.26	71.43	63.38	62.97	109.30	107.90
137.32	136.31	72.30	71.81	63.76	63.55	109.56	109.95
137.67	138.73	72.17	72.36	63.39	63.95	109.27	110.68
137.27	137.27	72.28	73.08	63.00	62.86	108.33	106.82
135.46	134.40	72.09	71.23	62.46	62.52	107.86	108.22
133.99	134.25	69.61	70.10	62.00	61.78	107.70	108.27
132.70	132.39	68.90	68.86	61.71	61.63	107.61	107.87
131.92	131.55	69.66	69.40	61.30	60.93	107.83	108.08
131.77	130.36	70.60	69.39	61.10	61.23	107.86	107.91
134.30	134.23	72.96	72.99	61.35	62.02	109.87	110.05
135.33	135.47	72.58	72.95	62.65	63.61	111.69	112.58
136.30	137.38	71.94	72.74	63.20	63.70	110.77	111.73
135.02	134.69	71.66	72.28	62.60	63.64	109.21	110.82
134.40	134.52	71.76	71.27	62.52	62.76	109.20	107.70
134.42	135.19	69.93	70.99	62.60	62.59	108.41	108.48
132.88	133.19	69.48	71.04	61.94	62.56	107.76	109.84
131.33	132.41	65.89	70.51	61.64	62.14	108.04	106.37
130.30	133.15	68.36	70.07	61.41	62.14	107.84	107.83
130.62	133.09	68.60	69.99	60.94	61.90	107.80	107.91
130.40	131.95	67.48	68.73	61.20	61.36	107.88	107.87
127.01	127.12	67.20	70.18	60.89	61.44	107.75	107.94
129.83	128.86	72.92	73.08	60.78	61.30	109.20	109.49
132.54	134.87	72.55	71.77	62.27	62.03	110.77	112.08
133.58	134.69	72.88	72.90	62.75	63.20	111.47	112.20
136.09	135.91	72.53	73.01	64.75	64.74	111.17	111.77
137.28	136.81	72.17	72.60	63.80	63.34	109.83	110.64
133.20	136.26	72.62	71.83	63.09	63.44	109.43	109.79
135.02	134.60	72.44	71.93	63.17	63.22	108.60	108.69
133.14	133.09	71.58	72.39	62.19	62.20	108.15	108.42

132.49	133.50	65.75	69.11	62.12	60.71	107.83	108.70
131.67	132.87	69.65	67.43	61.39	61.45	107.70	107.58
130.34	132.41	69.82	70.54	61.21	61.20	107.95	107.77
130.81	131.57	72.58	70.23	61.16	61.17	108.77	112.28
132.79	134.29	73.37	72.43	62.32	61.46	111.88	112.29
137.19	137.29	73.05	73.35	64.73	65.45	112.76	112.83
139.70	139.17	72.68	73.37	65.45	65.35	111.94	112.20
138.21	136.25	71.63	73.37	64.03	63.97	109.73	109.65
138.39	135.98	72.71	71.66	63.75	64.22	111.03	110.96
137.40	137.06	71.65	71.94	63.28	63.60	109.45	108.87
136.84	135.95	72.69	72.21	62.84	63.16	108.99	110.19
136.00	136.26	71.84	72.17	62.32	60.71	108.24	108.08
135.20	133.76	71.71	71.29	62.02	62.04	107.67	107.61
133.45	131.78	70.80	71.33	61.25	61.26	107.76	107.44
132.19	130.98	68.84	70.61	61.01	61.01	107.87	107.69
142.29	138.59	68.30	68.93	60.71	60.71	107.35	107.91
129.51	130.48	67.52	68.55	60.72	60.80	107.70	108.47
132.66	134.03	72.30	68.62	61.73	62.53	112.86	112.15
132.52	135.82	72.79	73.33	62.95	63.01	112.13	112.18
137.05	137.04	73.09	73.37	65.08	64.82	112.81	112.66
136.57	136.25	72.28	73.37	64.16	64.63	112.08	112.57
137.65	135.44	72.88	73.30	64.80	65.07	112.30	111.79
136.42	136.46	72.33	71.54	63.77	63.82	110.45	111.01
136.19	134.60	72.48	72.43	63.07	63.02	109.06	108.13
134.07	134.66	72.25	72.10	62.46	62.32	108.28	107.68
133.52	131.44	71.36	71.66	61.97	61.94	107.74	107.84
132.05	131.70	69.39	71.21	61.58	61.89	107.77	107.74
131.30	137.39	70.53	69.47	61.08	60.71	107.55	107.96
133.78	137.14	70.27	70.47	60.90	61.09	107.64	109.83

134.49	135.81	73.15	72.07	62.17	62.47	109.68	111.81
136.77	135.71	73.34	73.37	63.16	63.20	112.91	112.80
137.76	134.94	72.89	73.37	64.25	63.16	112.01	111.99
137.46	135.57	72.62	73.37	64.28	63.32	111.31	110.89
135.83	137.02	72.39	72.30	63.40	63.14	110.91	111.39
133.32	132.91	73.03	72.08	62.79	62.90	110.50	111.14
133.29	133.55	72.27	72.95	62.39	62.20	109.08	109.67
132.60	133.66	72.34	72.74	61.97	61.99	108.55	108.05
130.66	131.94	71.51	70.50	61.42	61.26	107.97	107.76
131.28	131.32	71.02	71.18	61.03	61.08	108.33	108.12
132.46	131.15	72.06	72.51	61.02	60.71	108.83	108.54
132.85	136.09	72.39	71.14	61.02	61.21	109.28	111.00
135.24	136.61	73.31	72.14	61.81	63.21	112.61	112.25
136.72	134.65	72.92	73.37	63.36	63.01	112.50	112.27
137.30	135.54	72.87	72.97	63.99	63.68	112.77	112.14
138.08	136.30	73.24	72.54	64.37	64.04	112.80	112.27
136.40	135.93	72.64	73.30	64.50	65.36	111.87	112.12
136.64	136.47	72.28	72.54	63.80	63.76	110.73	110.99

APPENDIX-III

Monthly precipitation data (mm) for the study period 2007-2021

Monthly precipitation data	2007	2008	2009	2010	2011	2012	2013	2014	2015	2016	2017	2018	2019	2020	2021
Jan	1.60	0.00	0.20	0.90	0.00	0.00	0.00	0.00	0.00	0.00	0.21	0.00	0.00	0.00	41.80
Feb	0.00	35.00	0.00	0.00	67.70	0.00	54.70	4.40	0.70	0.00	0.00	15.50	0.10	0.00	0.00
Mar	0.00	97.70	46.60	11.60	7.00	0.00	23.50	0.00	18.20	0.00	60.01	24.80	2.30	46.60	61.70
Apr	8.90	61.50	53.50	88.50	60.30	114.90	0.10	35.40	125.30	4.00	14.60	31.70	76.20	44.40	67.20
May	1.20	47.90	61.30	98.30	20.90	44.70	102.60	198.20	289.30	96.00	121.01	332.60	35.60	39.70	137.70
Jun	5.50	315.50	208.70	315.00	530.60	339.20	724.60	247.30	462.40	448.40	453.12	476.50	196.50	202.70	287.70
July	9.90	395.60	678.10	387.20	279.10	286.30	602.50	723.10	163.00	425.90	266.63	833.90	404.50	475.60	531.00
Aug	4.70	212.30	204.00	46.30	405.40	398.40	384.00	558.80	189.90	167.70	362.71	1004.70	995.00	665.50	286.70
Sept	4.20	171.10	184.30	121.50	246.40	165.80	337.70	273.80	74.00	92.60	327.00	70.40	584.30	459.20	312.00
Oct	2.80	357.50	173.30	192.80	177.40	177.70	382.00	220.80	104.00	56.80	136.62	219.10	366.30	120.50	442.00
Nov	0.30	41.70	230.00	244.30	221.90	48.20	45.90	5.10	176.40	69.00	37.31	19.70	173.30	66.30	230.00
Dec	0.40	8.10	14.70	12.70	17.70	0.00	3.70	12.40	8.80	35.80	46.30	0.30	5.20	29.80	16.30

APPENDIX-IV

Monthly max temperature for the study period 2007-2021

Monthly max temp	2007	2008	2009	2010	2011	2012	2013	2014	2015	2016	2017	2018	2019	2020	2021
Jan	32.03	32.75	33.72	33.72	33.12	32.95	33.24	31.78	32.07	32.58	33.67	32.61	32.11	32.60	30.60
Feb	34.54	33.94	35.78	35.78	34.34	35.41	34.47	34.52	34.16	35.73	35.16	34.36	35.31	34.20	33.40
Mar	36.45	33.86	37.10	37.10	35.56	35.60	36.78	36.71	35.21	38.41	36.98	36.46	38.14	37.10	36.50
Apr	36.39	34.14	35.65	35.65	34.55	35.28	37.77	37.81	36.27	39.89	37.87	37.13	38.82	37.70	36.10
May	34.00	33.91	33.95	33.95	33.66	33.56	36.47	35.16	34.00	36.44	35.95	33.62	36.97	37.00	34.30
Jun	30.29	30.30	30.79	30.79	29.84	30.61	28.24	31.83	31.79	30.50	30.37	29.63	32.99	31.50	31.50
July	28.29	29.59	29.55	29.55	29.43	29.95	27.60	29.11	30.72	29.58	30.38	28.61	29.96	30.50	30.70
Aug	29.58	30.18	29.41	29.41	29.64	29.25	30.01	29.63	31.53	30.69	30.14	28.58	28.95	30.20	29.90
Sept	28.45	29.50	30.66	30.66	30.17	30.59	30.67	31.43	33.06	30.97	31.63	33.23	30.77	30.10	30.50
Oct	30.45	31.75	30.47	30.47	32.14	32.40	31.67	32.10	32.42	33.08	32.87	32.77	32.60	31.60	31.30
Nov	32.10	32.51	30.70	30.70	31.52	32.01	32.50	31.72	31.79	33.56	33.02	32.37	31.98	32.10	30.60
Dec	32.10	32.33	30.99	30.99	32.44	33.19	31.11	31.47	32.17	32.81	31.70	32.33	30.68	30.30	29.10

APPENDIX-V

Monthly minimum temperature for the study period 2007-2021

Monthly min temperature	2007	2008	2009	2010	2011	2012	2013	2014	2015	2016	2017	2018	2019	2020	2021
Jan	20.21	19.63	19.92	21.42	20.78	20.01	23.48	23.90	22.94	23.65	23.61	22.86	22.14	24.10	24.10
Feb	20.82	21.63	20.80	22.86	19.81	21.14	23.75	23.65	23.56	24.76	23.60	23.46	24.68	24.60	23.70
Mar	23.84	22.09	23.71	24.21	23.20	23.89	25.45	24.90	24.19	26.28	24.89	24.65	25.09	25.90	24.80
Apr	24.65	24.79	24.82	25.29	24.28	25.01	26.31	25.86	24.83	27.51	26.52	25.97	26.39	26.10	25.60
May	24.72	24.97	24.53	25.66	24.75	25.48	26.60	25.26	25.07	26.04	25.61	24.48	26.49	26.70	25.70
Jun	24.12	23.77	23.65	24.24	23.77	24.13	23.26	24.65	24.32	23.97	24.16	24.05	25.43	24.30	24.30
July	23.42	23.69	22.89	23.51	23.35	23.87	23.04	23.26	23.99	23.51	23.67	23.24	23.81	23.90	24.00
Aug	23.42	23.94	23.72	23.65	23.46	23.78	23.65	23.44	24.24	23.93	23.99	23.24	23.53	24.00	23.70
Sept	22.85	23.30	23.80	23.63	23.33	23.66	23.58	23.84	24.39	23.66	24.17	24.18	23.74	23.90	24.10
Oct	23.23	23.37	23.81	23.45	23.58	23.65	23.68	24.28	24.22	24.11	24.36	24.20	23.96	23.90	24.20
Nov	21.59	22.79	23.39	23.15	21.98	22.30	24.83	24.32	24.05	23.80	24.54	25.15	24.93	24.80	23.90
Dec	21.11	20.50	22.75	21.09	21.03	21.70	23.32	23.73	25.06	23.15	24.05	24.52	24.90	23.90	22.80

APPENDIX-VI

SGI estimated by ANN predicted groundwater level for all wells

a)160 PKD-12	Jan	Feb	Mar	Apr	May
2007	0.6	0.4	-0.7	-1.5	-1.2
2008	0.6	0.4	0.3	-1.3	-1.3
2009	0.6	0.0	-0.1	-1.4	-0.5
2010	0.6	-0.1	-1.4	-1.4	-0.5
2011	0.6	0.4	-0.1	-0.3	-1.1
2012	0.6	0.0	-0.9	-0.7	-0.1
2013	0.5	0.0	-1.6	-2.6	-4.0
2014	0.0	-0.1	-1.6	-1.6	0.5
2015	0.6	0.1	-1.2	-0.2	0.3
2016	0.5	-1.5	-2.8	-2.3	-1.0
2017	0.3	-0.2	-1.5	-2.2	-1.2
2018	1.0	0.2	-0.5	-0.5	-0.2
2019	-0.3	-0.5	-1.5	-2.2	-0.8
2020	0.6	-0.6	-0.4	-2.0	-1.2
2021	0.3	0.7	-0.4	-0.4	-1.2

b)PKD -S3	Jan	Feb	Mar	Apr	May
2007	0.7	0.2	-1.4	-1.5	-0.6
2008	0.4	0.2	0.3	-0.8	-0.5
2009	0.3	-0.2	-1.0	-1.0	-0.5
2010	0.2	-1.2	-1.4	-1.2	0.4
2011	0.4	0.0	-1.4	-0.9	-0.4
2012	0.5	0.0	-1.3	-1.0	0.6
2013	-0.9	-0.9	-1.6	-2.2	-0.7
2014	0.2	-1.3	-1.6	-1.9	-0.5
2015	-0.2	-1.3	-1.2	-1.0	0.3
2016	-0.5	-1.4	-2.4	-2.0	-2.0
2017	-1.1	-1.4	-1.5	-2.5	-1.3
2018	0.4	-2.2	-3.5	-1.0	-1.3
2019	0.3	-0.4	-0.4	-1.0	-2.3
2020	0.5	0.2	-0.1	-0.5	-1.9
2021	0.9	0.7	-1.1	-0.5	0.5

c)PKD S4	Jan	Feb	Mar	Apr	May
2007	0.0	-0.7	-1.0	-1.7	-0.8
2008	0.5	-0.1	0.6	-0.5	-0.6
2009	0.0	-0.8	-1.9	-0.8	0.1
2010	-0.4	-0.2	-3.4	-2.0	-0.9
2011	-0.8	0.9	-0.8	-0.2	-0.5
2012	-0.1	-0.4	-0.6	-1.2	-0.9
2013	-0.8	-1.1	-3.0	-3.2	-3.1
2014	-0.5	-1.4	-2.1	-1.4	-0.8
2015	0.0	-1.2	-0.7	0.5	1.3
2016	-0.6	-1.4	-1.6	-1.3	-1.6
2017	-1.1	-1.3	-3.4	-1.5	-1.2
2018	0.0	-0.9	-2.6	-0.5	0.0
2019	-0.1	0.0	-0.2	-2.7	-1.2
2020	0.0	-0.2	-0.2	0.1	-0.6
2021	0.0	0.0	-0.7	-0.2	0.7

d)128	Jan	Feb	Mar	Apr	May
2007	0.0	-0.2	-1.1	-1.4	-0.6
2008	-0.1	-0.5	-0.9	-0.6	-0.4
2009	-0.1	-0.5	-1.2	-0.8	-0.5
2010	-0.1	-0.6	-1.2	-1.2	-0.3
2011	0.1	-0.1	-0.9	-1.0	-0.5
2012	0.0	-0.4	-1.2	-0.9	-0.1
2013	-1.0	-1.2	-1.7	-2.1	0.4
2014	-0.2	-1.2	-1.4	-2.1	-0.6
2015	-0.6	-1.1	-1.2	-1.1	1.2
2016	-0.7	-1.2	-2.2	-1.0	-1.6
2017	-1.1	-1.2	-1.5	-2.1	-1.4
2018	0.3	-1.0	-1.3	-1.7	1.1
2019	-0.3	-0.4	-1.4	-1.4	-1.7
2020	0.4	0.3	-1.6	-1.7	-1.7

e)129	Jan	Feb	Mar	Apr	May
2007	2.0	0.0	-0.7	-0.8	-0.9
2008	0.4	0.0	-0.1	-0.6	-0.6
2009	-0.4	0.0	-0.5	-0.7	-0.3
2010	0.1	-0.3	-0.7	-0.9	-1.0
2011	0.1	-0.5	-0.4	-0.5	-0.6
2012	0.0	0.0	-0.7	-0.7	-0.8
2013	-0.5	-0.4	-0.9	-1.1	-1.6
2014	0.1	-0.6	-0.8	-1.0	-1.1
2015	-0.3	-0.6	-0.7	-0.8	-1.1
2016	-0.3	-0.9	-1.0	-1.5	-1.3
2017	-0.6	-0.6	-0.8	-1.2	-1.1
2018	-0.6	-1.7	-1.1	-1.3	-1.3
2019	-1.7	-0.7	-1.3	-1.5	-1.7
2020	0.0	-0.5	-0.8	-0.8	-1.7
2021	-0.6	-0.7	-1.3	-1.4	-1.7

f)160 PKD- 8	Jan	Feb	Mar	Apr	May
2007	-0.1	-0.6	-1.7	-2.0	-1.2
2008	-0.8	0.2	1.1	-0.4	-0.3
2009	-0.7	-0.7	-0.6	-0.9	0.2
2010	-0.5	-1.2	-1.5	-1.2	0.2
2011	-0.4	0.5	-1.3	-0.7	-0.6
2012	-0.7	-0.8	-1.9	-0.3	-0.1
2013	-1.4	-0.5	-2.0	-2.1	-1.8
2014	-1.2	-1.7	-2.0	-2.1	0.8
2015	-1.4	-1.6	-1.7	0.3	0.6
2016	-1.3	-2.0	-2.1	-2.2	-1.7
2017	-1.5	-1.8	-1.5	-2.1	-0.9
2018	-0.6	-0.8	-1.0	-0.8	0.7
2019	-0.7	-0.8	-1.1	-1.3	-0.7
2020	-0.2	-0.4	-0.8	-1.0	-0.7
2021	0.4	-0.6	-0.9	-0.2	0.1

g)140	Jan	Feb	Mar	Apr	May
2007	0.7	-0.5	-1.2	-1.4	-1.2
2008	0.2	0.0	-0.3	-1.0	-1.1
2009	0.4	-0.5	-0.9	-1.3	-0.3
2010	0.1	0.1	-1.4	-1.6	-1.5
2011	0.6	0.5	-0.4	-0.7	-0.9
2012	0.5	0.2	-1.2	-1.5	-1.4
2013	-0.1	-0.3	-1.6	-1.9	-1.9
2014	0.0	-0.5	-1.5	-2.0	-1.4
2015	0.1	-0.2	-1.2	-1.7	0.5
2016	-0.2	-1.3	-2.0	-2.2	-1.9
2017	-0.1	-0.8	-1.7	-2.0	-1.8
2018	0.1	-0.4	-0.9	-1.6	-0.7
2019	0.1	-0.4	-0.9	-1.3	-1.7
2020	0.2	0.3	-1.5	-1.5	-1.8
2021	0.1	0.1	-1.0	-1.7	-1.8

h)142	Jan	Feb	Mar	Apr	May
2007	0.7	0.7	0.5	-0.4	-0.4
2008	0.7	0.7	1.0	0.2	0.2
2009	0.7	0.7	0.2	0.3	0.1
2010	0.7	0.8	-0.4	-0.9	-0.6
2011	0.7	0.7	0.0	0.0	-0.1
2012	0.7	0.7	-0.7	-0.2	-0.3
2013	-1.4	-0.8	-1.1	-1.2	-1.5
2014	0.5	-1.4	-1.1	-0.6	-1.6
2015	-0.5	-1.4	-0.4	0.1	-0.9
2016	-1.0	-0.3	-0.8	-1.8	-1.6
2017	-1.4	-1.2	-0.4	-1.4	-1.5
2018	-2.1	-0.9	-2.1	-2.3	-0.8
2019	-2.3	-2.3	-2.3	-2.4	-2.5
2020	-1.1	-2.0	-2.1	-2.4	-2.5
2021	0.2	-1.4	-1.5	-0.9	-0.2

i)133	Jan	Feb	Mar	Apr	May
2007	-0.5	-1.1	-0.9	-0.9	-0.5
2008	0.3	-0.7	-0.6	-0.7	-0.6
2009	-0.8	-0.8	-1.0	-0.7	-1.0
2010	-0.8	-1.2	-1.0	-0.9	-0.7
2011	-1.0	-0.4	-1.1	-0.9	-0.7
2012	-0.6	-0.6	-0.9	-0.9	-0.3
2013	-1.5	-1.0	-1.0	-1.0	-1.0
2014	-0.7	-1.3	-1.0	-1.0	-1.0
2015	-1.0	-1.7	-0.8	-1.0	-0.2
2016	-0.8	-0.8	-1.0	-0.9	-1.0
2017	-1.9	-1.1	-1.0	-1.0	-1.0
2018	-0.7	-0.6	-1.2	-1.1	1.4
2019	-0.9	-1.2	-1.3	-1.1	-1.0
2020	-0.9	-1.1	-1.1	-1.1	-1.0
2021	-0.1	-0.9	-1.1	-0.9	-0.7

j)PKD S 7	Jan	Feb	Mar	Apr	May
2007	0.5	1.0	-0.5	-1.0	-1.2
2008	0.2	0.0	-0.3	-1.0	-0.9
2009	-0.1	-0.4	-0.8	-1.1	-0.6
2010	0.5	-0.2	-0.3	-1.4	-0.5
2011	0.4	0.5	-0.7	-1.0	-0.9
2012	0.1	-0.2	-0.9	-1.3	-0.7
2013	-0.8	-0.8	-1.4	-1.9	-1.5
2014	-0.2	-0.9	-1.0	-1.3	-0.4
2015	-0.6	-0.8	-0.9	-0.5	1.4
2016	-0.6	-1.2	-1.4	-1.9	-1.5
2017	-0.9	-1.0	-1.1	-2.0	-1.5
2018	-1.3	-1.5	-2.0	-1.8	-2.0
2019	-0.1	-2.0	-2.0	-1.0	-0.9
2020	0.8	0.2	-0.4	-0.3	-0.5
2021	0.8	0.6	-2.0	0.7	0.3

k)139	Jan	Feb	Mar	Apr	May
2007	1.3	0.2	-0.6	-0.5	-0.9
2008	1.0	0.1	0.8	-0.3	-0.5
2009	0.8	0.1	-0.1	-0.4	-0.3
2010	0.1	0.3	-0.5	-0.4	0.0
2011	0.5	0.7	-0.3	-0.1	-0.7
2012	0.9	0.0	-0.8	-0.2	-0.4
2013	-1.2	-0.3	-1.5	-0.9	-0.6
2014	0.0	-1.2	0.8	-0.4	-0.7
2015	0.6	-1.3	-0.6	-0.5	0.5
2016	-0.6	-0.7	-1.3	-1.6	-2.0
2017	-1.3	-1.0	-1.1	-1.5	-3.1
2018	-1.1	-0.9	-1.1	-1.3	-1.6
2019	0.0	-0.8	-1.5	-1.8	0.8
2020	-0.6	-0.5	-1.6	-1.5	0.4
2021	-0.9	-0.9	-1.5	-1.7	-1.7

l)PKD S 7	Jan	Feb	Mar	Apr	May
2007	0.5	1.0	-0.5	-1.0	-1.2
2008	0.2	0.0	-0.3	-1.0	-0.9
2009	-0.1	-0.4	-0.8	-1.1	-0.6
2010	0.5	-0.2	-0.3	-1.4	-0.5
2011	0.4	0.5	-0.7	-1.0	-0.9
2012	0.1	-0.2	-0.9	-1.3	-0.7
2013	-0.8	-0.8	-1.4	-1.9	-1.5
2014	-0.2	-0.9	-1.0	-1.3	-0.4
2015	-0.6	-0.8	-0.9	-0.5	1.4
2016	-0.6	-1.2	-1.4	-1.9	-1.5
2017	-0.9	-1.0	-1.1	-2.0	-1.5
2018	-1.3	-1.5	-2.0	-1.8	-2.0
2019	-0.1	-2.0	-2.0	-1.0	-0.9
2020	0.8	0.2	-0.4	-0.3	-0.5
2021	0.8	0.6	-2.0	0.7	0.3

**SPATIO-TEMPORAL GROUNDWATER DROUGHT
ASSESSMENT BASED ON ANN MODEL AND GIS FOR A
SUB-BASIN OF BHARATHAPUZHA**

By

RABEEA ASSAINAR K K

(2020-18-005)

ABSTRACT OF THESIS

Submitted in partial fulfilment of the requirement for the degree of

MASTER OF TECHNOLOGY

IN

AGRICULTURAL ENGINEERING

(Soil and Water Engineering)

Faculty of Agricultural Engineering & Technology

Kerala Agricultural University



**DEPARTMENT OF IRRIGATION AND DRAINAGE ENGINEERING
KELAPPAJI COLLEGE OF AGRICULTURAL ENGINEERING AND
TECHNOLOGY**

TAVANUR - 679573, MALAPPURAM

KERALA, INDIA

2022

ABSTRACT

Groundwater is one of the most precious and significant sources of water in the world. Understanding the effects of both natural and human-made factors on groundwater reserves and exploitation is crucial for developing appropriate management strategies to deal with unsustainable use. The understanding of groundwater level variability and trend is crucial for water resource planning in a region. The groundwater level fluctuation is a non-linear phenomenon. Hence, Artificial Neural Networks (ANN) proves to be one of the best tools for modelling non-linear relationship between input and output datasets. Once the groundwater level is modelled, it is easy to assess the groundwater drought conditions of a region using Standardized Groundwater level Index (SGI). Therefore, systematic information about likely occurrence and distribution of drought may assist in preparedness and mitigation of drought disasters.

The present study was conducted in Kalpathypuzha sub-basin of Bharathapuzha to analyze the variability and trend of groundwater level, to develop ANN model for groundwater level prediction and to assess the groundwater drought using Standardised Groundwater level Index (SGI). Twelve observation wells evenly distributed in the blocks of Kuzhalmannam, Palakkad, Malampuzha and Chittur were selected. The groundwater level variability was analyzed by various descriptive statistics such as mean, standard deviation, coefficient of variation, skewness and kurtosis. The groundwater level trend was estimated using Mann-Kendall test and Sens slope estimator. ANN models were developed separately for each well to predict the groundwater level using MATLAB R2016a software. The input parameters used were precipitation, maximum and minimum temperature and output data used was groundwater level collected for a period of 15 years from 2007 to 2021. SGI values were estimated for both observed and predicted groundwater level data to assess the groundwater drought scenario of the study area and to develop spatio-temporal groundwater drought map. Monthly groundwater level and drought conditions were predicted for the year 2023 using the developed ANN model.

Results of trend analysis showed a decreasing pre-monsoon groundwater level trend in three wells, well 129 of Palakkad block and wells 133 and 142 of Malampuzha block while decreasing post-monsoon groundwater level trend in well 139 of Chittur block. But there was no trend in all other wells for both pre-monsoon and post-monsoon. Feed forward ANN models were developed for all the twelve wells in the study area and the performance indicators correlation coefficient r (0.93 to 0.74), Root Mean Square Error RMSE (0.11 to 0.45 m), and coefficient of determination R^2 (0.87 to 0.69) were found in the acceptable range. The best model performance for training was for the well PKD S-4 with model configuration 3-10-1 and $r = 0.92$ whereas, during testing it was found for the well 129 with model configuration 3-14-1 and $r = 0.93$. ANN predicted groundwater level was found in close agreement with that of the observed groundwater level in this study. Hence the model developed could be safely and effectively applied in the study area.

The SGI was estimated for pre-monsoon months Jan, Feb, Mar, Apr and May of the study period from 2007 to 2021 for all the twelve wells as drought was more severe during these months. SGI values ranged from -3.7 to 1.1 indicated exceptional to no drought condition in the study area. The computed SGI values indicated that the years 2013, 2016, 2017 were the severe drought years of the study area. According to Spatial distribution of SGI values for the years 2013, 2016 and 2017 Chittur and Malampuzha block were the most drought affected areas followed by Kuzhalmannam and Palakkad block. Hence the study revealed that the majority of Kapathypuzha sub-basin is drought prone and immediate measures are to be adopted to prevent the extend of severity in the area.